HYDROCARBON PROCESSING®

Cover Image: A worker inspects a gas turbine rotor at a Siemens' gas turbine plant. Photo courtesy of Siemens.

100TH
1922–2022
ANNIVERSARY

HP Industry Perspectives

New project market share down 19% 1H 2021 vs. 1H 2022

In 1H 2022, new capital projects have declined 19% vs. 1H 2021. Gulf Energy Information's Global Energy Infrastructure (GEI) database tracked 108 new projects in 1H 2021. Conversely, new project announcements have fallen to below 90 in the first half of this year. In total, newly announced projects this year represent more than $90 B in capital investments.

Market share. At 40% market share, most new project announcements this year have been in the Asia-Pacific region (**FIG. 1**). This region is followed by the Middle East (16%) and Eastern Europe, Russia and the Commonwealth of Independent States (CIS) at 15%.

In Asia, China and India continue to be the leaders in new project announcements this year. In total, these two countries account for 80% of new projects announced this year in the Asia-Pacific region, with China's market share alone at nearly 55%. Most of these projects in both countries are within the petrochemicals industry.

The Middle East is continuing to invest in building out downstream processing capacity, especially new petrochemical units. Most of the newly announced projects this year are in Iran and Saudi Arabia.

In Eastern Europe, Russia and the CIS, new capital projects are focused on expanding petrochemicals production capacity and additional refining units to produce cleaner transportation fuels. Western Europe has not only witnessed an uptick in new renewable fuel projects, but also in several LNG terminal projects (primarily floating vessels such as FLNGs and FRSUs) to find new natural gas supplies as the region weans off the use of Russian natural gas. **HP**

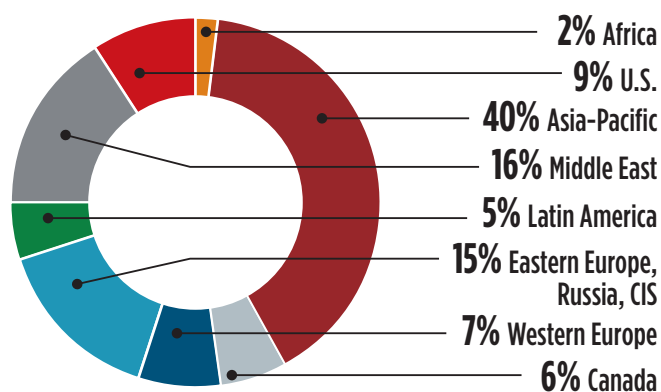

2% Africa
9% U.S.
40% Asia-Pacific
16% Middle East
5% Latin America
15% Eastern Europe, Russia, CIS
7% Western Europe
6% Canada

FIG. 1. New project announcements market share by region, 1H 2022.

LEE NICHOLS, EDITOR-IN-CHIEF/ASSOCIATE PUBLISHER
Lee.Nichols@HydrocarbonProcessing.com

No flow, no go: Stressing the importance of flow control technologies

One of the most critical aspects of plant operations is controlling the flow of liquids and gases throughout refining and petrochemical process units. For an average-sized refinery, a significant amount of feedstock, products and fuel travel through miles of piping, equipment and processing units to be converted into the multitude of products used every day around the world.

These flow systems consist of thousands of valves and pumps that must be monitored to ensure efficiency and optimum operation. Any breakdown of these systems can result in significant maintenance costs, downtime, loss of profitability and/or even safety issues that can put plant personnel in harm's way. Ensuring these systems are working properly is paramount for refining and petrochemical personnel.

Technologies and optimizing performance. Since the use of valves, pumps and turbomachinery is so prevalent within the hydrocarbon processing industry, it is imperative to provide the latest technologies, products and know-how to help plant personnel ensure the proper operation of these pieces of equipment.

For this reason, *Hydrocarbon Processing* has not only devoted this issue to the subject, but has also made the topic of valves, pumps and turbomachinery a regular feature throughout its editorial lineup. This issue features several in-depth technical articles to help refineries and petrochemical plants better manage and optimize various equipment within their flow systems.

The following is a preview of the technical articles within this issue that focus on valves, pumps and turbomachinery.

Non-OEM valve components. This month's Business Trends section focuses on the prevalence of non-OEM (original equipment manufacturer) parts being used in processing facilities. These pieces of equipment can look identical to their OEM counterparts, but tend to be less efficient and can be dangerous should they fail during operations. This article provides an overview of non-OEM valve components and several case studies on the detrimental effects when non-OEM equipment fails.

A new equation for pressure relief valves (PRVs). PRVs protect process equipment from the hazards of excessive over-pressure. A simple liquid equation is widely used as a standard method for sizing incompressible fluids. This Special Focus (SF) article proposes an alternative solution for a constant isentropic expansion coefficient. The new method is based on the classical homogeneous equilibrium model chosen by API 520 Part 1 and AIChE/DIERS for emergency pressure relief system designs.

Fouling. Hydrogen recycle gas compressors are one of the most significant rotating equipment in oil refineries, petrochemical plants and upgraders. The risk of fouling is high in recycle gas compressors due to chemical injection and reactions in the reactor. This SF article explains the hydrotreating process and addresses compressor fouling, which impacts the recycle gas compressor's performance and reliability.

Calculating flowrate in turbulent flow regimes. Calculating flowrate through long, straight pipe in a zone of complete turbulence is easy using standard fluid mechanics equations. This SF article presents equations that accurately calculate flowrate through valves, fittings and pipe under a turbulent flow regime.

Corrosive fluids. Refineries and petrochemical plants contain highly corrosive fluids that are used in operations. These fluids can wreak havoc on equipment such as valves. This SF article details the effects of highly corrosive valves and steps plant personnel can take to avoid safety issues. **HP**

INSIDE THIS ISSUE

22 Special Focus. Hundreds of pieces of crucial equipment ensure the continued flow of fluid throughout processing plants. Any disruption in this fluid flow system can severely impact refining and petrochemical plant operations. Therefore, it is necessary to properly design, operate and maintain these systems for optimal operations.

37 Modularization. Modular construction allows for standardization and repeatability, which translates to the ability to establish a definitive estimate early in the project development phase. This article details the benefits of using truckable modularization technology, including scalability, installation flexibility, repeatability, project predictability and risk mitigation.

40 History of the HPI. This month's History of the HPI section examines the major events and technologies in the refining and petrochemicals industry in the 1980s. These include a third oil price crisis in 15 yr, the creation of novel coal gasification and heavy oil upgrading processes, research on liquid crystals and conducting polymers, new safety measures born from tragedies, and the rise of virtual and augmented reality.

77 Maintenance and Reliability. When identifying solutions that can offer assurance and longevity, the maintenance and reliability of asset repairs can be challenging. This article introduces a novel, two-component, solvent-free toughened epoxy adhesive material that provides high adhesion to metallic substrates, while also being able to withstand high movement or cyclic fatigue vs. general epoxy materials.

B. BOYLE, Emerson

Non-OEM parts–Buyer beware

What is the harm in wearing a knock-off Rolex watch? It looks the same, keeps time, and if no one inspects it too closely, appears impressive. How about wearing a name-brand replica pair of jeans, or perhaps a counterfeit pair of top-tier athletic shoes? That might create some discomfort and even a blister or two, but the cost savings may more than compensate.

Now, consider the ramifications of using non-OEM (original equipment manufacturer) airbags or brakes on your car. Would it be acceptable if passenger trains began using these types of parts to repair their braking systems? Suddenly, a non-OEM replacement part might be seen in a very different light.

In some industries, such as aviation, legal requirements cover service and repair situations, making it against the law to use non-OEM parts. The same types of regulations apply to the use of valves in some industrial applications, such as in safety systems; while most industrial applications for valves do not expressly prohibit the use of non-OEM parts, this certainly does not lessen the risk of their use.

All types of non-OEM parts present potential problems. Issues are not limited to poor performance and downtime due to failure, as civil lawsuits can result if personnel injury occurs due to failure of a sub-standard part. If a company loses its case in court due to the use of non-OEM parts, insurance rates will certainly rise, and future visits by adjusters will become more frequent and exacting.

Imagine non-OEM valve body components in 1500# service, as isolation valves for natural gas service, and even in a nuclear power plant. Each of these situations has the potential to create catastrophic damage and, in the worst-case scenario, injury to plant personnel.

A burgeoning problem. It is disconcerting that the scenarios posed above have actually occurred. Certainly, the world is awash in fake watches, name-brand clothes and designer shoes, but it is a less-publicized fact that non-OEM auto parts are common in every world market, with some countries estimating that 20% of car accidents stem from these substandard components. Despite laws prohibiting their use, at least one fatal airline crash was directly attributable to non-OEM engine mount bolts.

In a similar vein, non-OEM valves and valve components are invading various sectors of industry. In some cases, these components are used within a plant unknowingly, as some are marketed as the real thing and provided by a new supplier. In other cases, maintenance and procurement departments order the cheaper components in an attempt to save money or fill a pressing need. The problem is the number of non-OEM parts is growing explosively, and spotting them is becoming more difficult (**FIG. 1**).
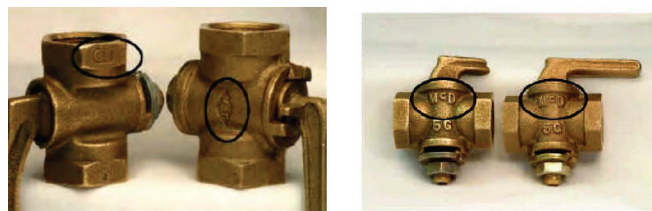
FIG. 1. The non-OEM gas valve on the left will not close properly. Other than some markings and a few dimensional variations, the part looks very similar to the authentic valve on the right. (Reprinted from Department of Energy's Counterfeit Training Manual.)

In the past, non-OEM parts may have been easier to spot, with parts that were wrapped in newspaper, labels that had misspelled words and prices that were significantly reduced. However, some non-OEM parts are now shipped in authentic packaging with fairly accurate equipment labels, and prices have been raised to make the part cost seem reasonable—although still attractive. It is certainly possible for a plant to pay nearly full price for a non-OEM part and not realize it was not genuine.

What are the critical differences? Non-OEM valve parts can look identical to their OEM counterparts. The color, dimensions and labeling may appear to be exactly the same. Some are openly marketed as a "direct replacement" for the original component, while others are presented as an authentic OEM part. What are the differences between an OEM and a non-OEM part? The answer, while not obvious, can be significant.

A parts replicator looks to fabricate a non-OEM part as cheaply as possible. The part itself must look the same, of course, and in that regard the replicator is usually fairly successful. They start with an OEM part, often used, and measure its dimensions. They then use a positive material identification (PMI) gun to scan the part and identify the alloy of construction (**FIG. 2**). Based on that data, the fabricator creates the replacement part, often painting it the same color and affixing a similar label. The part is then sold as a direct replacement, and in some cases, it is even packaged and marketed as an actual OEM part.

While the component may look identical, a more thorough examination can reveal a host of problems, starting with those seemingly simple dimension measurements. Any machining process involves a target dimension with an allowable manufacturing tolerance (**FIG. 3,** left). As long as the final dimensions fall within the allowable range, the part is considered "in specification" and released. This process works well for the OEM fabricator, which has designed the part, knows the fabrication toleranc-

es, and has set that tolerance band to ensure the finished part will consistently fall within specification and perform as expected.

> Despite their near identical appearance, non-OEM components are still likely to underperform, resulting in significant costs in terms of downtime, equipment damage and personnel hazards.

In contrast, the replicator has a single, and typically used, part that they measure to determine the target dimension. They then use that dimension as their new target and will fabricate parts in a tolerance around that measured value. The replicator does not know the OEM target dimension or the allowable tolerance, so the resulting parts will often fall outside OEM specifications, as shown on the right of **FIG. 3**. This can create significant performance issues when the component is placed into service.

FIG. 2. While a PMI gun can reveal some details regarding materials of construction, it does not provide a complete picture. Source: Emerson.
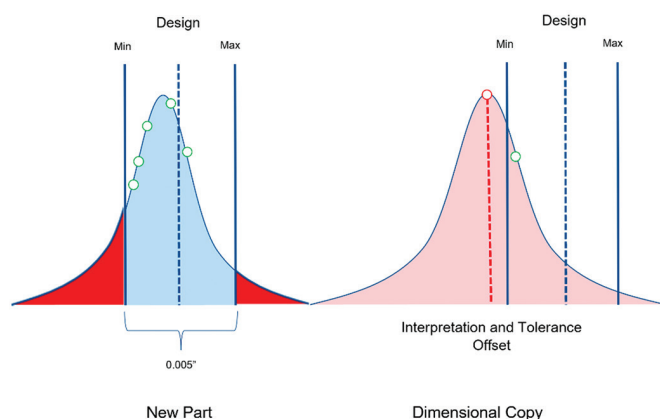
FIG. 3. The OEM part (left) is fabricated to a design dimension and falls within an allowable tolerance band. The non-OEM part (right) is based on a single dimension taken from a used part. The resulting dimensions will often fall outside the allowable OEM tolerance band. Source: Emerson.

Now consider the replica part's material of construction. The x-ray fluorescence analyzer in the PMI gun can identify the chemical composition and grade of the part, but that is only a small piece of a much broader specification. Every OEM part has detailed specifications for external coating materials and thickness, heat treatment, hardness and surface finish (**TABLE 1**).

These processes are carefully chosen to extend part life, minimize friction, manage specific stresses expected in normal operation, and perform as expected. The non-OEM part manufacturer has no way to determine any of this information from a PMI gun reading, so they finish the part until it "looks right," and then box it up for shipment to a hapless customer.

The difference in part performance can be significant. Hardness and surface finish impact the friction of the component as it moves, which can cause control valves to hunt around setpoint. The non-OEM parts also tend to gall and wear earlier, as well as leak and fail prematurely in cavitation or flashing conditions.

Additional value from OEM parts. The dimensions and material of construction obviously have a significant impact on the performance and service life of a valve component. However, another significant benefit is associated with OEM parts: the knowledge and expertise of the manufacturer itself.

A host of professional standards organizations are dedicated to maintaining the safety and reliability of process control valves, while ensuring the metallurgical fabrication techniques are the best available. Nearly every OEM control valve supplier has active representation on many of these standards committees, offering valuable knowledge and staying current on the latest industry developments.

That knowledge is translated into continuous improvements in the materials of construction and manufacturing techniques that are used to fabricate valve parts. Just as every product has a

TABLE 1. A PMI gun reading can indicate the specific material of construction, but it cannot determine the host of other material specifications, post-treatment and testing a typical valve part requires

Replication vs. OEM design: Materials

	ASTM A494	Fisher ASTM A494
Raw material control		x
Chemistry control	x	x
Heat qualification bend test		x
Liquid penetrant (LP) examination		x
Heat treat temperature control	x	x
Heat treat time control		x
Quench method control		x
PWHT major repairs		x
Weld filler control		x
Interpass temperature control		x
LP examination weld repairs		x
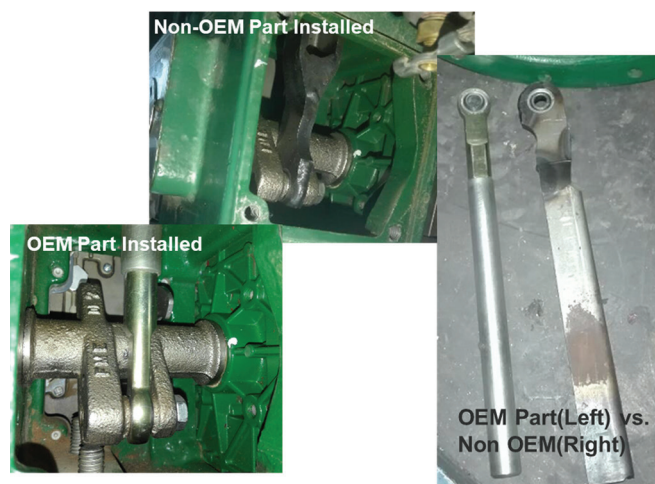
FIG. 4. An unauthorized valve repair shop decided to replace the actuator shaft assembly with a reverse engineered version (right). The non-OEM part dimensions were incorrect and kept the valve from fully closing, forcing an additional 24 hr of unplanned downtime. Source: Emerson.

lifecycle, so does every part. In some cases, the part remains the same throughout its lifecycle; in many other instances, the part is upgraded throughout its lifecycle, sometimes more than once.

An upgraded part may be quite different from the original part used in the original valve because it has often been redesigned to perform better and/or last longer than the original. When an OEM part is purchased, the user is taking advantage of this expertise and obtaining a part that reflects the most up-to-date knowledge available.

Another benefit of buying OEM parts is the opportunity to benefit from a vendor's extensive application and domain expertise. Process changes occur often, subjecting valve components to more difficult conditions than were originally considered in the original purchase. If a part fails prematurely, the OEM has the expertise to evaluate the part, determine why it failed and possibly offer an upgraded part better suited to the new conditions and requirements. Replicators will simply offer their best efforts at a duplicate (but not exact) replacement, which is destined to fail again soon.

Another valuable service provided by OEMs is the ability to quickly provide stocked parts anywhere in the world. In many cases, the part can be delivered within hours, with upgraded parts supplied as a matter of course.

The wages of non-OEM parts are serious incidents. Innumerable examples exist where non-OEM electronic, piping and valve components found their way into plants and caused serious damage and lost production. A few recent examples are detailed here.

A massive fire in India's Hazira gas plant forced the immediate shutdown of the plant's 30-MMm^{3}d capacity, blocked production from several gas fields, and curtailed 40% of a downstream user's supply. The cause of the fire was traced to a set of non-OEM gaskets and O-rings installed in a gas meter during refurbishment. The meter was returned to service and the meter seals failed shortly thereafter, sparking the blaze that forced the large gas processing plant out of production.

In another incident, an end user sent a control valve to an unauthorized repair facility for refurbishment. The valve was repaired, returned to the site and placed into service (**FIG. 4**). Upon startup, the valve immediately began leaking and forced the plant to shut down again to address the problem. Upon investigation, the plant determined that the shop had replaced the actuator shaft assembly with a non-OEM part that was not dimensionally correct and kept the control valve from fully closing, creating the leaks noticed at startup. Ultimately, the plant incurred an additional 24 hr of unexpected downtime due to minuscule savings on a part that could have been purchased from the OEM for $200 from stock at a nearby warehouse.

Steam desuperheaters are a critical application in many combined-cycle power stations, with downstream equipment and piping dependent on their performance to avoid significant damage. After an extended time in service, a set of desuperheaters was removed and sent to an authorized repair facility for refurbishment, with the plant purchasing the repair components and providing them to the service center.

The repair facility examined the non-OEM parts and noticed significant differences in the design. Further investigation revealed that the plant had purchased the "OEM" parts from a non-OEM supplier, and the replacement components were actually substandard. There is no way to know how these parts would have performed, but any deviation could have easily damaged downstream piping, warped boiler tubes and cost hundreds of thousands of dollars in equipment and downtime. The plant was unwilling to take the risk, so the non-OEM parts were returned and replaced with OEM parts, and the repaired desuperheaters were returned to service without incident.

Takeaways. The case studies presented here are just a small sample of the thousands of cases of non-OEM valve components encountered daily in industrial plants and facilities worldwide. Valve bodies have failed, internal seal components have quickly deteriorated, and control valves have leaked both internally and externally—all due to the use of non-OEM parts.

Eliminating this problem has become increasingly difficult because suppliers of substandard parts have stepped up their game. Non-OEM parts are no longer so easily recognized, with these parts packaged, priced and sold into non-OEM supply channels and marketed as authentic OEM parts. Despite their near identical appearance, these types of components are still likely to underperform, resulting in significant costs in terms of downtime, equipment damage and personnel hazards.

A repair savings of a few hundred dollars can easily result in an unplanned loss and equipment damage worth hundreds of thousands of dollars. Is that deal worth the risk? Certainly not when the results can include extended downtime, associated economic loss, equipment damage, environmental incidents, injury to personnel, civil lawsuits, increased insurance rates and long-lasting damage to a company's brand and reputation. **HP**

BOB BOYLE is Vice President of the Fisher Parts Business Unit at Emerson. Prior to joining Emerson, he spent 20 yr with Deere & Co. in a variety of roles related to aftermarket, precision agriculture, business strategy and M&A. Mr. Boyle holds a BS degree in management from the University of Maryland, and an MBA and an MS degree in finance from Loyola University Maryland.

MIKE RHODES, MANAGING EDITOR
Mike.Rhodes@HydrocarbonProcessing.com

HP| Innovations

Net-zero mass spectrometer

The Thermo Scientific Delta Q isotope ratio mass spectrometer (IRMS) is a next-generation gas IRMS designed to enable detailed analysis with greater precision and accuracy. In addition to its improved specifications, including an upgrade in software to Qtegra ISDS to dramatically improve ease-of-use and laboratory productivity, the system's carbon footprint will be neutralized, allowing scientists to conduct their work while minimizing their environmental impact. The Delta Q IRMS (**FIG. 1**) is the first product to be released as part of the IsoFootprint campaign, an initiative to permanently remove carbon dioxide (CO_2) emissions associated with the manufacture and supply chain of all new inorganic IRMS products.

The Inorganic MS (IOMS) team at Thermo Fisher has committed to removing all embodied carbon in its new instrumentation, using technologies like direct air capture and bio-oil sequestration that lock away carbon from the atmosphere permanently. The company states that by 2026, its IOMS instruments will become carbon neutral, removing ~4,500 tCO_2e from the atmosphere each year.

FCC additive for emissions and regenerator afterburn control

BASF has launched Enable™, its next-generation carbon monoxide (CO) promoter additive. Enable significantly enhances activity and delivers superior performance for refiners with more efficient use of precious metal, optimizing durability via support surface morphology modification. The combination of differentiating design features offers customers significant performance improvement in controlling regenerator afterburn. Enable is the latest addition to BASF's advanced refinery additives portfolio, supporting customers by enabling

environmental compliance with a cost-effective solution.

Extracting RSH, H_2S, CO_2 and COS from liquid and gas streams

Merichem Company's THIOLEX™ technology removes mercaptan compounds (RSH), hydrogen sulfide (H_2S), carbon dioxide (CO_2), carbonyl sulfide (COS) and elemental sulfur from liquid and gas hydrocarbon streams. THIOLEX units (**FIG. 2**) use proprietary, non-dispersive FIBER FILM® Contactors (FFC) as a mass transfer device, with caustic and/or amine as the treating reagent in liquid and gas hydrocarbon streams. The technology removes H_2S, RSH and CO_2 and some elemental sulfur using caustic alone; with other additives, it can remove COS.

Typical treatment to remove H_2S and RSH uses 14 wt%–20 wt% sodium hydroxide (caustic). For COS removal, the system uses monoethanolamine (MEA)/caustic, which is effective at hydrolyzing COS to meet clients' specifications.

The FFC is a vertical pipe or vessel packed with proprietary fiber that achieves non-dispersive-phase contact without the

problems inherent in conventional dispersive mixing devices, such as aqueous phase carryover, hydrocarbon losses, lack of turndown ability, long settling times, plugging and flooding. Because the aqueous phase adheres to the fibers rather than being dispersed into the hydrocarbon phase, carryover and uncontrollable emulsions are virtually eliminated.

This technology can be fully automated and typically requires minimal

FIG. 1. The Thermo Scientific Delta Q Isotope Ratio Mass Spectrometer (IRMS).
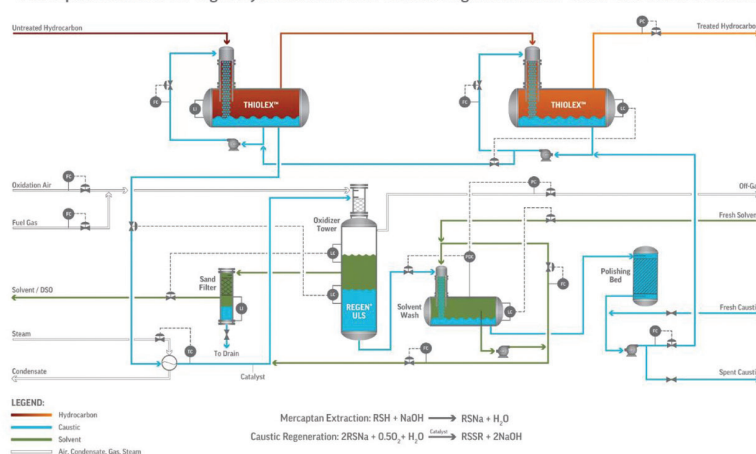

FIG. 2. Merichem's THIOLEX™ removes light hydrocarbons with caustic regeneration for ultra-low sulfur product.

operator support. It operates efficiently over a wide range of throughputs and operating conditions, and is not limited by hydrocarbon-to-caustic ratios that typically limit counter-current systems. An ideal situation is operation over a wide range of caustic strengths, which achieves a high utilization of the caustic due to the efficiency of the mass transfer.

Merichem Company's FIBER FILM technologies can be retrofitted into existing units or built new in stick-built or modular systems. Retrofitting existing vessels saves cost and space, and fabrication using modules offers "plug and play" opportunities to drive more efficient installation and improve safety at the site due to the minimal interface requirements of a modular system. From a pure treatment aspect, Merichem Company has designed new FFC Plus offerings that can be used in THIOLEX systems that increase the amount of sulfur that can be removed using a smaller FIBER FILM Contactor with even better separation, further reducing carryover.

High-accuracy ultrasonic flowmeter for process cooling systems

AW-Lake Company has introduced a Water Inline (WIN) Ultrasonic Flow Meter for highly accurate and reliable flow measurement of cooling water, condensing water and water/glycol solutions. Designed for process cooling applications, including industrial cooling circuits, the WIN Ultrasonic Flow Meter has no moving parts for long-term reliability and low maintenance costs. By incorporating two wetted ultrasonic transducers that face each other directly

FIG. 3. AW-Lake Company's Water Inline (WIN) Ultrasonic Flow Meter provides accurate and reliable flow measurement of cooling water, condensing water and water/glycol solutions.

in the flow tube, the ultrasonic flowmeter reduces wear associated with moving parts and maximizes signal strength.

The WIN Ultrasonic Flow Meter (**FIG. 3**) offers high accuracy (+1.0% of reading over 25:1 turndown, 100:1 total turndown) over a wide flow range with minimal pressure drop. An innovative flow tube design simplifies installation in limited straight runs and ensures no obstruction in the flow path. Holding an IP67 (NEMA 6) rating, the WIN Ultrasonic Flow Meter operates safely when temporarily submerged in water.

An LCD display version comes standard with Modbus RTU communications, providing an output of flowrate, volume total, run hours, alarms and diagnostics. The display is detachable for remote mount installation up to 5 ft. from the sensor. A built-in data logger enables easy data access vis Modbus. Units without a display come standard with analog and pulse outputs, 24V AC/DC power, one pulse and one analog output.

Cognitive AI software products for refining

Beyond Limits, an industrial and enterprise-grade AI software company built for the most demanding sectors, has made available its new LUMINAI Refinery Advisor. Developed in collaboration with bp, this cloud-based offering leverages Beyond Limits' Cognitive AI software to better adhere to commercial operating plans, capture and operationalize expert knowledge, reduce production material costs, maximize operational efficiencies, accelerate time to market, and reduce waste in critical downstream oil and gas sectors.

Beyond Limits' LUMINAI Refinery Advisor allows plant operators to meet refinery operating plans more consistently and adapt to ever-changing constraints by providing real-time guidance and specific instructions based on expert engineering, operator knowledge and process conditions. The no-code solution provides an easily integrated and affordable application to optimize plant-wide process functions in a unified, digital space, improving alignment between planning, engineering and operations to ensure all teams have the specific directions they need to keep the refinery running at enhanced efficiency.

The company's industrial-grade AI solutions provide plant operators and R&D organizations with explainable real-time recommendations to optimize operations and improve decision-making speed and accuracy across a broader decision space. These AI-powered extensions allow companies to maximize profits and gain a competitive advantage.

Global Standardized Plan 54 designed to fit a wide range of challenging, dual-pressurized seal applications

John Crane, a global leader in rotating equipment solutions, supplying engineered technologies and services to process industries, has launched its Global Standardized Plan 54 (GS 54), an API Plan 54 support system designed to fit a wide range of challenging, dual-pressurized seal applications.

The new GS 54 uses best-practice design to provide clean, cooled and filtered barrier fluid, optimal seal performance and pump up-time, and supports API Plan 54 standards for leakage prevention. In tough and technically challenging processes where reliability is a prerequisite, the API Plan 54 support system provides a standard solution, removing avoidable complexity from the design and selection process. Applicable for challenging applications in the oil and gas, chemical, pharmaceutical and other high-purity industries, the support system's pre-engineered design offers high reliability and expedited customer delivery.

Designed with a focus on operational efficiency and reliability, features of the new booster include:
- Streamlined design to minimize footprint and obstruction
- System reservoir that provides a nominal volume of 30 gal (114 l) of barrier fluid
- Filter housing with 10-micron filter elements
- Shell-and-tube, water-cooled designed heat exchanger. **HP**

When to consider liquid-ring compressors

Liquid-ring compressors (**FIG. 1**) use the centrifugal whirling of a sealing liquid to create a series of piston-like water columns to trap gas or vapor between the impeller cells of a rotor installed eccentric to its casing. During operation, the trapped space occupied by the gas or vapor in each impeller cell progressively decreases around the rotor. By sealing liquid being flung outward from the center of the rotation, the volume of the gas is progressively reduced. Therefore, the pressure increases, and the gas leaves the discharge port at some elevated pressure.

As the gas discharges, entrained vaporized liquid (originating from the sealing liquid) is discharged along with the gas. However, this loss of sealing liquid is continuously replaced by a fresh flow of sealing liquid.

The overwhelming majority of these machines are in the range of 15 kW–150 kW, although larger machines exist. Their traditional application range is detailed in **FIG. 2.**

The heat from compression increases the sealing liquid temperature approximately 10°F to 15°F during its passage from entry to discharge. Water is generally used as the sealing liquid; however, some processes cannot tolerate water. In those cases, substitute liquids can be used.

Several process applications for liquid-ring compressors include:
- Flare gas recovery
- Flare gas compression
- Vinyl chloride monomer recovery
- Vent gas recovery
- Vapor recovery
- Hydrogen compression
- Oxygen/ozone compression
- Wastewater treatment methane compression
- Carbon dioxide compression
- Waste gas compression, power plants. **HP**

FIG. 1. Schematic illustrating operating principle.
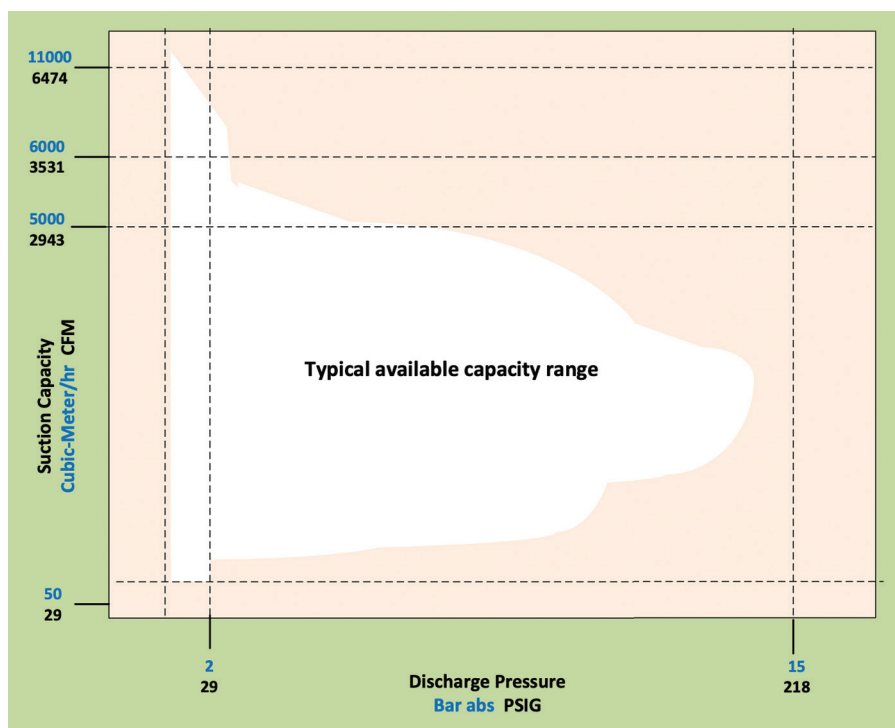
FIG. 2. Typical operating range for liquid-ring compressors.

REFERENCE
[1] Elliott, H. G. and H. Bloch, *Compressor Technology Advances: Beyond 2020,* DeGruyter, Berlin, Germany, 2021.

HEINZ P. BLOCH resides in Montgomery, Texas. His professional career commenced in 1962 and included long-term assignments as Exxon Chemical's Regional Machinery Specialist for the U.S. He has authored or co-written more than 800 publications, among them 24 comprehensive books on practical machinery management, failure analysis, failure avoidance, compressors, steam turbines, pumps and the recently released *Compressor Technology Advances,* from which this excerpt was condensed.

Integrity operating windows management

Operations in the oil and gas, petrochemical and refining industries pose a higher risk when failures occur in identifying ongoing damage mechanisms within static equipment. Often, inspections use a risk-based approach that enables the determination of fit-for-purpose inspection frequencies, methods and coverage to suit the allotted budget window. Therefore, it has become even more important to maintain a closer view of the process conditions within the static equipment.

Data being fed to the risk-based inspection management software should always remain updated and dynamic to provide the best output to ensure asset integrity. The inability to monitor process conditions—a vital component in determining the lifecycle of any asset—can lead to improper inspection frequencies, methods and coverage that endanger overall asset management. That is where the management of integrity operating windows (IOWs), shown in **FIG. 1,** comes into focus.

In some processes, a range of changes is acceptable and may not cause any adverse effects on asset integrity; however, cases exist where the slightest change in process conditions can negatively affect the health of the asset, leading to unnoticed damage and potential health, safety and environmental (HSE) impact. Improper control over temperature in a stream where sulfidation (a form of high-temperature hot corrosion) is expected to occur can lead to metallurgical damages; if not inspected in a timely manner, this carries the potential for a loss of process containment.

Temperatures of furnaces and heaters exceeding specific temperature limits can lead to hot spots and possibly internal refractory damage. Operating acid lines with concentrations different than those suitable for the metallurgy under operation can adversely affect the piping system. If an inspection function is not
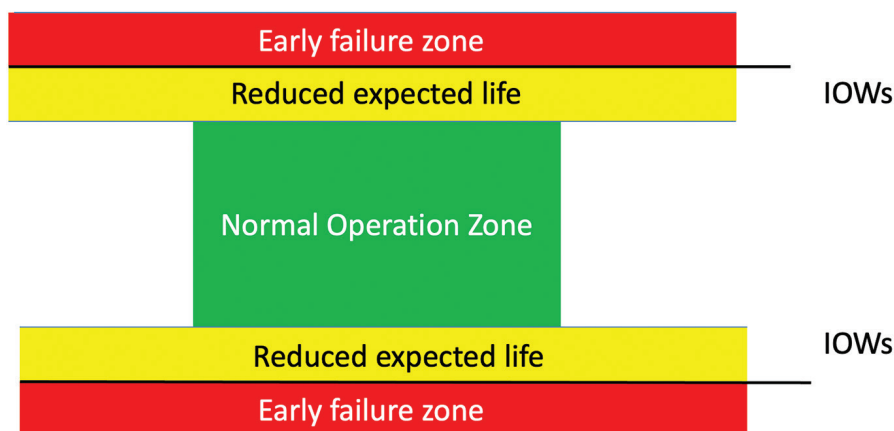
FIG. 1. A simplified representation of integrity operating windows (IOWs).

informed about these changes, an early detection of the extent of damage and appropriate action would be delayed.

Every critical piece of equipment and piping system within a facility should have a defined set of IOWs that must be monitored regularly. Any breaches should not only be recorded for the slightest changes, but must be shared with the responsible asset integrity function to review and obtain inputs from other functions, such as inspection and reliability. Defining IOWs requires the formation of a team comprising operations, process and asset integrity personnel to perform an asset level study of normal operating parameters and then establish the limits of continuous safe operations beyond them. This should be completed for all static equipment and then documented so any breach of defined limits can be identified immediately for further reporting and analysis.

A system-dependent monitoring of IOWs should be required in any hydrocarbon operating facility to reduce risk and ensure asset integrity. The minimum expectations from such a system include determining the types of breaches, their magnitude and the time duration. An initial review by the plant operations team should obtain this data daily so that vali-

dation can be achieved—this validation will ensure the recording of breaches and their authenticity. It is quite possible that the system may detect breaches resulting from a faulty instrument or some planned or breakdown maintenance that is in progress and causing communication of such irregularities.

After achieving validation from the plant operations representative, this data should be shared with the teams responsible to ensure asset integrity. The data should be consistently analyzed so that the impact of exceeding the IOWs can be evaluated. A single incident of exceeding an IOW may not necessitate the revision of an existing plan; however, multiple instances (if not recorded and analyzed properly) may cause long-term damage. This is when response time matters. For each defined IOW, the appropriate action for operations and the response time should be predefined. This must be completed while developing each IOW work process.

Note: The reporting and validation of initial breaches is the responsibility of the plant operations team, but further review, trend-making and analysis should be done by the relevant functions responsible for ensuring asset integrity. Some

sites have assigned the responsibility of reviewing all such breaches to a site risk-based inspection (RBI) engineer. Most site RBI engineers are equipped with software enabling them to quantitatively enter the data and obtain recommended inspection coverages and frequencies that will eventually support them in identifying any credible damage mechanism. In all cases, data should be recorded and kept for further analysis should further breaches occur on the same system.

To manage IOWs, the plant operations team is expected to address and manage breaches in parameters. Breaches should be justified with an early action to deter recurrence. In the absence of a short-term action to control or prevent repeated breaches, data should be shared with process teams to initiate corrective action(s) with studies or by implementing change(s) in plant operations. This ensures that breaches do not cause long-term effects on asset integrity.

Takeaway. While each change can bring potential improvement, it can also pose an additional risk to existing facilities—this risk should be analyzed by a multidisciplinary team. During this risk analysis, IOWs must be examined for any required revision, which should be communicated to the respective sections. Teams responsible for studying, reviewing and implementing plant changes must ensure that every change approved for implementation should include a review of existing IOWs.

While the operations team is collecting, maintaining and communicating the data, the inspection and other relevant field teams performing necessary preventive checks on equipment and systems should be equipped with the applicable integrity operating windows exceedance reports to identify exceeded parameters that indicate damage. This check is in addition to regular communication of data through operations to the relevant teams, and should avoid any miscommunications.

IOWs should be established while considering and maintaining safe operating windows limits, as well. Safe operating windows fall within the normal zone, as shown in **FIG. 1.** Any exceedance of those limits should also be recorded, reported, shared and analyzed. This helps to alert the responsible teams ahead of an actual breach in IOWs so that proactive actions may then be taken to avoid affecting asset integrity.

Periodic audits for the management of IOWs—if in place—can help ensure asset integrity. If defined IOWs are correctly followed, maintained and communicated to the relevant field inspection and reliability teams, long-term asset integrity becomes simpler and damages can be identified earlier, requiring fewer resources to maintain safe and profitable operations. **HP**

ASHFAQ ANWER is an Asset Integrity Engineer with 17 yr of experience in the field of inspection for static equipment in the oil and gas, petrochemical and fertilizer industries. He has actively participated in inspection data analysis, inspection planning and management, fitness for service and other field activities related to static equipment.

A. RASTOGI
Fluor Daniel India Pvt. Ltd., New Delhi, India

Gas flaring: Necessary, or a waste of resources and a source of greenhouse gases?

Flaring is the controlled burning of hydrocarbons at oil refineries, gas processing plants and petrochemical plants. It is required for plant safety by burning all reliefs of the plant in emergency condition—this is called "safety flaring." However, many upstream and downstream facilities use flaring to destroy unwanted gases produced along with the main product—such flaring is called "routine flaring." Typical examples are oil refineries and petrochemical plants (FIG. 1), gas processing plants and crude oil production facilities. Both of these methods of flaring involve the waste of natural resources and produce harmful emissions to the environment.

Routine flaring involves the burning of all unwanted and uneconomical gases that cannot be sold to local markets or exported to wider markets. This flaring generates maximum pollutants by wastefully burning valuable natural resources and emitting large amounts of carbon dioxide (CO_2), methane (CH_4), black soot and other greenhouse gases (GHGs) that significantly impact the environment. It is estimated that if even half of the gas burned in routine flaring is used for power generation, it could provide approximately 400 BkWh (billion kilowatt hours) of electricity.

Zero flaring: An initiative from the World Bank. As per a World Bank report:

"Thousands of gas flares at oil production sites worldwide burned approximately 142 Bm^3 of gas in 2020. Assuming a 'typical' associated gas composition—a flare combustion efficiency of 98% and a global warming potential for CH_4 of 25—each cubic meter of associated gas flared results in about 2.8 kg of CO_2 equivalent (CO_2e) emissions, resulting in more than 400 MMtpy of

FIG. 1. Routine flaring in refineries and petrochemical plants involves the burning of all unwanted and uneconomical gases that cannot be sold to local markets or exported to wider markets.

CO_2e emissions. The CH_4 emissions resulting from the inefficiency of flare combustion contribute significantly to global warming. This is particularly true in the short to medium term as, according to the Intergovernmental Panel on Climate Change, CH_4 is > 80 times more powerful than CO_2 as a warming gas over a 20-yr period. On this basis, the annual CO_2e emissions are increased by nearly 100 MMt."

To mitigate this global pollution issue, the World Bank instituted an initiative in 2015 to end routine flaring by 2030.

Achieving zero flaring. A few technical solutions to reduce the extent of gases to be flared are listed here. Some of them are already utilized by oil, gas and petrochemical companies with the aim of zero flaring by 2030:

- Flare gas recovery system (FGRS)—This is one of the cleanest solutions to minimize or eliminate gas flaring in refineries.

It is a specialized compression system to recover gases that would otherwise be burned during the flaring process. This system utilizes a liquid ring compressor and three-phase separator to capture gases from the flare header. The recovered gases can be reused within the facility's fuel gas system. An example of an FGRS is shown in FIG. 2.

- On-demand flaring—This methodology utilizes a high-pressure ballistic ignition system to ignite the flame at the flare tip on an on-demand basis when flammable gas is present. Emissions are minimized by eliminating the need for continuous flaring operation, as it involves burning a predetermined minimum amount of fuel gas. This ignition system is used where flare gas is recovered and recycled, as with an FGRS.
- Gas-powered electricity generation plants—These facilities utilize a
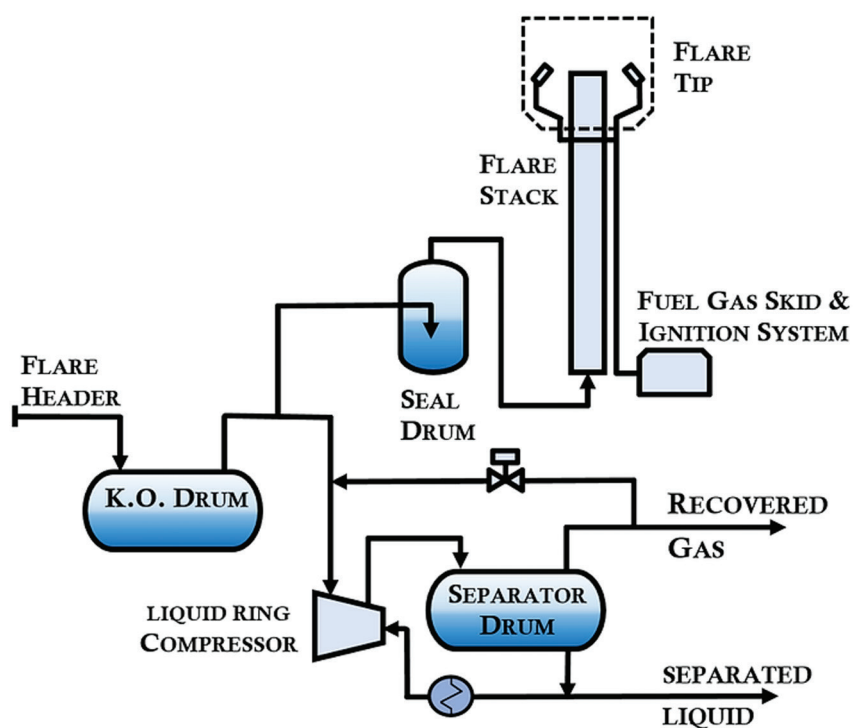
FIG. 2. A typical flare gas recovery system.

gas-turbine generator running on the field gas to generate electricity. Electricity generated can be stored and transmitted to other facilities to meet their daily operational needs, or it can be sold to other users and to generate revenue. The amount of gas to be flared is reduced, as electricity is generated by using site-produced gas that otherwise would have been flared, resulting in GHG emissions reductions.

- Gas-powered e-frac fleets— This system utilizes modular gas turbine generators that run on site-produced gas rather than diesel used in a conventional system. Electricity generated is used to power pressure pumps and other electrical items onsite.
- Gas-powered onsite equipment— Some companies manufacture heavy machines or equipment that utilize gas as fuel. They also offer the service to modify the existing machineries and heavy vehicles to run on gas against conventional fuel diesel. Utilizing the site-produced gas in these machines can save fuel costs and reduce gas flaring.
- Small-scale gas-to-liquid conversion plants—This

alternative can be economically viable if unwanted gas is produced at mass scale by a plant or by many gas-producing facilities that are in close vicinity. Unwanted gas produced in all facilities can be stored and cooled at a common "gas-to-liquid conversion plant" and then transported to other local and international market for sale.

Takeaway. While these strategies will not completely eliminate gas flaring, they provide viable paths to reduce the extent of gases to be flared and means to utilize them more effectively. Companies should utilize flaring strictly for the safety of plants in upset or emergency conditions. Routine flaring should be diminished progressively to zero flaring by applying strict regulations. Government and companies should collaborate and support each other for effective monetization of such hydrocarbon resources and unwanted gases to eliminate routine flaring. HP

ANUJ RASTOGI is a Mechanical Engineer with Fluor Daniel India Private Ltd. New Delhi and has been with the company for 11 yr. He has more than 16 yr of experience in packaged equipment and holds a BE degree in mechanical engineering.

HP Digital

O. RODRIGUEZ
Lloyd's Register, Houston, Texas

Layering up to avoid the cold realities of asset performance silos

Operators may use a variety of tools and techniques—hardware solutions, software packages and sensor technologies—to monitor and manage different aspects of plant performance. However, are they compromising their pursuit of net-zero goals or asset performance if they are not integrating that effort into their overall management of individual assets?

Everyone has an angle when it comes to managing critical pieces of infrastructure within a plant. The integrity professional is managing the asset from one distinctive perspective, while it is likely that others will have a specialist focus on areas such as safety, reliability, productivity and environmental impact.

However, if they are managing their remit within a siloed structure with no common platform where they can quickly share data to expedite decision-making, then is not each discipline operating under a degree of avoidable constraint? In turn, does not that mean the asset is not being run at optimum efficiency?

Every element of a system is part of an interconnected process and implementation of discrete maintenance and repair regimes since each of those in isolation would never prove successful. It makes perfect sense. If you go to the doctor with an ailment, they will check the bigger picture (e.g., medical history, other health issues, allergies) before prescribing a remedy that not only targets the problem but also factors in your overall wellbeing.

Those same principles should apply if one narrows the focus down to an individual piece of equipment. Each discipline with a stake in its performance and wellbeing should not be going about their work in isolation either. With access to all asset data, they should be equipped to make fully informed decisions not only in the context of their specialist layer, but also in the best interests of the asset, and the business as a whole.

This topic has the potential to help deliver on global sustainability goals in the wake of COP26: an asset's optimum working performance will embrace its energy consumption and emissions levels.

As mentioned earlier, the integrity expert has a particular focus, but any integrity failure has potential consequences in a much wider context—across areas ranging from safety and productivity to environmental. The expert's counterparts in those disciplines have their own specific responsibilities and indicators that constitute good performance. They are all using specialist technologies and practices to deliver on their remit, but not necessarily as part of a complete plant strategy. They are deploying the right tools and making the right decisions within their own scope of duty, but could they be impacting the other areas of asset performance, as well?

This scenario presents the possibility of wider challenges of someone, at some point, missing something of operational or commercial significance. It is also why companies are exploring technology-led concepts that can serve to underpin a new approach, allowing businesses to focus inspection and maintenance where it counts and address risk beyond that of only what its known. This can be referred to as a layered model, fully aligning the various disciplines and offering a shared, centralized view of all areas of asset activity.

Creating a centralized view not tied to certain technologies or vendors that anyone in an organization can access at any time and anywhere would eliminate the shortcomings associated with this form of tunnel vision. This approach offers every stakeholder full and live visibility of not only their own data, but also the changes and decisions others are making. For example, an instant oversight of the impact (positive or negative) that pro-duction variations have on energy use or emissions management can only support optimum performance. Having full oversight enables people to make smart use of data, to speak the same language as their assets and unlock their knowledge.

More broadly, it would better inform strategic business decisions on asset maintenance or replacement. Managers could better understand where their best long-term options lie. For example, do the prospects of much enhanced energy consumption and emissions performance outweigh the cost of investing to replace aging assets? Or, is the current repair and maintenance program still the best route to take in efficiency terms?

The concept of interconnected layers would also facilitate the introduction of new elements, if necessary; this is significant given that many operators are looking to introduce new emissions and energy consumption-specific tools in pursuit of net-zero objectives, enabling them to drive better business value in both digital and energy transitions.

Bringing new technology onboard without integrating it into the full asset performance structure may undermine its power (e.g., "just another data point" is not contributing to the complete asset strategy because not every factor is being considered). Certainly, the new application might help monitor and control emissions, for example, but not the production regime, energy use or integrity program, all of which are part of the bigger net-zero picture.

The digital transformation journey has delivered numerous industry gains, but it is the author's experience that people are, to a large extent, still working in isolation, albeit with more advanced solutions at their disposal. There is an opportunity to harness the power of digital technologies to fully connect asset layers with their corresponding actors. **HP**

Achieving the right installation torque with a virtual calculation

Determining the required installation torque for a tight flange system is a daily challenge for industrial valve manufacturers and plant operators. All components within the flange system have installation requirements and environmental regulations, which add further difficulty to any project. Collaboration between the manufacturers of individual components and the plant operator and holistic approaches are crucial to achieving operational efficiency.

The author's company has recognized this challenge and remains committed to complying with its customers' installation requirements. This article describes the challenges and workable solutions.

There are different approaches to selecting the required installation torque. In addition to manufacturer information for individual components, calculation standards such as DIN EN 1591-1 or the AD 2000 set of rules can calculate conventional flange systems analytically. According to the stated calculation standards, a conventional flange system (**FIG. 1**) is defined as a flange inlet (Flange I), a flange outlet (Flange O), gasket and connecting elements (e.g., bolts). In practice, additional components expand the flange system. These can include a pressure protection mechanism, such as a rupture disc. A rupture disc is usually installed with a mounting unit (Holder), consisting of a holder inlet (Holder I) and holder outlet (Holder O). A second gasket (Gasket I) is also required. In this case, four additional components must be considered at once.

Conventional/stated calculation standards become invalid for these expanded flange systems, as the equations underlying these standards do not consider any additional components. Metallic sealing surface contact has also been excluded, as have systems with stiffness that fluctuates greatly over the width of the gasket. Both of these cases are valid with the expanded flange system. Due to the Technical Instructions on Air Quality Control amendment—the set of regulations to decrease the emissions of air pollutants—metallic sealing surface contact will be a requirement.

The functionality of the rupture disc primarily determines the requirements of the flange connection design. For the connection between the holder and rupture disc, the contact pressure must be sufficient to hold the rupture disc and stop it from being pulled out. This ensures the functionality of the rupture disc. The system must also be tight so none of the medium can leak out. Conversely, the contact pressure must not be so high that it leads to the destruction of the rupture disc material. These factors/prerequisites result in a range for the permitted surface pressure in this connection, which must be set via the installation torque.

A gasket manufacturer must focus on the sealing point between the flange and gasket. Every gasket manufacturer specifies a minimum and a maximum sealing surface pressure. This results in a range for the permitted surface pressure at the sealing point, which must also be set via the installation torque. Two different requirements for the necessary installation torque are produced.

In most applications, rupture discs are manufactured from stainless steel, and gaskets are often made from non-metallic materials. Different materials with different material properties experience a required surface pressure. However, to adjust this surface pressure, only one shared installation torque is set for both cases, which creates an optimization problem.

The solution lies in the geometric alteration of the contact surfaces between the rupture disc and holder, and therefore falls to the rupture disc manufacturer.
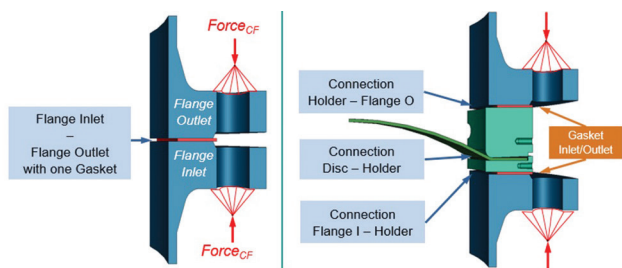
FIG. 1. Comparison of conventional flange system (left) and flange system with rupture disc and holder (right).

FIG. 2. Flange system with rupture disc and holder.

Due to the metallic sealing in this connection, the required surface pressures in this range are generally higher than the permitted gasket tension. Excessive tension is created in the sealing surface between the rupture disc and holder with targeted design measures. This allows the optimum surface pressure to be set in the sealing surface without the surface pressure in the gaskets increasing to an unacceptable extent.

In addition, when calculating the installation torque, it must be determined whether the components of the flange system are overloaded in the respective constellation. Installing a rupture disc and a holder in a flange system causes the mechanical properties of the overall system to change. This results in greater flange rotation and, consequently, a higher tension level in the flange.

The rupture disc and gaskets must be replaced if an overloading of the process triggers the rupture disc. However, the flange and holder are usually used multiple times. The flange and holder must retain function-securing geometry after repeated dismantling and installation. Therefore, permanent plastic deformations in the loading conditions installation, testing and operation are not permitted. A strength test must be carried out for the configuration, ensuring a sufficient distance from the material's elasticity limit for all loading conditions.

All required calculations for configuring the installation torque cannot be performed with sufficient precision using analytical calculation principles. The author's company uses virtual engineering with the finite element method to consider the complexity and the ever-greater challenges of the installation torque configuration. This makes it possible to depict the flange system, including all components, as a digital twin and simulate its mechanical behavior before manufacture and commissioning. With this digital twin, the mutual influences of all components are considered in advance.

The simulation results and empirical knowledge are then used to optimize the individual components until all are in accordance with their installation requirements; then, the parts are manufactured and installed.

The author's company is one of the first rupture disc manufacturers to offer such calculation services. Involving an engineering firm or similar service provider for plant operators is no longer necessary. The customer receives a complete solution with added value—reliable simulation results calculated by specialists, which then flow into the customer-specific manufacture of the rupture discs. **HP**

CARINA WEGENER has worked for more than 10 yr in process safety, namely pressure relief, helping to protect processes in various industries, including chemical, pharmaceutical, and oil and gas. Ms. Wegener has studied mechanical engineering, focusing on numerical calculation methods, especially finite element methods, computational fluid dynamics and fluid-structure interaction. Since joining REMBE GmbH Safety + Control in 2012, she has been responsible for all calculation tasks as the Head of REMBE Computer Aided Engineering. Operational safety is a mission to which REMBE has dedicated itself for almost 50 yr through consulting, engineering, products and service.

J. S. KIM, J. LOPEZ, P. LI and **R. HAINES**,
Covestro LLC, Baytown, Texas

Use a simple vapor equation for sizing two-phase pressure relief valves

Pressure relief valves (PRVs) protect process equipment from the hazards of excessive over-pressure. A simple liquid equation is widely used as a standard method for sizing incompressible fluids. A simple vapor equation is also widely used when sizing for ideal vapors. For non-ideal vapors, an isentropic expansion coefficient typically evaluated at the relief conditions is used. Alternatively, API 520 Part 1 suggests averaging the isentropic expansion coefficients calculated at the upstream pressure and the pressure in the throat of the valve nozzle.[1] Using the average isentropic expansion coefficient with a simple vapor equation can result in undersized PRVs due to the assumption of an ideal vapor in the simple vapor equation.

This article proposes an alternative solution for a constant isentropic expansion coefficient. For two-phases, the Leung Omega method—often referred to as a two-point method—is widely used. In addition, the homogeneous direct integration (HDI) method requires significant computational efforts but is considered the most rigorous and accurate method.

No standardized PRV specification sheet is in use for non-ideal vapors and two-phases because no simple unified methodology exists for compressible fluids (non-ideal vapors and two-phases). For two-phases, the mass flux and the basis for the calculations are specified in accordance with the API 520 Part 1, Annex D.[1] However, no guidelines are available for non-ideal vapors. This article introduces a new method for sizing any compressible fluid PRV using a simple vapor equation. The proposed approach generates rigorous results validated against the existing rigorous HDI method. This method is applicable to vapors and two-phases, including slightly subcooled liquids if the three-point data is available from isentropic flash calculations. In addition, it significantly reduces the computational efforts necessary for the numerical integration method. The new method using a simple vapor equation will improve the communication between the valve manufacturer and the relief system engineer for non-ideal vapors and two-phases, including slightly subcooled liquids.

A simple vapor equation. For vapors, the critical flow through a PRV is represented by Eq. 1, which assumes the vapor behaves ideally when a compressible vapor expands across a PRV nozzle. The simple vapor equation provides satisfactory sizing results over a wide range of applications. However, to ensure the appropriate sizing results, the vapor compressibility factor should be no less than approximately 0.8 or greater than approximately 1.1.[1] Recently, API 520 Part 1 noted that the va-

lidity of Eq. 1 may diminish when the reduced volume of the fluid is less than 2 at the valve inlet pressure:

$$A = \frac{W}{C \times K_d \times P_0 \times K_b \times K_c} \times \sqrt{\frac{T \times Z}{M}} \qquad (1)$$

where,
A = the required discharge area of the device, in.^{2}
W = the required flow through the device, lb/hr
C = a function of the ratio of the ideal gas-specific heats at the inlet relieving temperature
K_d = the coefficient of discharge
P_0 = the inlet relieving pressure, psia
K_b = the capacity correction factor due to backpressure
K_c = the combination correction factor for installations with a rupture disk upstream of PRV
T = the relieving temperature of the inlet vapor, °R
Z = the compressibility factor at inlet relieving conditions
M = the molecular weight of the vapor at inlet relieving conditions.

For real gases, API 520 Part 1 recommends using an isentropic expansion coefficient evaluated at the relief conditions. **Note**: A real gas-specific heat ratio does not provide a good representation of the isentropic expansion coefficient.[1] Alternatively, an average isentropic expansion coefficient between the upstream pressure and the pressure in the throat of the nozzle is recommended.[1] However, the isentropic expansion coefficient is not used in the API 520 PRV specification sheets.

Numerical integration method. API 520 Part 1 contains the most rigorous method for calculating the mass flux for PRVs. The method applicable to all phases is known as the HDI method, evaluated numerically by direct summation over small pressure intervals using an appropriate technique (e.g., Simpson's method).[2] The HDI method can be used for any homogeneous fluid provided fluid property data at constant entropy is available. The critical mass flux can be estimated by integrating (as shown in Eq. 2) until the mass flux reaches a maximum mass flux. If the fluid is subcritical, the subcritical mass flux can be estimated by integrating until the actual backpressure on the nozzle is reached, as shown in Eq. 3:

$$G_c{}^2 = \left[\frac{-2 \times \int_{P_0}^{p} v \times dp}{v_t^2} \right]_{max} \qquad (2)$$

$$G^2 = \left[\frac{-2 \times \int_{p_0}^{p} v \times dp}{v_t^2} \right] \qquad (3)$$

where,

G = the mass flux through the nozzle, lb/sec-ft^2
P = the pressure of the fluid, psia
v = the specific volume of the fluid, ft^3/lb
t = the throat of the nozzle.

The calculation precision associated with the HDI method is determined by the size of the pressure intervals, with smaller pressure intervals providing better results. Some cases may require many data sets for acceptable sizing results. The HDI method requires intensive computational efforts; however, the numerical integral result can also be obtained accurately and quickly if evaluated analytically with pressure-specific volume (P-v) models or employed P-v models.

Reduced P-v models. The equation of state (EOS) typically involves four variables. Simpson presented a total of six reduced P-v models involving only two variables.[2] The reduced P-v model is obtained by a few constant entropy flash calculations, for which the specific volume reflects changes in the compressibility factor, pressure and temperature. The reduced P-v model based on the homogeneous equilibrium model (HEM) well represents the pressure expansion processes in the PRV.

This article evaluates two out of the six P-v models and a conventional model in a simple vapor equation to select the best P-v model for isentropic expansion flow. Eq. 4 is good for ideal vapors, but not suitable for flashing liquids. Eq. 5, the Omega method, is good for flashing liquids, but not so suitable for vapors. The two-point Omega method is most widely used for sizing two-phases. Eq. 6 is a combination of Eqs. 4 and 5, so it should be suitable for both vapors and two-phases. Simpson noted that Eq. 6 is the only reduced P-v model that gave consistently outstanding fits of the data.

$$v = v_0 \times \left(\frac{p_0}{p} \right)^{\frac{1}{n}} \qquad (4)$$

$$\frac{v}{v_0} - 1 = \omega \times \left[\frac{P_0}{P} - 1 \right] \qquad (5)$$

$$\frac{v}{v_0} - 1 = \alpha \times \left[\left(\frac{P_0}{P} \right)^{\beta} - 1 \right] \qquad (6)$$

where,

n, ω, α, β = the P-v model constants.

For subcooled liquids, the initial pressure (P_0) shall be at the saturated pressure, ignoring subcooled conditions. Eq. 5, a two-point method, uses two data sets at initial pressure and typically 90% of the initial pressure. Eq. 6, a three-point method, uses three data sets at initial pressure, a middle pressure and 50% of the initial pressure (not greater than the critical pressure).

Upgrading the numerical integration method. A new approach to make the rigorous HDI method more convenient is discussed here. To reduce significant computational efforts,

Kim, et al. proposed Eqs. 7–9, which are based on Eq. 6.[3] A compressible fluid reaches a condition of maximum flow when the velocity at the nozzle reaches the speed of sound. The isentropic maximum mass flux for Eq. 2 is given by Eq. 7. Eqs. 7 and 8 are in an identical derivative form.

An identical and simple equation form for both critical mass flux and subcritical mass flux is preferred to simplify the calculation method. This allows for an analytical solution for mass flux calculations to make the numerical integration easier. Eqs. 2 and 3 are in an identical integral form rather than derivative. The integral form does not allow the analytical solution for mass flux calculations. Eq. 9 is derived from Eqs. 3 and 8, and has been upgraded here to handle slightly subcooled liquids. Eq. 9 simplifies the numerical integration and provides rigorous results. Both Eqs. 7 and 8 provide the results of P-v equation-based integration. This new method is applicable to compressible fluids (vapors and two-phases, including slightly subcooled liquids):

$$G_c = \sqrt{\left(\frac{-\partial P}{\partial v} \right)_s} = 68.07 \times \sqrt{\frac{p_{ec-max}^{\beta+1}}{\alpha \times \beta \times p_0^{\beta} \times v_0}} \qquad (7)$$

$$G = 68.07 \times \sqrt{\frac{p_{ec}^{\beta+1}}{\alpha \times \beta \times p_0^{\beta} \times v_0}} \qquad (8)$$

$$P_{ec} = \left[-2 \times \alpha \times \beta \times P_0^{\beta} \times \left[\alpha \times \left(\frac{p_0}{p} \right)^{\beta} - \alpha + 1 \right]^{-2} \times \left((p_0 - p_{sc}) + \frac{\alpha \times p_0^{\beta}}{1-\beta} \times \left(p^{1-\beta} - p_0^{1-\beta} \right) + (1-\alpha) \times (p - p_0) \right) \right]^{\frac{1}{\beta+1}} \qquad (9)$$

where,

$ec–max$ = the critical pressure (P_c), maximum equivalent pressure
ec = the equivalent critical pressure at the calculated mass flux
sc = the subcooled liquid.

Eq. 10 has been developed to determine if a subcooled liquid is compressible or incompressible. Eq. 10 is similar to the API 520 Part 1 Equation (C.32), but easier to follow. If the subcooled pressure is greater than the calculated P_{ec-max}, the fluid is incompressible; the fluid is not considered a slightly subcooled liquid because there is no change in density during the expansion process. In this case, the fluid should be sized using a liquid equation and the fluid chokes at the saturated pressure. If the subcooled pressure is not greater than the calculated P_{ec-max}, the fluid is compressible. In this case, the fluid should be sized as a two-phase fluid:

$$P_{sc-max} = p_0 + \frac{p_0}{2 \times \alpha \times \beta} \qquad (10)$$

For subcritical mass flux, use Eqs. 8 and 9. The P_{ec} in Eq. 8 is calculated using Eq. 9 at P (typically at backpressure) without iteration. For critical mass flux, use Eqs. 7 and 9. The P_{ec-max} in Eq. 7 is also calculated using Eq. 9 at P (initially at backpressure) with iteration until P_{ec} is equal to P. The calculated P_{ec} replaces P in the next trial. The maximum P_{ec} value (P_{ec-max}) is obtained when P_{ec} is equal to P.

Critical pressure can also be obtained from the following approximations (Eqs. 11 and 12) developed based on the Omega method.

$$p_c = n_c^{\beta^{-0.727144}} \times p_0 + \left(1 - n_c^{\beta^{-0.727144}}\right) \times p_0 \times \qquad (11)$$

$$\left(1 - \cfrac{1 - 2 \times \alpha \times \beta + \cfrac{p_0}{p_{sc}} \times (1 + 2 \times \alpha \times \beta) \times \left[1 - \sqrt{1 - \cfrac{p_{sc}}{p_0} \times \left(\cfrac{2 \times \alpha \times \beta - 1}{2 \times \alpha \times \beta}\right)}\right]}{1 - 2 \times \alpha \times \beta + (1 + 2 \times \alpha \times \beta) \times \left[1 - \sqrt{\cfrac{1}{2 \times \alpha \times \beta}}\right]} \right)$$

$$n_c = \left[1 + \left(1.0446 - 0.0093431 \times \alpha^{0.5}\right) \times \alpha^{-0.56261}\right]^{\left(-0.70356 + 0.014685 \times \ln \alpha\right)} \qquad (12)$$

All values of nozzle pressure and P_{ec}, along with mass flux, are plotted in **FIG. 1** to tangibly illustrate the relations among nozzle pressure, P_{ec}, P_c and mass flux for API 520 Part 1, Example B.3.3. The green line shows the subcritical mass flux calculations for a known backpressure (at P, greater than the critical pressure). In subcritical flow, there is no iteration. Because Eq.9 provides a result of equivalent critical pressure at the integrated mass flux from initial pressure to the backpressure, the calculated P_{ec} is directly used for the mass flux calculation. The calculated P_{ec} value shall be less than the known backpressure (P).

The red line shows the critical mass flux calculations for a known backpressure (at initial P, the backpressure is not greater than the critical pressure). In critical flow, the calculations are repeated until the calculated P_{ec} is equal to P. The mass flux and P_{ec} are maximized at the critical pressure (P_c). In the critical flow region, the maximum mass flux is taken at P_c because a further decrease in nozzle pressure does not affect the mass flux. The calculated P_{ec} also decreases as the P is further decreased below the critical pressure.

The HDI method uses only one blue graph. The upgraded integration method uses two graphs (blue graph and gold graph). The two graphs intersect at P_c. Using the two graphs significantly improves obtaining the critical pressure point quickly and accurately. Eq. 9 is used to calculate both the P_{ec} for subcritical mass flux and the P_{ec-max} (P_c) for critical mass flux. The upgraded integration method quickly determines if the flow is critical or subcritical. However, the HDI method should complement the Eq. 2 calculations to determine if the flow is critical or subcritical.

Isentropic expansion coefficient. Estimating the isentropic expansion coefficient during the expansion process is not simple because it is a function of pressure, volume and the ratio of real gas-specific heats, as shown in Eq. 13. It also varies throughout the expansion process, during which condensation may occur. The isentropic expansion coefficient for non-ideal vapors at the relief conditions is often used because it is readily available. A constant isentropic expansion coefficient can be easily back-calculated using Eq. 14 if the C value is known. Eq. 14 can be expressed in terms of two-parameters in a P-v model, critical pressure and initial relief pressure, as shown in Eq. 15. The C value can be calculated by other methods if the mass flux result is validated. Eq. 15 is recommended as the calculation method of choice as a result of the reduced P-v model evaluation.

$$n = -\frac{v}{P} \times \left(\frac{\partial p}{\partial v}\right)_T \times \frac{C_p}{C_v} \qquad (13)$$

$$C = 520 \times \sqrt{n \times \left(\frac{2}{n+1}\right)^{\frac{n+1}{n-1}}} \qquad (14)$$

$$C = 520 \times \sqrt{\frac{1}{\alpha \times \beta} \times \left(\frac{p_c}{p_0}\right)^{\beta+1}} \qquad (15)$$

Kim proposed Eqs. 15–17 at the API SCPRC Meeting.[4] Eq. 15 is derived from Eqs. 1 and 7.

The polynomial Eqs. 16 and 17 are used to estimate the constant isentropic expansion coefficient for two different C ranges. The C value is a result of the most rigorous calculation method. This may be an outstanding solution for constant isentropic expansion coefficients. This approach allows a simple vapor equation to be extended to any compressible fluid, including slightly subcooled liquids because Eq. 1 is based on Eq. 4. Therefore, a simple vapor equation can be applied to any compressible fluid, not only to ideal vapors.

However, n should be a constant isentropic expansion coefficient obtained from Eq. 14 to be compatible with a simple vapor equation. The constant isentropic expansion coefficient reflects the assumption of ideal vapor relationship in Eq. 14 since it is simplified for ideal vapors with the ratio of the ideal gas-specific heats; therefore, the constant isentropic expansion coefficient is different from the average isentropic expansion coefficient. For a non-ideal vapor, an average isentropic expansion coefficient can result in undersized PRVs. For an ideal vapor, an ideal gas-specific heat ratio at the relief inlet conditions can be used as a constant isentropic expansion coefficient.
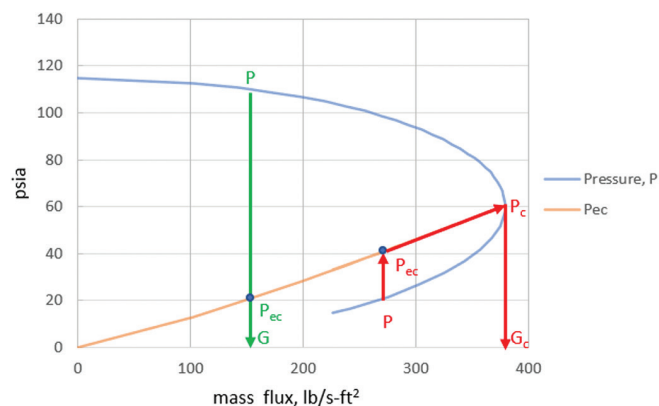

FIG. 1. Plot of nozzle pressure, P_{ec} and mass flux.

For $12 < C \leq 160$:

$n = 2.5343\text{E-}11 \times C^4 - 8.3347\text{E-}10 \times C^3 + 7.4632\text{E-}6 \times$
$\quad C^2 - 2.433\text{E-}6 \times C + 3.3047\text{E-}5$ (16)

For $C > 160$:

$n = 3.8459\text{E-}13 \times C^5 - 3.7986\text{E-}10 \times C^4 + 1.7953\text{E-}7 \times$
$\quad C^3 - 3.3542\text{E-}5 \times C^2 + 4.6767\text{E-}3 \times C - 2.1238\text{E-}1$ (17)

A new method for sizing compressible fluids. Sizing methods for significantly non-ideal vapors and two-phases—including slightly subcooled liquids—have not yet been standardized. However, many effective new methods have been developed over the last few decades. A new method for sizing compressible fluids using a simple vapor equation is proposed here to be a standard sizing method. All equations required for the new method are summarized here based on the standard steps in a work procedure (Eqs. 1, 6, 9, 10, 15, 16 and 17):

$$A = \frac{W}{C \times K_d \times P_0 \times K_b \times K_c} \times \sqrt{\frac{T \times Z}{M}} \quad (1)$$

$$\frac{v}{v_0} - 1 = \alpha \times \left[\left(\frac{P_0}{P} \right)^\beta - 1 \right] \quad (6)$$

$$P_{ec} = \left[\begin{array}{c} -2 \times \alpha \times \beta \times P_0^\beta \times \left[\alpha \times \left(\frac{p_0}{p} \right)^\beta - \alpha + 1 \right]^{-2} \times \\ \left((p_0 - p_{sc}) + \frac{\alpha \times p_0^\beta}{1-\beta} \times \left(p^{1-\beta} - p_0^{1-\beta} \right) + \right) \\ (1-\alpha) \times (p - p_0) \end{array} \right]^{\frac{1}{\beta+1}} \quad (9)$$

$$P_{sc-max} = p_0 + \frac{p_0}{2 \times \alpha \times \beta} \quad (10)$$

$$C = 520 \times \sqrt{\frac{1}{\alpha \times \beta} \times \left(\frac{p_c}{p_0} \right)^{\beta+1}} \quad (15)$$

For $12 < C \leq 160$:

$n = 2.5343\text{E-}11 \times C^4 - 8.3347\text{E-}10 \times C^3 + 7.4632\text{E-}6 \times$
$\quad C^2 - 2.433\text{E-}6 \times C + 3.3047\text{E-}5$ (16)

For $C > 160$:

$n = 3.8459\text{E-}13 \times C^5 - 3.7986\text{E-}10 \times C^4 + 1.7953\text{E-}7 \times$
$\quad C^3 - 3.3542\text{E-}5 \times C^2 + 4.6767\text{E-}3 \times C - 2.1238\text{E-}1$ (17)

Detailed standard steps in a work procedure. The following procedure can be used for sizing compressible fluids (including slightly subcooled liquids) using a simple vapor equation:

1. Calculate the two parameters, α and β, in Eq. 6 using three pressure-specific volume data:
   - Two flash calculations should be carried out at constant entropy
   - P_0 is at the PRV inlet
   - P_0 is at the saturated pressure for slightly subcooled liquids; do not include the subcooled region
   - P_2 is at the backpressure or 50% of P_0

(not greater than the critical pressure)
   - Higher P_2 would improve the calculation accuracy
   - P_1 is the average pressure of P_0 and P_2
   - Use a goal seek feature or a simple macro program.
2. Calculate the C value in Eq. 15:
   - For subcooled liquids, determine if the fluid is compressible or incompressible using Eq. 10; do not use this method for incompressible fluids
   - $P_{sc} = P_0$ if the fluid is not subcooled
   - Specify the P_{sc} if the fluid is slightly subcooled ($P_{sc} \leq P_{sc-max}$)
   - Calculate the P_c (P_{ec-max}) iteratively using Eq. 9 until the P_{ec} is equal to P; alternatively, Eq. 11 can be used to avoid iteration
   - For a subcritical flow with conventional valves, calculate the P_{ec} without iteration; use the P_{ec} instead of P_c (P_{ec-max}) and use $K_b = 1$, or calculate the P_c (P_{ec-max}) using Eq. 9 until the P_{ec} is equal to P and use $K_b = C_{at\,Pec}/C_{at\,Pc}$
   - For a subcritical flow with balanced valves, use the P_c (P_{ec-max}), and apply the backpressure correction factor (K_b) supplied by valve manufacturers
   - Use a goal seek feature or a simple macro program.
3. Calculate the n using Eqs. 16 and 17:
   - n (constant isentropic expansion coefficient) is specified on the PRV specification sheet.
4. As usual , size PRVs using Eq. 1:
   - Eq. 1 can size vapors and two-phases, including slightly subcooled liquids.

Validation of new method. This section is included to validate the proposed method by comparing it with the existing HDI and Omega methods using readily available example problems from API 520 Part 1—API 520 Part 1 does not cite an example for slightly subcooled liquids. Case 1 is from Simpson's Example 1.[2] **TABLE 1** shows comparisons with different sizing method results for the following four cases.

Case 1 : Simpson's Example 1
Fluid: Subcooled water at 66 psia and 298°F (148°C), saturated at 65 psi
HDI: Used 12-point data at 0.2 psi constant pressure intervals
Omega: Used two-point data at 65 psia (0.017433 ft³/lb) and 58.5 psia (0.074177 ft³/lb)
New: Used three-point data at 65 psia (0.017433 ft³/lb), 48 psia (0.205211 ft³/lb), and 32 psia (0.612741 ft³/lb)

Case 2: API 520 Part 1, Example Problem C.2.1.2
Fluid: Two-phase containing a significant amount of hydrogen at 2,168.5 psia and 80.3°F (27°C)
HDI: Used 14-point data at 86.7 psi constant pressure intervals
Omega: Used two-point data at 2,168.5 psia (5.18 lb/ft³) and 1,908.3 psia (4.77 lb/ft³)
New: Used three-point data at 2,168.5 psia (5.18 lb/ft³), 1,648.1 psia (4.28 lb/ft³) and 1,040.9 psia (2.96 lb/ft³)

Case 3: API 520 Part 1, Example Problem B.1.3
Fluid: Supercritical ethylene at 797.7 psia and 80.33°F (27°C)

HDI: Used 44-point data at 7.8 psi constant
    pressure intervals
Omega: Used two-point data at 797.7 psia (0.152 ft³/lb)
    and 719.4 psia (0.165 ft³/lb)
New: Used three-point data at 797.7 psia (0.152 ft³/lb),
    625.4 psia (0.185 ft³/lb) and 445.3 psia (0.248 ft³/lb)

Case 4: API 520 Part 1, Example Problem B.3.3
Fluid: Low-pressure air at 114.7 psia and 80.33°F (27°C)
HDI: Used 60-point data at 1 psi constant pressure intervals
Omega: Used two-point data at 114.7 psia (1.741 ft³/lb)
    and 103.7 psia (1.870 ft³/lb)
New: Used three-point data at 114.7 psia (1.741 ft³/lb),
    85.7 psia (2.141 ft³/lb) and 55.7 psia (2.907 ft³/lb)

A simple vapor equation satisfactorily sizes PRVs for all four cases. Red color values in **TABLE 1** represent the deviation in mass flux of > 2% and the deviation in critical pressure more than the constant pressure interval from the HDI method. The new method is in excellent agreement with the HDI method for all four cases. Blue color values in **TABLE 1** represent calculated C values and constant isentropic expansion coefficients for all four cases.

For Case 1 (slightly subcooled water), a commercial process simulator using the ASME steam property package provides the average isentropic expansion coefficient of 0.0729. The ASME steam specific volume data is in good agreement with the Case 1 data. The new method predicts the constant isentropic expansion coefficient of 0.0671. The average isentropic expansion coefficient with a simple vapor equation results in undersized PRVs. This fluid is compressible because P_{sc}, 66 psia ≤ calculated P_{sc-max}, 66.13 psia. The C value and constant isentropic expansion coefficient are much less than the other cases. The new method predicts better critical pressure than the HDI method because Simpson used specific volume data from the same P-v model and numerically integrated at a constant pressure interval of 0.2 psi.

For Case 2 (two-phase containing hydrogen), there is no composition information available to evaluate the constant isentropic expansion coefficient.

For Case 3 (supercritical ethylene), a commercial process simulator using the SRK (Soave-Redlich-Kwong) property package provides the average isentropic expansion coefficient of 1.2424. The SRK specific volume data agrees well with the Case 3 data. The new method predicts a constant isentropic expansion coefficient of 1.1863. The average isentropic expansion coefficient with a simple vapor equation results in slightly undersized PRVs.

For Case 4 (low-pressure air), a commercial process simulator using the SRK (Soave-Redlich-Kwong) property package gives the average isentropic expansion coefficient of 1.4203. The SRK specific volume data is in good agreement with the Case 4 data. The new method predicts the constant isentropic expansion coefficient of 1.4091. This is an acceptable difference in two isentropic expansion coefficients for air. This confirms that Eq. 14 is acceptable for ideal vapors or relatively constant isentropic expansion coefficients.

Takeaways. The above proposed method for sizing compressible fluid PRVs using a simple vapor equation is an out-

TABLE 1. Comparisons with different sizing method results

		HDI	Omega	New method
Case 1	Mass flux, lb/sec-ft²	751.76	748.25	751.87
	Critical pressure, psia	63.4	63.21	63.33
	ω or α/β	N/A	29.294583	21.279825 / 1.350907
	C/n	N/A	N/A	94.1 / 0.0671
Case 2	Mass flux, lb/sec-ft²	4,830.8	4,960.50	4,852.1
	Critical pressure, psia	1,214.4	1,183.8	1,227.1
	ω or α/β	N/A	0.630383	0.57015 / 1.143954
	C/n	N/A	N/A	349.7 / 1.3296
Case 3	Mass flux, lb/sec-ft²	3,201	3,199	3,184.8
	Critical pressure, psia	468.8	458.7	463.6
	ω or α/β	N/A	0.785794	0.733619 / 1.065312
	C/n	N/A	N/A	335.8 / 1.1863
Case 4	Mass flux, lb/sec-ft²	379.1	369.9	379.2
	Critical pressure, psia	60.7	64.2	60.4
	ω or α/β	N/A	0.698517	0.99802 / 0.710831
	C/n	N/A	N/A	356.8 / 1.4091

standing approach. The new method is based on the classical homogeneous equilibrium model chosen by API 520 Part 1 and AIChE/DIERS for emergency pressure relief system designs. Most pressure relief system engineers are familiar with the simple vapor equation.

For non-ideal vapors, an average isentropic expansion coefficient does not give the corresponding correct mass flux because Eq. 14 assumes ideal vapor. Generally, using the average isentropic expansion coefficient with a simple vapor equation can result in undersized PRVs. The new method provides the most practical solution for a constant isentropic expansion coefficient that is compatible with a simple vapor equation. For ideal vapors, an ideal gas-specific heat ratio at the relief inlet conditions can be used as a constant isentropic expansion coefficient. The proposed method allows a simple vapor equation to size compressible fluids (vapors and two-phases including slightly subcooled liquids) if the three-point data is available from isentropic flash calculations. This approach produces rigorous results validated against the existing rigorous HDI method, while significantly reducing computational efforts necessary for the numerical integration method.

Presently, there is no standardized PRV specification sheet for non-ideal vapors and two-phases. The proposed method using a simple vapor equation will improve the communication between the valve manufacturer and the relief system designer for non-ideal vapors and two-phases, including slightly subcooled liquids. The proposed method using a simple vapor equation is recommended as the standard sizing methodology for compressible fluids, including slightly subcooled liquids. **HP**

LITERATURE CITED
Complete literature cited available online at www.HydrocarbonProcessing.com.

The effects of highly corrosive fluids on valves and disasters that can be avoided

Some of the highly corrosive fluids in the oil and gas industry contain the following compounds: carbon dioxide (CO_2), hydrogen sulfide (H_2S), chlorides and moisture. These corrosive fluids have different chemical interaction mechanisms with the valve's body and demonstrate distinct behavioral tendencies when in contact with specific metallic materials. In crude oil, the concentration of H_2S is between 0.05% and 15%. Sulfide concentrations above 0.15% are sufficient to cause sulfidation corrosion in plain steels and low-alloy steels.

CO_2 becomes corrosive after its reaction with moisture, where it converts into carbonic acid. The kinetics of this reaction becomes favorable for the formation of carbonic acid (H_2CO_3) once partial pressure of CO_2 reaches 0.5 bar, which is often the case in the industry. H_2CO_3 is a weak acid, and it becomes aggressive in acidic regions when it attacks steel, creating iron carbonate. Lastly, the chloride ions and their concentration in the pipeline should be accurately determined since they have one of the fastest adsorption rates to the steel surface. Once they penetrate through the coating layer, their reaction with metal oxides is very rapid. As a result, chlorides often cause a localized breakdown, a corrosion mechanism commonly known as pitting.

Corrosion-resistant check valve materials. One of the optimal anticorrosive materials for a valve's body (such as the industrial check valve shown in **FIG. 1**) is stainless steel 316, due to the 2%–3% molybdenum content that improves 316's corrosion resistance. Unreactive, non-metallic materials are suitable for other wetted components, such as valve seals, seats or linings. Piping systems with high corrosion rates due to the availabili-

ty of chloride traces in the fluid use valves made from alloys with higher pitting resistance equivalent numbers (PREN). Alloys with higher PREN values are more resistant to corrosion than steel.

Any severe service valve must provide sufficient sealing throughout its service life. While graphite-based packing materials provide excellent sealing at higher temperatures, they are likely to undergo galvanic corrosion. An alternative to such corrosive flow operations is using polytetrafluoroethylene (PTFE) valve packings.

Monel, an alloy of nickel, has better corrosion and chemical resistance compared to steel-based valve materials. Other alloys that perform well in corrosive and aggressive fluid service are Alloy C-276, which is commonly referenced as Hastelloy C-276 and is composed of nickel-molybdenum-chromium alloys and tungsten. Inconel is an alloy of nick-

el and chromium and resists oxidation at high temperatures and pressure.

Corrosion effects upon check valves. The safety of severe service pipelines relies on the integrity of check valves. These valves guarantee directional and volumetric control of hazardous fluids while preventing leakage. When corrosion occurs, the valves weaken, increasing the probability of fluid media leakages and fugitive emissions of toxic gases. Valve components consist of dissimilar materials (metals and non-metals) that react differently to the corrosive service media. Valve corrosion occurs in any or a combination of the following ways.

General corrosion. This occurs due to chemical or electrochemical reactions within the valve. Concentrations of sulfur, chlorides or carbonates mix with moisture and oxygen in the piping system to form weak acids that attack metal surfaces

FIG. 1. The use of optimal anticorrosive materials, such as stainless steel 316, is suggested for equipment like industrial check valves.

in a process called chemical corrosion. Elevated temperatures speed up the chain of chemical reactions, causing a rapid deterioration of the valve body. Electrochemical corrosion occurs when dissimilar valve materials come into contact with electrolytes and initiate a flow of electrons that causes gradual damage to metallic surfaces. The different metals form galvanic pairs: the strong metal is the cathode and the weaker one is the anode. The anode corrodes faster than the cathode. The rate of electrochemical corrosion in valves depends on the pH concentration of the service media (alkalinity or acidity) and the amount of oxygen in the pipeline. Low oxygen levels increase the rate of flow-accelerated electrochemical corrosion.

Pitting and crevice corrosion. Valves made from steel contain a protective oxide layer that inhibits chemical reactions. Exposing the valves to corrosive, aqueous fluid media initiates oxidation and causes the ferrous metal to lose some electrons, leading to the formation of small pits, which expand as the valve cycles increase. Crevice corrosion is predominant in valve connectors and welded joints. Crevices, which are as small as 0.025 mm–0.1 mm, permit the leakage of corrosive electrolyte solutions to form a galvanic cell that creates perfect conditions for localized corrosion (**FIG. 2**).

Frictional corrosion. Also known as erosion corrosion, this type of corrosion occurs when a viscous and corrosive fluid repeatedly passes through the valve at high speed. The viscous service media leaves behind small debris around the valve, scouring the metallic surface and gradually wearing out the protective oxide layers. As frictional wear continues, the underneath steel components are exposed to the corrosive media, increasing the rates of chemical and electrochemical attacks on the valve. Choke valves installed in oilfields to balance the pressure of the common manifolds are prone to this type of corrosion due to the aggressive nature of the oil well stream (mixture of oil, gases, semi-solids and water).

Stress corrosion cracking. Varying the operating temperatures of oil and gas processes causes expansion and contraction of valves and other components of the piping system. With time, these variations cause minute cracks on internal valve components, escalating check valve corrosion.

When check valves corrode, their performance drops. Frictional corrosion reduces the thickness of the flapper or disc. It also affects the geometry of the valve seat, leaving behind irregular seat surfaces and increasing the probability of leakage from valves. As the structural integrity of the disc deteriorates, its shutoff characteristics degrade. As the valve's shutoff characteristics degrade and its disc loses efficiency, it becomes susceptible to upstream fluid flow even at pressures well below the designed cracking pressure.[1,2] Because these factors lead to delays in valve closures, they also leave room for small backflows. Such instances result in downstream contamination and other adverse effects, such as water hammers and cavitation. Weakened discs/flappers frequently slam against the valve seats, with significant losses in the sealing capabilities.

Pitting, crevice corrosion and general corrosion attack the disc/flapper, valve stem and valve packing. As the corrosive action of the fluid attacks the stem, the diametral tolerance between the valve stem and the packing increases. This creates conditions for leakages and fugitive emissions around the valve body, escalating operational safety risks. Fluid leakages result in increased pressure drops across the valve, a situation that will affect the efficiency of downstream processes.[3] Over time, the corrosive fluids attack the external components like the actuators, affecting the responsiveness of valves to process controls.

FIG. 2. Crevices permit the leakage of corrosive electrolyte solutions to form a galvanic cell, which creates perfect conditions for localized corrosion.

As rust accumulates around the valve, the opening and closing limits of the valves reduce. The check valves cannot provide a full path for fluids to pass. At the same time, the process operating conditions are kept constant, with the pumps supplying fluids at optimum capacity. The partially open check valve disc obstructs the flow of corrosive fluids, resulting in a rapid buildup of pressure in the upstream piping equipment. With time, the excess fluid pressure weakens the pipes, causing rupture and explosion.

Prevention and maintenance. Selecting the appropriate valve for corrosive fluid service eliminates safety risks arising from the gradual degradation of valve components. One way to protect valves used for corrosive fluid service is by performing metal surface treatment. A protective, non-reactive coating is applied between a metal surface and its surroundings to create a physical barrier. This prevents chemical reactions at the surface of the metallic component. Other treatment methods include surface coating, passivation or oxidation. The protective coatings use corrosion-resistant materials and alloys like chromium, zinc, metal oxides and phosphates.[4,5] To protect valves against electrochemical corrosion, manufacturers use anodic or cathodic protection, which converts galvanic pairs into passive components to prevent electron flow. Other valves use non-metallic corrosion inhibitors like ceramics, metal oxide ceramic coatings and non-metal substrates. To combat and inhibit corrosion, operators should remain vigilant in their inspection and maintenance procedures (**FIG. 3**).

Heavy-duty, severe service valves contain ports for the lubrication of internal valve surfaces to enable the smooth movement of dynamic parts. This reduces the impact of frictional corrosion.

Corrosion predominantly attacks a check valve's disc, as it is the most dynamic component. To minimize the impacts of corrosive chemical attacks on the check valve discs, they are often coated with 0.3 mm–0.6 mm of ethylene chlorotrifluoroethylene (Halar) material. Another way to protect the discs is by coating metallic valve components with polyethylene or perfluoroalkoxy (PFA) materials. These thermoplastic materials possess better mechanical and chemical resistance than Halar.

FIG. 3. To combat and inhibit corrosion, operators should remain vigilant in their inspection and maintenance procedures.

The choice of valve material varies depending on the concentration of the dominant corrosive compounds. Piping systems with high concentrations of sulfur, with suitable conditions for the formation of sulfuric acid (H_2SO_4), should use valves made from alloy stainless steel, such as Alloy-20. Fluoroplastic valves can be used for low-pressure, low-temperature H_2SO_4 service.

Pipelines conveying fluids with less than 30% hydrochloric acid concentrations at temperatures below 120°F (50°C) can use valves made from steel alloys containing suitable quantities of molybdenum. Non-metallic valve materials are appropriate for hydrochloric acid service as long as the process temperatures do not exceed 300°F (150°C). High-temperature nitric acid service pipelines use titanium alloy valves. Nitric acid corrodes most metals at room temperature and pressure. Where there is a high concentration of H_2S gas in the service media, the valve stem is electroplated using phosphorous and nickel coatings.

Non-metallic materials such as PTFE, synthetic rubbers, nylon and strong thermoplastics are used to create seals in valves. Although they provide sufficient sealing, their use is limited to low-temperature applications.

When installing non-metallic valves for corrosive fluid service, avoid distorting the flanges. The machining of non-metallic flanges is not as smooth as that of most metallic valves and can be a source of external leakages.

Always use the correct valve and piping materials that are resistant to the service media. Installing the valves in the appropriate locations and orientations prevents instances of choked flows, stagnation or contamination that can exacerbate the corrosive action of the working fluid. **HP**

LITERATURE CITED
[1] Driscoll, R., "What is the cracking pressure of a check valve?" Valveman, online: https://valveman.com/blog/what-is-the-cracking-pressure-of-a-check-valve/
[2] Wood, R., "Erosion-corrosion interactions and their effect on marine and offshore components," U.S. Department of Energy, Office of Scientific and Technical Information, 2004, online: https://www.osti.gov/etdeweb/biblio/20671857
[3] Zulkarnaini, M. A., et al., "Analysing petroleum leakage from ground penetrating radar signal," ResearchGate, January 2019, online: https://www.researchgate.net/publication/325115239_Analysing_Petroleum_Leakage_from_Ground_Penetrating_Radar_Signal
[4] Waters, R., "Selection of severe service valves," Chemical Engineering, June 2017.
[5] SpecialChem, "Corrosion resistance and anti-corrosion coatings—All you need to know," SpecialChem: The material selection platform, online: https://coatings.specialchem.com/coatings-properties/corrosion-resistance

GILBERT WELSFORD JR. is the Founder of Valveman.com and a 3rd-generation valve entrepreneur. He has learned valves since a young age and brought his entrepreneurial ingenuity to the family business in 2011 by creating the online valve store Valveman.com. Mr. Welsford's focus is building on the legacy his grandfather started, his father grew, and he has amplified.

S. ZARDYNEZHAD, TurboTech Consulting Corporation, Calgary, Alberta, Canada

Fouling in hydrogen recycle gas compressors

Hydrogen (H_2) recycle gas compressors are one of the most significant rotating equipment in oil refineries, petrochemical plants and upgraders. The compressor is usually a centrifugal gas compressor between bearings. A single-shaft centrifugal compressor design is based on the API Standard 617.[1] Without the compressor, a plant's production will be stopped. **FIG. 1** shows a typical H_2 recycle gas compressor in a hydrotreating unit.

H_2 recycle compressors are used with oil refinery processing equipment, including hydrocrackers, hydrotreaters, platformers and isomerization units. The hydrotreating process is similar in oil refineries and petrochemical plants like aromatic plants and upgraders. Depending on the licensor, the number and configuration of the equipment may be different; however, the process is very similar.

The risk of fouling is high in recycle gas compressors due to chemical injection and reactions in the reactor. Stress corrosion cracking, possibly combined with high cycle fatigue, causes impeller and rotor failures.

This article will explain the hydrotreating process and address compressor fouling, which impacts the recycle gas compressor's performance and reliability, based on the author's experience working in large oil refineries, petrochemical plants and upgrader plants.

The hydrotreating process. The hydrotreating process reduces mercaptan, sulfur, metal content, nitrogen, oxygen, organic halides (chlorides and bromides), olefins and aromatic components of the feedstock while enhancing the cetane/octane number in oil refining and the density and smoke point of the product. Some hydrocracking and thermal cracking reactions may take place in the hydrotreating process. **FIG. 1** shows a typical sketch of the hydrotreating process in oil refineries, upgraders and petrochemical plants. The primary duty of the recycle gas compressor is to move the feedstock (Point A) through a fired heater, reactor, reactor feed effluent exchanger, air and trim cooler, separator and finally, the compressor's suction. Make-up gas (Point C) supplied by a separate reciprocating gas compressor replaces the H_2 consumed. The large quantity of H_2 gas recycled from the separator to the reactor has the following purposes:

- Absorbing some of the heat of reaction, minimizing the catalyst bed temperatures.
- Lowering the heater and feed effluent exchanger tube wall temperatures by increasing the flow through the equipment.
- Preventing coke formation as the feedstock is heated to the reaction temperature.
- Ensuring the reactions are carried out completely.

FIG. 1 shows a liquid feedstock sent to the heater by a charge pump, normally a centrifugal pump. Consider the pump shutoff pressure when designing the compressor to prevent surging. Typically, two check valves are placed close to the injection point to prevent reverse liquid flow towards the pump. Another check valve is required downstream of the anti-surge valve.

H_2 gas. H_2 gas is colorless, odorless and highly flammable. H_2 gas forms explosive mixtures with air at concentrations from 4%–74% and with chlorine at 5%–95%. A spark, heat or sunlight can trigger explosive reactions. The H_2 auto-ignition temperature—the temperature of spontaneous ignition in the air—is 500°C (932°F). Pure H_2-oxygen flames emit ultraviolet light, and high-oxygen mixes are nearly in-
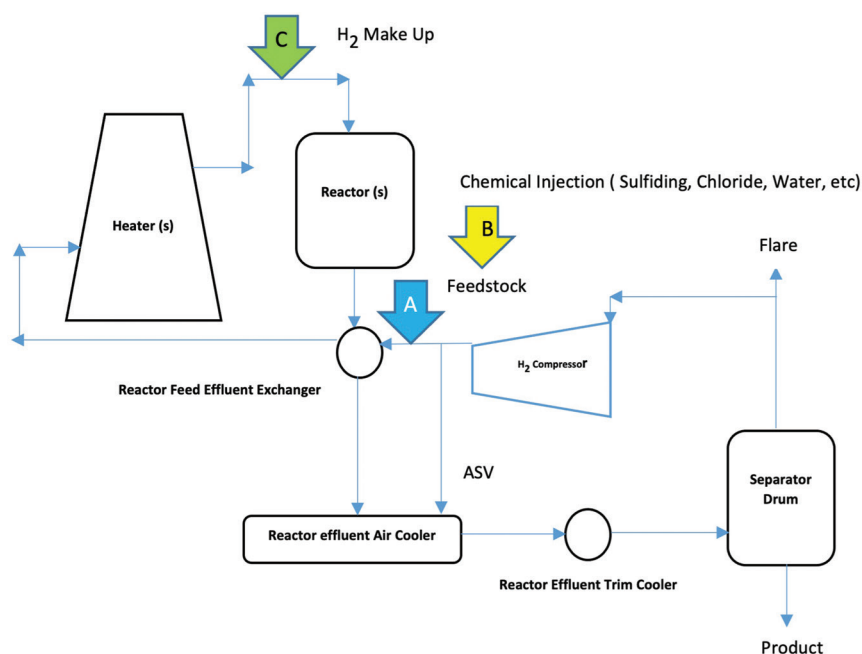

FIG. 1. Simplified hydrotreating process.

visible to the naked eye. Detecting a burning H_2 leak may require a flame detector, and a leak can be hazardous. Working around H_2 compressors, especially reciprocating gas compressors, requires knowledge, understanding and experience.

H_2 recycle gas compressors. The compressor is typically a centrifugal type based on the API 617 design and consists of a vertically split main casing, which houses the rotor, inlet guide vanes, diaphragms and intake/discharge walls. The balancing piston seal, shaft end and interstage seals are also contained in the main casing. By pulling the barrel out of the compressor casing and lifting off the top half of the inner barrel, all compressor internals are accessible for inspection.

The compressor gas is mainly H_2 with a low molecular weight. Low molecular weights are difficult to compress and have little pressure rise or volume reduction per stage. Due to this, the H_2 recycle compressors normally have 6–12 stages, run at high speeds like a steam turbine, or both. The compressor location is generally at the mezzanine and driven by a steam turbine. The compressor seal is a dry gas seal tandem. The purpose of the recycle gas compressors is to circulate H_2 gas to the reactor circuit to provide H_2 for reaction and quench gas for reaction temperature control.

Compressor fouling-reliability improvement. Compressor gas composition shall be specified in detail in the datasheet and clarify to the various prospective vendor's the amount of condensable liquid, water, hydrogen sulfides (H_2S), chlorides and various amines. Within the reactor, in the presence of a catalyst, sulfur compounds are decomposed to form hydrocarbon and H_2S. Oxygen compounds convert to hydrocarbon and water, and nitrogen compounds convert to hydrocarbon and ammonia (NH_3). The sulfur and nitrogen contained in the feed convert to H_2S and NH_3 in the reactor.

These two reaction products combine to form ammonium salts that can solidify and precipitate as the reactor effluent is cooled. Likewise, ammonium chloride may form if there is any chloride in the system. The purpose of the water is to dissolve these salts before they precipitate. Water is injected in a vertical run of pipe through an injection quill that facilitates mixing the water with the reactor effluent.

Chloride and ammonium chloride build up on casing diffusers and impellers reduce a compressor's efficiency. The build-up can reduce the seal gas supply flow from the compressor casing port to dry the gas seal console, and it can build up on the orifices and the seal gas filter casing. The following is recommended to solve compressor fouling:

- Carefully monitor all heat exchanger differential pressure trends upstream of the compressor with the proper process software.
- Carefully monitor compressor efficiency and plan to shutdown the compressor to perform internal cleaning. Consult with a dry gas seal manufacturer for online cleaning provisions. Depending on the process, loss of efficiency is expected to occur roughly every 1 yr–2 yr.
- Install a coalescer filter to remove entrained water within the process stream.
- Place the wash water injection point properly to minimize the entrained water.
- Run higher suction inlet temperatures to sublimate the chloride solids back into the gas stream.
- Consider an engineered and sufficiently sized recycle gas scrubber upstream of the compressor. The recycle compressor suction line exiting the scrubber should be heat traced and insulated to prevent condensation, which causes recycle compressor damage.
- Refer to API 571[2] for more detail. **HP**

NOTE
The recommendations outlined in this article are based on personal experience and not related to any company.

LITERATURE CITED
Complete literature cited available online at www.HydrocarbonProcessing.com.

SHAHAB ZARDYNEZHAD is a registered Senior Mechanical Engineer in Alberta with more than 30 yr of experience working on many of the world's largest oil, gas and petrochemical projects. He has experience in engineering, procurement services, manufacturing, shop/field inspection, installation, commissioning, startup, reliability, and the maintenance and operation of pumps, compressors and turbines. Mr. Zardynezhad holds a BS degree in mechanical engineering from the University of Petroleum of Iran, an MS degree in industrial engineering from I.U.S.T-Iran, an MS degree in project management and an MS degree in mechanical engineering from the University of Calgary. He is a certified API inspector for rotating equipment.

Accurately calculate flowrate through valves, fittings and pipe under a turbulent flow regime

Calculating flowrate through long, straight pipe in a zone of complete turbulence is easy using standard fluid mechanics equations. In most industrial process designs, real piping systems lie in the area known as the transition zone, meaning that the friction factor depends on both the Reynolds (Re) number of the flow and the relative roughness of the pipe. Conversely, most real piping systems have valves and fittings that make calculating flowrate more difficult.

This article presents equations that accurately calculate flowrate through valves, fittings and pipe under a turbulent flow regime (Re > 4,000) in systems where the energy loss is then the sum of the losses of pipes and fittings.

Two equations provide a reasonable value of equivalent length of straight pipe to account for valves and fittings, and two other equations determine precise values of the friction factor in smooth, new and rough pipes. These equations are excellent resources to calculate flowrate in piping systems where fittings cannot be disregarded. In this type of problem, the following information is known:

1. Physical properties of fluid (density and viscosity)
2. Pipe size and its schedule
3. Total pressure drop or total head loss in the piping system
4. Straight length of pipe
5. Character of internal surface of the pipe wall
6. Number and types of valves and fittings installed in the piping system.[1–5]

Equivalent length of pipe. The following equations estimate an equivalent length of pipe for valves and fittings. As a general rule, the values of this equivalent length of pipe are not real, but they allow the actual value of the friction factor to be determined.

For smooth and clean commercial pipe (Eq. 1):

$$L_e = 33 \times \sum K \times \left(\frac{\mu}{\rho} \right)^{-0.24} \times (D)^{1.36} \times \left(\frac{h_f}{L_s} \right)^{0.12} \tag{1}$$

For rough pipe, use Eq. 2:

$$L_e = 44 \times \sum K \times \varepsilon^{-0.263} \times D^{1.263} \tag{2}$$

where $\sum K$ is determined as follows (Eq. 3):

$$\sum K = \sum (L/D)_{eq} \times f_t + \sum K_0 \tag{3}$$

Many books and handbooks tabulate $(L/D)_{eq}$ and f_t values for numerous fittings and valves. The adjusted length of pipe is then (Eq. 4):

$$L_a = L_e + L_s \tag{4}$$

Friction factor. The value of the friction factor can be calculated by the following equations. For smooth pipe (Eq. 5):

$$f = 0.0056 + 0.0189 \Lambda^{-0.36} \tag{5}$$

For clean commercial and rough pipe (Eq. 6):

$$f = \frac{0.25}{\left[log \left(\frac{0.000576}{\Lambda} + 0.27 \frac{\varepsilon}{d} \right) \right]^2} \tag{6}$$

where Λ is a conventional number defined as (Eq. 7):

$$\Lambda = \frac{\rho}{\mu} \times \sqrt{h_f \times \frac{D^3}{L_a}} \tag{7}$$

Additionally, the number Λ is calculated with the actual length of pipe defined as (Eq. 8):

$$\Lambda = 0.0002258 \times Re \times \sqrt{f} \tag{8}$$

Actual equivalent length of pipe. Based on the friction factor obtained above, the equivalent length of pipe is precisely determined using Eq. 9, and the adjusted length of pipe is checked by Eq. 4.

$$L_e = \frac{\sum K}{f} \times D \tag{9}$$

The desired flowrate is obtained using Eq. 10:

$$q = 3.47835 \times D^{2.5} \times \sqrt{\frac{h_f}{f \times L_a}} \tag{10}$$

Checking the result. The mean velocity of flow, the Re number and the relative roughness of the pipe (if any) are calculated by traditional fluid flow equations. The friction factor is then obtained by the Moody diagram or by equations published in many papers, which agree with the calculations achieved by Eqs. 5 and 6.

A sample problem demonstrates the usefulness of this flow-rate calculation method. Light oil ($\rho = 960$ kg/m³, $\mu = 1.2$ Cp) is flowing through a valve station. This piping system contains 20 m of horizontal new commercial 3 in.-diameter Schedule 40 pipe, three gate valves, four 90° welded elbows ($r/d = 1.5$), one conventional globe valve and one thin orifice plate with a loss coefficient of $k = 3.6$. With all valves wide open, the pressure drop in this system is 11,844 Pa. Calculate the flowrate of oil in l/min (liters per minute) as shown below.

1. The 3 in.-diameter Schedule 40 pipe data is: $d = 77.9$ mm; $D = 0.0779$ m; $f_t = 0.018$; and $\varepsilon = 0.046$ mm.

2. Kinematic viscosity (Eq. 11):

$$\nu = [1.2/(1{,}000 \times 960)] = 1.25 \times 10^{-6}\ \text{m}^2/\text{sec} \qquad (11)$$

3. Summarizing K for valves and fittings (Eq. 12):

$$\sum K = (3 \times 8 + 4 \times 20 + 1 \times 340)0.018 + 3.6 = 11.592 \quad (12)$$

4. Total head loss applying Bernoulli equations (Eq. 13):

$$h_f = [11{,}844 / (960 \times 9.806)] = 1.2581\ \text{m} \qquad (13)$$

5. Equivalent length of pipe estimated for valves and fittings (Eq. 14):

$$L_e = 33 \times 11.592 \times \left(\frac{1.2}{960}\right)^{-0.24} \times$$
$$0.0779^{1.36} \times \left(\frac{1.2581}{20}\right)^{0.12} \approx 42m \qquad (14)$$

6. Estimated for adjusted pipe (Eq. 15):

$$L_a = 42 + 20 \approx 62\text{m} \qquad (15)$$

7. Conventional number Λ (Eq. 16):

$$\Lambda = \frac{960}{1.2} \times \sqrt{1.2581 \times \frac{0.0779^3}{62}} = 2.478 \qquad (16)$$

8. Friction factor (Eq. 17):

$$f = \frac{0.25}{\left[log\left(\dfrac{0.000576}{2.478} + 0.27\dfrac{0.046}{77.9}\right)\right]^2} = 0.0215 \qquad (17)$$

9. Actual equivalent length of pipe (Eq. 18):

$$L_e = (11.592 / 0.0215) \times 0.0779 = 42\ \text{m} \qquad (18)$$

10. Flowrate (Eq. 19):

$$q = 3.47835 \times 0.0779^{2.5} \times \sqrt{\frac{1.2581}{0.0215 \times 62}} = \qquad (19)$$
$$0.00572347\ \text{m}^3/\text{sec}$$

$$Q = q \times 60{,}000 = 343.4\ \text{l/min}$$

11. Checking results (Eq. 20):

$$\nu = [(4 \times 0.00572347) / (3.1416 \times 0.0779^2)] = 1.2\ \text{m/s} \qquad (20)$$
$$Re = [(1.2 \times 0.0779 \times 10^6) / 1.25] = 74{,}784$$
$$\varepsilon/\text{D} = (0.046 / 77.9) = 0.0005905$$
$$f = 0.0216$$
$$\Lambda = 0.0002258 \times 74{,}784 \times \sqrt{0.0216} = 2.48$$

The friction factor calculated in Step 8 (Eq. 17) is slightly less than the calculation above, but the difference is small enough to forego any correction of the equivalent length of pipe and flowrate. Therefore, the calculated flowrate is correct and the condition given in Eq. 8 is fulfilled.

Takeaway. The proposed calculation methods here determine flowrate trough valves, fittings and pipe for most liquid and vapors without tedious trial and error methods. The equations to determinate unknown parameters are derived from classical equations published in literature.[1,4,5] These methods are also applicable in open tanks draining through piping systems and in piping systems with elevation above the reference level containing numerous fittings and valves. **HP**

NOMENCLATURE

d = Internal diameter of pipe, mm
D = Internal diameter of pipe, m
f = Darcy friction factor
f_t = Friction factor in zone of complete turbulence
h_f = Total head loss, m
K = Fitting loss coefficient
K_0 = Fitting loss coefficient for a specific type of fitting
L_e = Equivalent length of pipe, m
L_s = Straight length of pipe, m
L_a = Adjusted length of pipe, m
$(L/D)_e$ = Equivalent length of pipe in numbers of pipe diameters
q = Flowrate, m³/sec
Q = Flowrate, l/min
Re = Reynolds number
μ = Dynamic viscosity of fluid, cP
ν = Kinematic viscosity of fluid, m²/sec

LITERATURE CITED

[1] Churchill, S. W., "Friction factor equations spans all fluid flow regime," *Chemical Engineering,* November 1977.
[2] Crane Valve Group (CVG), "Flow of fluids through valves, fittings & pipe," Crane Technical Paper No. 410 (TP-410), 1988.
[3] Darby, R., "Correlate pressure drops through fittings," *Chemical Engineering,* July 1999.
[4] Mott, R. L., *Applied fluid mechanics,* 4th Ed., Prentice Hall PTR, 1996.
[5] Verma, C. P., "Solve pipe flow problems directly," *Hydrocarbon Processing,* August 1979.

ISRAEL GARCIA graduated from the University of Cienfuegos Cuba with an MS degree in mechanical engineering. Mr. Rodriguez has been attached to the mechanical engineering faculty of that university since 1985 as a Professor in fluid mechanics, heat transfer and science materials. Mr. Garcia has more than 30 yr of industrial experience in chemical plants and power stations and has presented several papers that deal with the design of heat exchangers, pressure vessels and piping systems. The author can be reached at isgaro47@gmail.com.

ALEJANDRO GARCIA is a mechanical engineer that graduated from the University of Cienfuegos Cuba. He received his MS degree in mechanical engineering with a specialty in materials from the Autonomous University of Nuevo Leon, Mexico. He gained several years of experience in power plants and the automotive industry as a static and dynamic equipment specialist. He now works in a steel and wire plant in Houston, Texas as a mechanical engineer. The author can be reached alessandromilan88@gmail.com.

M. VILLEGAS, Koch Modular Process Systems, Houston, Texas

Enabling a circular economy delivery model through truckable modularization

As resources become scarcer, and as costs continue to rise, companies are looking for new methods to reduce their material feedstock costs and remain competitive. Societal pressures on companies to minimize their impact on the environment and reduce their carbon emissions further compound this situation.

One of the key strategies for achieving a competitive advantage, while also meeting corporate sustainability goals, is to create a circular economy. This can either be done by developing the circular economy from the start or by converting a linear economy to a circular economy (**FIG. 1**). To close this loop, many companies leverage chemistry and related process technologies (including process intensification and decarbonization) to bridge the gap.

Recent examples of areas in the chemical processing industry that have successfully implemented circular economies include bio-derived materials and fuels, recycled plastics and recycled oils. For bio-derived materials and fuels, products sourced from living matter (also known as biomass) are processed as a substitute feedstock for petroleum-based raw materials. In the case of recycled plastics, waste plastic is chemically converted back into feedstock-grade plastic, rather than having it end up in a landfill. Then, this recovered plastic is reintroduced as feedstock, eliminating the need for petroleum-based raw materials to manufacture new plastic goods. Similarly, the recycled oil industry cleans and reprocesses previously used oils and then reintroduces these oils back into the marketplace, thus replacing the demand for petroleum-based oils.

Creating a circular economy. Enabling a circular economy can be accomplished by either developing new processes to utilize renewable feedstocks or by redesigning existing processes to substitute current non-renewable raw material feedstocks. Renewable feedstock examples include bio-derived, recycled or recovered materials. These feedstocks could be the result of waste byproducts that originate from other internal manufacturing processes or even from completely different industries. The goal is to reclaim one's own manufactured product upon end-of-life use and then reintroduce it into the beginning of the manufacturing process as recycled feedstock.

When it comes to feedstock sourcing, the traditional linear economic manufacturing model no longer works in many circular economy-based models. Because bio-derived, recycled or recovered materials are typically generated in smaller quantities and/or across multiple geographies, it is uneconomical to transport multiple feedstocks to a single, centralized manufacturing facility. The added cost in transportation due to increased source locations would also raise the manufacturing carbon footprint rather than lower it. Therefore, in a circular economy-based manufacturing model, a hub-and-spoke feedstock delivery model is more efficient and economical.

Hub-and-spoke feedstock delivery model. A hub-and-spoke feedstock delivery model consists of smaller centralized processing facilities acting as hubs located relatively close to the feedstock origin locations. The spokes extend into surrounding communities, collecting feedstocks from multiple municipal recycling facilities, farms and other point sources. Typically, spokes extend only a few hundred miles from the hub.

For example, a hub could be placed in the middle of a 500-mi circle containing no feedstock, provided there were 3–5 facilities on the circumference located very near feedstock, albeit outside the circle. This structure economically optimizes efficiency by processing feedstock locally and minimizing transportation costs.

Using this model, multiple hubs are required to service extended geographical regions or to provide national and interna-
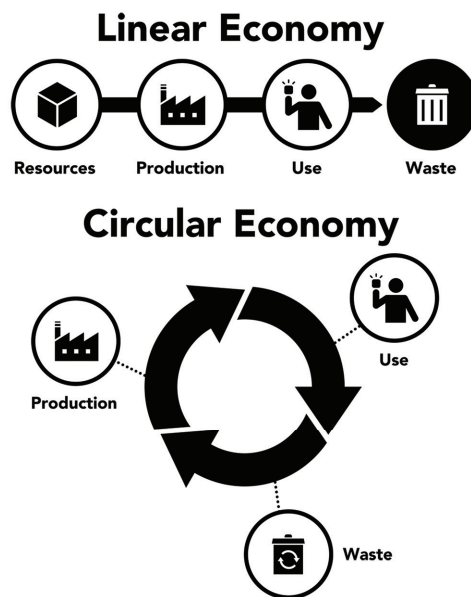

FIG. 1. A circular economy can be created from the start or by converting a linear economy to a circular economy.

tional footprints. Furthermore, in some cases, feedstock sources may be fluid and may change over time. Creating multiple, smaller processing hubs that are designed and built to be mobile allows economical relocation as needed to follow feedstock sources.

Also, given that a hub-and-spoke feedstock delivery model drives the need for employing multiple smaller and potentially mobile processing facilities, the project delivery model, along with the construction and design of these process facilities, must be reevaluated. Building truckable modules (**FIG. 2**) vs. traditional field construction or even traditional modularization creates considerable advantages.

Right-sized truckable modular solution. Modularization is described as the process of shifting as much of the labor-intensive field construction activities as possible from the field to an offsite fabrication facility. This mitigates the inherent risks associated with field construction. Typically, a modular system includes complete process units that are fabricated remotely from the plant site.

Modular construction allows for standardization and repeatability, which translates to the ability to establish a definitive estimate early in the project development phase—much earlier than is typically possible with a field construction execution strategy. Furthermore, with modularization, issued for construction (IFC) drawings are also frozen much earlier than with field construction, thus enabling a fixed-price contracting strategy to ensure cost certainty. This is especially beneficial with developing-technology projects, which typically rely on bank and venture capital funding to advance projects from the proof-of-concept stage to commercialization. Another added benefit of being able to freeze the design early in the project is that it mitigates the opportunity for scope creep in the field, which can have a direct impact on cost and schedule.

The benefits of modularization over field construction can include:

- A reduction in workplace hazards and injuries
- Shorter project delivery schedules and time to market
- Minimized site interruptions
- Increased productivity
- The ability to commence module fabrication during the permitting phase
- Advanced definitive estimates and fixed-price contracts
- Overall project cost savings.

Considering the smaller capacity and size of the hub facilities

FIG. 2. A view of Origin Materials' biomass truckable modular process system.

in the hub-and-spoke model, truckable modular construction is best suited as a project delivery model vs. both traditional field construction and modularization. Unlike traditional modules, which can weigh up to 6,000 t and require highly specialized transportation, truckable modules generally have footprints of 12 ft × 14 ft × (up to) 90 ft, which means that these modules can fit easily on a standard truck. Consequently, these modular systems are well-suited for facilities with manufacturing capacities that are best served by a hub-and-spoke feedstock delivery model.

Truckable modular process systems are typically built in a horizontal assembly line fashion in a controlled indoor environment. This helps minimize the amount of work and resources needed vs. field construction. When arriving onsite, the truckable modules are approximately 90% complete, and include all necessary components and equipment placed within the structural steel frame required to deliver a complete process system. This frame serves as support during shipment, and provides access to the equipment for operation and maintenance after installation at the plant site. Once delivered onsite, the only remaining activities include making interconnects, utility and electrical tie-ins, and commissioning and startup activities.

Benefits of truckable module project delivery models. In addition to the typical benefits of executing projects modularly, selecting a truckable module project delivery model introduces additional advantages, including:

1. **Scalability:** When a project is designed up front as a modular facility, then it is possible to employ a plug-and-play design strategy for adjusting the facility size, design capacity, layout and other design parameters to fit the regional requirements. This facilitates the ease of reconfiguring, adding or eliminating process modules. Furthermore, scalability creates the ability to quickly and economically move from proof-of-concept pilot scale to commercial scale.

2. **Installation flexibility:** Once erected in the field, truckable modules can be installed in either a horizontal or vertical orientation. For distillation column applications, where the column height exceeds the overall erected height of a given module, the columns can be dropped into the module and flanged together at the site, or two vertically oriented modules can be bolted together. Additionally, where process systems require multiple modules to form a complete operating process system, these modules can be interconnected both horizontally and vertically.

3. **Repeatability:** One of the inherent benefits of designing for scalability is that designs can be standardized for repeatability. Given the nature of a hub-and-spoke feedstock delivery model, facilities may need to be installed in various locations across multiple regions. Therefore, a design-one/build-many approach can be employed as a base design while implementing minor design modifications that consider local factors such as codes and specifications, as well as special environmental conditions.

4. **Project predictability and risk mitigation:** All the inherent benefits of modularization, along with the addition of the special benefits afforded by opting for

a truckable module solution, stack the deck for project success. Transferring construction from the field to an offsite controlled environment—and introducing a scalable, repeatable design that can be frozen prior to fabrication and before ever going into the field—has a significant, positive impact on project predictability. Therefore, truckable modular solutions provide the enhanced ability to mitigate project execution risk vis-à-vis cost, schedule, safety and quality.

Getting the right modular support to create a circular economy. Utilizing a truckable module project delivery model requires specialized expertise unlike that of traditional modules, especially with respect to field construction. While traditional modularization already requires a completely different mindset to design, engineer, procure, project-manage, fabricate and deliver the module to the site, delivering truckable modules requires a further degree of expertise. Every nuance of the process from "feedstock in" to "product out" must fit within the constraints of a 12-ft $\times$ 14-ft $\times$ 90-ft footprint, while remaining scalable, repeatable and cost-competitive to ultimately deliver project certainty. For this reason, specific truckable process module expertise is paramount.

When creating or moving to a circular economy delivery model, the use of truckable modules should be seriously considered. Once selected as a project delivery model, it is important to engage an experienced process development and engineering firm with direct experience designing and delivering truckable modules. To realize the full benefit that this solution can provide, it is equally important to engage the chosen firm as early as possible in the project development phase. Ideally, the selected engineering firm will also have the capability to support pilot testing during the proof-of-concept phase, which will help de-risk the project and, in many cases, offer a final process performance guarantee. The sooner an engineering firm can get involved and perform a modularization study, as well as provide pilot-scale testing and process optimization for truckable modularization, the sooner a definitive estimate can be established to support the financial investment decision process.

Overall, creating a circular economy brings significant benefits to companies that employ this model, from both competitive advantage and corporate sustainability standpoints. Using a truckable module project delivery model helps to execute this initiative in a cost-effective way while also mitigating risk—ultimately, helping companies in the chemical process industry to adapt and remain successful far into the future. **HP**

MAURICIO VILLEGAS is the Manager of Business Development at Koch Modular Process Systems. He has more than 25 yr of experience in the engineering and construction industry, delivering projects across industries ranging from small brownfield projects to greenfield mega-projects. Prior to joining Koch Modular Process Systems, he held various management roles at WorleyParsons, Technip, IHI E&C and Arcadis. Mr. Villegas earned a BS degree in business administration and management from Northeastern University in Boston, Massachusetts.

The 1980s: Oil spike/collapse, liquid crystals, conducting polymers and the rise of AR/VR

Several major impactful events took place in the global oil and gas and petrochemical industries in the 1980s. Nations around the world were hit with another spike in global oil prices, followed by a price collapse. This third crisis in 15 yr led many nations to invest in finding alternative fuels and/or feedstocks to produce transportation fuels and petrochemical products, including the discovery of a new coal gasification technology for chemicals production. The discovery of liquid crystals and conducting polymers not only created new fields of research, but also advanced the creation of a new host of electronic display devices and led to a Nobel Prize in Chemistry.

The 1980s also witnessed a greater focus on mitigating vehicle emissions and the continued phase-out of lead in transportation fuels. For example, the U.S. Environmental Protection Agency enacted a new standard in the mid-1980s to severely limit lead content in gasoline. The standard, enacted in 1986, decreased lead content in gasoline from 1.1 g/gal to 0.1 g/gal.[180] U.S. refiners also began to increase the use of methyl tertiary butyl ether (MTBE) in gasoline. MTBE was used as a replacement for tetraethyllead as an anti-knocking agent (i.e., octane enhancer).

Regions such as Asia and the Middle East experienced sizable increases in refining and petrochemicals production capacity during the decade. For example, the Middle East's refining capacity increased from 3.5 MMbpd in 1980 to more than 5.6 MMbpd in 1990.[181] Saudi Arabian petrochemical producer SABIC increased petrochemical production capacity by more than 6 MMtpy to 13 MMtpy by 1990 (this included the launch of several JVs, including KEMYA, YANPET, PETROKEMYA, SADAF and SHARQ)—the creation of SABIC, as well as the construction of Al-

Jubail and Yanbu industrial cities and the country's master gas system, would propel Saudi Arabia to be the leading petrochemical producer in the region (these events were detailed in the History of the HPI section of the June issue). The Asia-Pacific region's net refining capacity expanded more than 1 MMbpd to more than 13.6 MMbpd from 1980–1990 (Japan's refining capacity declined more than 1.3 MMbpd in the 1980s).[181] The region's largest refining capacity increase occurred in China, which added nearly 1.2 MMbpd in the 1980s. China was followed by India, which added more than 560,000 bpd; Indonesia doubled domestic refining capacity to nearly 950,000 bpd in the same period.

The decade also witnessed the creation of three novel heavy-oil upgrading technologies, the popularization of new digital technologies that would enhance multiple facets of the oil and gas and petrochemicals industries in the future, and notable industrial accidents and ensuing directives that led to enhanced safety regulations still in use today.

A spike, an oil glut and a collapse. In the 1970s, two major oil crises—the oil embargo of 1973 and the oil crisis of 1979—significantly affected importing nations (both crises were detailed in the History of the HPI section in the June issue). The oil embargo of 1973 led to a quadrupling of oil prices globally and was an impetus for oil importing nations to intently focus on energy security. The embargo also led to the creation of the International Energy Agency in 1974 as a way for major energy consuming nations to discuss energy policies and strategize pathways for the security of supplies.[182]

The oil crisis of 1979—caused by the Iranian Revolution, which led to a sizable increase in global crude oil prices—had

lingering effects into the early 1980s. The year-long revolution was responsible for knocking approximately 4.8 MMbpd of oil production offline. Although this represented only 7% of the world's oil production at the time, it led to global oil prices nearly doubling to $39/bbl (equates to nearly $140/bbl in today's currency after adjusting for inflation).[140]

As oil prices skyrocketed, oil producers swiftly ramped up production and fought for market share. Led by OPEC-producing countries, global crude oil production reached nearly 64 MMbpd in 1979–1980. However, a global economic recession from 1980–1983 led to a steep decline in oil consumption. Many industrialized nations (e.g., Canada, Japan, West Germany, the UK and the U.S.) witnessed high inflation rates and unemployment during this period. With oil production having ramped up over the past few years, the world was awash in oil, leading to a global glut that sent oil prices on a freefall.

During this timeframe, newly-elected U.S. President Ronald Reagan deregulated the U.S. oil and gas industry through executive order by removing price controls on gasoline, propane and U.S.-produced crude oil.[183] Although the policy helped reduced high pump prices and put market forces at the helm of crude oil and products pricing, it removed several beneficial incentives for smaller U.S. refiners. According to the U.S. Energy Information Administration, this led many small, simple refiners to shut operations. From 1980–1990, operable refineries in the U.S. decreased from nearly 320 to just over 200.[183] Most of these closures were within 2 yr after the decontrol of the U.S. oil and gas industry. This led the country's remaining refineries to expand operations and invest in increasing processing complexity.

To mitigate wild fluctuations in crude oil prices, OPEC tried to stabilize the market by implementing production cuts. The OPEC London agreement of 1983 was a notable action taken by the cartel to try and prevent a crude oil price collapse (**FIG. 1**). The agreement contained two important accords: OPEC lowered the benchmark price of its light crude oil by $5/bbl to $29/bbl and agreed to cut production rates.[184] This was a historic occasion, as it was the first time that the cartel had lowered oil prices. By 1985, global oil production had declined from nearly 64 MMbpd in 1980 to less than 57 MMbpd.[185]

However, many OPEC nations disregarded agreed-upon production cuts and began to increase production rates. In late 1985, tired of trying to stabilize the oil market, Saudi Arabia boosted oil production, flooding the already oversupplied market. By March 1986, the tremendous spike in crude oil supplies led to prices collapsing to $10/bbl—adjusted for inflation, prices collapsed from nearly $140/bbl in early 1980 to nearly $27.50/bbl in 1Q 1986.[186,187] Within a 15-yr timespan, the world had experienced three major oil price crises. It would not be for several years afterwards that the

FIG. 1. OPEC's extraordinary meeting in London in 1983 to try and stabilize the global oil market. The outcome of the meeting became known as the OPEC London agreement of 1983. Photo courtesy of OPEC.

FIG. 2. View of Eastman Chemicals Co.'s Kingsport plant in Tennessee (U.S.), the site of the company's proprietary coal gasification process. Photo courtesy of the American Chemical Society.

global oil market would fall into balance. However, it would not be the last oil price collapse or spike the global oil market would see. Several other significant price swings would occur over the next 30 yr.

A new coal gasification process. Due to the effects of the oil crises in the 1970s (especially the oil embargo of 1973), several nations conducted extensive research on finding alternative energy sources to produce fuels and chemicals besides using crude oil as a feedstock. The stark increase in crude oil prices significantly increased both refiners' and petrochemical producers' feedstock costs—most petrochemicals produced at the time used oil-derived feedstocks; the same is true today.

In an effort to wean off using high-priced petroleum feedstocks for fuels and chemical products production, several companies set their sights on coal gasification and coal liquefaction technologies. Since coal was a cheap commodity, converting it into transportation fuels and/or using it as a feedstock for petrochemicals production looked to be a viable alternative vs. using high-priced crude oil. Coal gasification/liquefaction technologies were not new at the time. Technologies such as the Bergius process and Fischer-Tropsch process had been around for decades (these technologies are detailed in the History of the HPI section of the January issue). Countries with abundant supplies of coal reserves could make use of existing coal gasification/liquefaction technologies to not only produce fuels and petrochemicals at a cost-effective rate, but also strengthen domestic energy security.

As global oil prices stabilized, many efforts to switch to other feedstocks fizzled out.[188] Conversely, the Eastman Chemical Co. continued research and development on coal-derived chemicals production. Like many chemical companies in the 1970s, Eastman was heavily dependent on crude oil and natural gas to produce petrochemicals. However, the company's petrochemical facility in northeast Tennessee (U.S.) was in close proximity to vast coal reserves in the Appalachian region of the eastern U.S.[189]

In the mid-1970s, Eastman conducted extensive research on utilizing coal to produce chemicals, especially acetic anhydride. At the time, the company consumed more than 1 Blb/yr of acetic anhy-

dride to produce various products. Acetic anhydride was first synthesized by French chemist Charles Frédéric Gerhardt in 1852; it is used to produce acetate fibers, plastics, coatings and film.[189,190,191] The company began pilot plant operations in 1977, followed by construction and operations on a commercial facility in 1980 and 1983, respectively.

According to literature,[189] the facility used several different technologies to produce acetic anhydride from coal. Synthesis gas was produced using the Texaco Coal Gasification Process. The proprietary coal gasification technology would eventually be licensed by ChevronTexaco after the companies merged in 2001. It fell into the hands of GE Energy after the company purchased ChevronTexaco's gasification business in 2004. Air Products became the current owner of the technology after purchasing the GE gasification business in 2018.[192,193]

According to literature,[189] the coal gasification process used oxygen and coal/water slurry as feedstock for a gasifier, which used high temperature and pressure to produce two gas streams: shifted gas and raw synthesis gas. The two product gas streams left the gasifier and were purified—hydrogen sulfide (H_2S) and carbon dioxide (CO_2) were removed via the Rectisol process (licensed by Linde and Air Liquide). The H_2S was converted to elemental sulfur in a Shell Claus offgas treating unit, while the CO_2 was recovered and sold to make carbonated beverages.[186] The purified raw synthesis gas was cryogenically separated into hydrogen and carbon monoxide, with hydrogen used for methanol production and the carbon monoxide used for acetic anhydride production.[189] The final step used an Eastman proprietary reactive distillation process and catalyst system to produce acetic anhydride—purified carbon monoxide reacted with methyl acetate to form acetic anhydride.[189] In May 1983, operations began at the Kingsport plant (**FIG. 2**), which became the first U.S. facility to use a novel coal gasification process to produce a modern generation of industrial chemicals.[189]

Liquid crystals and conducting polymers. For more than 30 yr, electronic providers have produced items such as cell phones, personal computers/laptops and televisions with ever-increasing ultra-clear displays. These technologies would not be

possible without the advancement of liquid crystal polymers technology.

Although first discovered in the late 1800s by Austrian botanist and chemist Friedrich Reinitzer, liquid crystals did not find commercial success until nearly 100 yr later. In the late 1880s, Reinitzer was experimenting with cholesteryl benzoate. While heating the organic chemical, he noticed that it changed from a white solid to a hazy liquid, which then turned clear at higher temperatures. According to literature, Reinitzer observed that the liquid passed through two different color forms before returning to the original white solid form. Reinitzer concluded that the substance passed through two different melting points, which should not exist—German chemist Wilhelm Heintz observed the same phenomenon while conducting similar experiments on fatty acids in the mid-1850s.[194]

Reinitzer sent his findings to German physicist Otto Lehmann. Upon heating the material, Lehmann viewed the reaction under a microscope. As the solid changed into a milky liquid, Lehmann observed multiple small crystalline formations with irregular borders.[194] After additional testing and review, Lehmann believed this phase was a new state of matter, one between a solid and a liquid. He named the substance liquid crystals and published his findings "About floating crystals" in Zeitschrift für Physikalische Chemie (*Journal of Physical Chemistry*) in 1889. This was the first publication on liquid crystals.[195]

However, no commercial applications were discovered using liquid crystals. It was not until the late 1940s that extensive research began to be conducted on liquid crystals applications for commercial endeavors. This included works from the following references described in literature:[196]

- English researcher George William Gray: His book *Molecular Structure and the Properties of Liquid Crystals* provided a detailed understanding on designing molecules that exhibit the liquid crystalline state. His work would be instrumental in the future adoption of liquid-crystal displays (LCDs).
- American chemist Glenn H. Brown: His liquid crystals conference in the mid-1960s gathered the world's most-prominent scientists on the subject and was a catalyst for worldwide research efforts on the advancement of liquid crystals technologies research.
- Richard Williams and George Heilmeier: Their work at RCA Laboratories in the U.S. in 1962 were the origins of using a liquid crystal-based flat panel display to replace the cathode ray vacuum tube used in televisions. However, to be used effectively, the compound used in the process (para-azoxyanisole) to create a nematic liquid crystal state required too high of a temperature ($> 116°C$) to make it a practical application for television displays. In 1966, while working within the Heilmeier group, Scientists Joel Goldmacher and Joseph Castellano were able to create nematic liquid crystals at room temperature by altering the compounds used in the process. This enabled RCA to produce the first practical display device.

In 1972, George Gray and Ken Harrison worked with the Royal Radar Establishment in Malvern, England to produce stable liquid crystals for small LCDs within electronic products.[196] Additional research in the 1980s led to an extensive use of liquid crystal polymers in display devices (i.e., LCDs for television, mobile phones, personal computers and laptops) and other products within the automotive, electronics and medical sectors. Today, many companies produce liquid crystal polymers (e.g., Celanese, Polyplastics, Solvay, Sumitomo Chemicals and Toray Industries), and forecasts show the liquid crystals polymers market to reach nearly $2.5 B by 2030.[197]

Conducting polymers. Prior to the 1970s, it was a common belief that plastics could not conduct electricity. However, research by three scientists changed the fundamental thought on the conductivity of polymers. This research would not only lead to the production of many different products for various industries, but also earned these men the Nobel Prize in Chemistry.

Conductive polymers are organic polymers that conduct electricity.[198] Research and discovery of partly conductive polymers date back to 1862. While working at the College of London Hospital, English chemist Henry Letheby obtained a partly-conductive material by anodic oxidation of aniline in sulfuric acid.[199] Additional research in the 1970s found that polythiazyl (polymeric sulfur nitrade) was superconductive at low temperatures, while several other conductive organic compounds were superconductive at high temperatures.[199]

In the early 1970s, Japanese chemist and engineer Hideki Shirakawa led a group that adapted Ziegler-Natta polymerization to produce well-defined, silvery films of polyacetylene (the work of Karl Ziegler and Giulio Natta is detailed in the History of the HPI section of the April issue).[199,200] During the same timeframe, American physicist Alan Heeger and New Zealand-born American chemist Alan MacDiarmid were researching the metallic properties of polythiazyl. The two scientists shifted their focus to polyacetylene after MacDiarmid met with Shirakawa in Tokyo.

In 1976, MacDiarmid, Shirakawa and Heeger (**FIG. 3**) collaborated on additional research focused on the conductivity of polyacetylene. In 1977, additional

FIG. 3. MacDiarmid, Shirakawa and Heeger were awarded the Nobel Prize in Chemistry in 2000 for their work on conductive polymers. Photo courtesy of the Nobel Foundation archives.

experiments showed that doping poly-acetylene with iodine increased its conductivity by seven orders of magnitude; similar results occurred using chlorine and bromine, as well. The trio published their findings in the article "Synthesis of electrically conducting organic polymers: Halogen derivatives of polyacetylene, $(CH)_x$,"[201] followed by two separate deeper dive articles into the technical research and conclusions of their work.

The efforts of MacDiarmid, Shirakawa and Heeger were instrumental in creating a new field of plastic electronics research, which gained prominence in the 1980s and led to numerous products and applications. These included anti-static substances for photographic film, shields for computer screens and smart windows that absorb sunlight, light-emitting diodes (LEDs), solar cells, displays in mobile phones and small television screens, batteries, specialty coatings, and many other applications.[198,202] For their contributions in the field of conducting polymers, MacDiarmid, Shirakawa and Heeger were awarded the Nobel Prize in Chemistry in 2000.

From tragedy to a safer industry. Notable industrial accidents occurred in the mid-1970s through the 1980s that led to stark changes in the way industry views safety. These included the Bhopal and Seveso disasters and the Phillips 66 Houston Chemical Complex explosion.

In July 1976, a chemical leak at a small chemical plant north of Milan, Italy exposed the surrounding region to high levels of 2,3,7,8-tetrachlorodibenzo-p-dioxin. The leak severely affected humans, wildlife and the environment. It was later determined that the plant had very rudimentary safety systems, it had not considered environmental protection during construction/operation and had no warning system or health-protection protocols for the surrounding communities.[203]

The Seveso disaster led to the adoption of the Seveso Directive in 1983. The directive (82/501/EC) aims to control major accident hazards involving dangerous substances, especially chemicals, and contributes to the technological disaster risk reduction effort.[204] The directive was superseded by Seveso 2 (1996)—also referred to as Control of Major Accident Hazards (COMAH)—and Seveso 3 (2012). These amendments were the re-sults of other industrial accidents that severely affected surrounding populations and the environment. The major take-aways from the Seveso Directives were the obligations placed on plant operators, which included mandatory safety reports, the establishment of a detailed safety management system and emergency action plans, and the deployment of major accident prevention policy, among others.[205] Today, the Seveso Directive applies to more then 12,000 industrial establishments in the EU and is widely considered a benchmark for industrial accident policy for nations around the world.[204]

Two other major industrial accidents in the 1980s changed the way the industry views process safety management: the Bhopal disaster and the Phillips 66 chemical plant explosion. The Bhopal disaster occurred in the late evening/early morning of December 2–3, 1984 in Bhopal, India. Shortly after midnight on December 3, up to 40 t of toxic methyl isocyanate leaked from the plant's storage tank and drifted downwind into the surrounding community.[206] The highly toxic material claimed the lives of thousands of people and resulted in more than 550,000 injuries.

The Bhopal tragedy led to new safety and environmental measures and government regulations in India. This included the Environmental Protection Act of 1986, which created the Ministry of Environment and Forests—the ministry was responsible for enforcing environmental laws and policies. It also led to the Factories Act of 1987; the Hazardous Wastes (Management and Handling) Rules; and the Manufacture, Storage and Import of Hazardous Chemical rules, both enacted in 1989, among other rules and regulations.[207] The Bhopal disaster also influenced the Seveso 2 amendment in Europe and raised awareness from governing bodies around the world that enhanced safety management systems were needed in industry.

In the mid- to late-1980s, several governmental safety organizations proceeded with advancing new safety management system regulations. For example, the Occupational Safety and Health Administration (OSHA) in the U.S developed the process safety management system regulation in the late 1980s. The regulation—still in use today—focuses on the handling, manufacturing, storage and onsite movement of highly hazardous chemicals.[208]

However, new regulations in process safety management in the U.S. were still a work in progress when an explosion happened at the Phillips 66 high-density polyethylene plant in Houston, Texas (U.S.). The series of explosions—caused by the release of flammable process gases that contacted an ignition source—on October 23, 1989, claimed the lives of nearly two dozen and resulted in hundreds of injuries.[209] The tragedy increased the focus on better process safety systems in dangerous work environments, especially in the refining and petrochemical industries. According to literature, several insights prevailed in the aftermath of the accident, including a better adherence to safe work practices and a better overall process safety and risk management program, the creation and adoption of new standards and regulations, the detrimental effects that can occur when safeguards are removed or disabled, and the need for operational discipline in plant operations.[210]

Unfortunately, the three industrial accidents mentioned here were not the last to occur within the processing industries. However, these major industrial tragedies led to an increased focus on process safety management at both refineries and chemical plants. They have left a lasting impression and have been responsible for new directives, standards and safety guidelines throughout the processing industries in an effort to keep plant personnel and surrounding communities safe.

Heavy oil upgrading. In 1984, the Association for the Valorization of Heavy Oils (ASVAHL) was assembled in France. The ASVAHL Analytical Group was comprised of the Institut Français du Pétrole [French Institute of Petroleum (IFP), which would later take the name IFP Energies nouvelles], Elf Aquitaine (a French petroleum and natural resources group that was acquired by Total Fina in 2000 and is now Total Energies)[211] and Total (now Total Energies).

The group's primary function was to research and develop new heavy-oil upgrading technologies. According to literature, the group's main objectives included developing straightforward methods for the conversion of heavy products and a better knowledge of the structure of heavy products.[212]

ASVAHL's research and findings led to the development of three major heavy-oil processing technologies: Hyvahl, Solvahl and Tervahl. The Hyvahol technology is a fixed-bed residue desulfurization process that enables refiners to produce ultra-low-sulfur fuel oil and low-sulfur diesel—the process is now licensed by Axens (the company was created by IFP in mid-2001 through its merger with Procatalyse Catalysts and Adsorbents).[213,214] The Solvahl technology (also licensed by Axens) is a solvent deasphalting process that removes asphaltenes, most metals and other impurities contained in atmospheric or vacuum residues.[215] Tervahl is a residue and heavy-oil conversion process by using thermal cracking.[216] These heavy-oil processing technologies are still in use today.

The rise of virtual/augmented reality: A precursor to the digital transformation. The 1980s not only witnessed the beginning of the rise in video gaming systems (Atari and Nintendo rose to prominence in the decade)—a market that would reach nearly $200 B in 2021—but also in the popularization of virtual reality (VR).[217]

One of the earliest VR systems was the Sensorama created by Morton Heilig in the mid-1950s. This "theater" included a stereoscopic color display, fans, odor emitters, a stereo sound system and a motion chair.[218] The mechanical device would use sights and sounds to simulate reality for the viewer. Heilig followed up his Sensorama invention with the telesphere mask in 1960 (**FIG. 4**). This mask was the first iteration of a head-mounted display (HMD) device for VR and is a rudimentary version of the HMDs available in consumer and industrial markets today.

In 1969, Myron Krueger created computer-generated environments that responded to the user. This system eventually progressed, leading to the creation of VIDEOPLACE. According to literature, this virtual world could analyze and process the user's actions in the real world and translate them into interactions with the system's virtual objects.[219] Krueger eventually termed this type of system "artificial reality."

Both VR and artificial reality [also known as augmented reality (AR)] research and development increased exponentially over the next several decades.
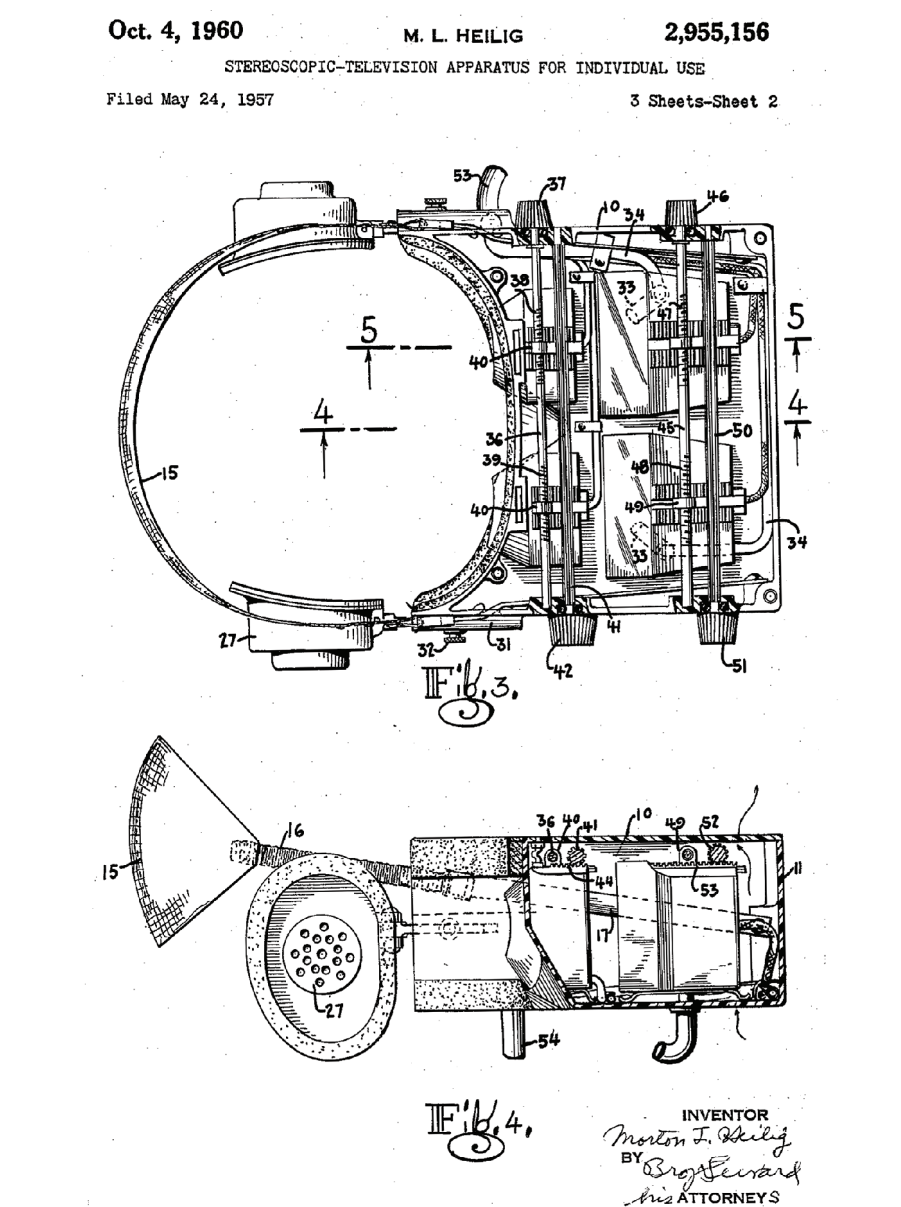

FIG. 4. Drawings of Heilig's telesphere mask from his patent Stereoscopic-Television Apparatus for Individual Use. Source: U.S. Patent Office, patent no. 2,955,156.

For example, many advances in VR/AR technologies happened in the 1980s. These included the creation of Sayre gloves that used optical sensors to detect finger movements, the creation of VPL Research by Jaron Lanier and Thomas Zimmerman (the company was the first to sell HMDs and gloves to consumers, and Lanier was the first to coin the term "virtual reality"), advanced flight simulators for pilots, and VR to train National Aeronautics and Space Administration (NASA) astronauts, among many others.[220]

Today, AR and VR are advancing technologies within the oil and gas and petrochemical sectors, primarily due to the industry's digital transformation. HPI professionals utilize AR/VR technologies for training, maintenance, planning, safety, engineering and design. The advancements in AR/VR systems are enabling the HPI to digitally enhance operations and safety throughout all sectors of the oil and gas and petrochemicals industries. The adoption of these technologies is forecast to increase the AR/VR market in the oil and gas industry to nearly $1 B by 2027.[221] **HP**

LITERATURE CITED

Complete literature cited available online at www.HydrocarbonProcessing.com

Excerpts from the 1980s: Energy efficiency, advanced process controls, improved maintenance and a focus on the environment

Can a computer reduce your maintenance?
J. H. Redding, January 1980

How do computers reduce costs and improve operations? What are some of the limitations? How do you justify a computer system? How large should your system be? These questions are answered here.

How to select hydrotreating catalyst
T. F. Kellett, A. F. Sartor and C. A. Trevino, May 1980

A comparison between cobalt/molybdenum (Co/Mo) and nickel/Mo (Ni/Mo) catalyst shows applications for desulfurization, denitrogenation and hydrogen uptake. Specifics are given for Shell catalysts to emphasize differences.

Make olefins from syngas
V. U. S. Rao and R. J. Gormley, November 1980

This catalyst of silicalite impregnated with iron and promoted with potassium has an exceptionally high selectivity for producing C_2–C_4 olefins from synthesis gas.

Chemicals from methanol
M. B. Sherwin, March 1981

Current and developing chemical synthesis based on methanol indicate dramatic demand growth as a feedstock.

How to evaluate distributed computer control systems
S. Cocheo, June 1981

Control systems and process engineers are faced with a wide variety of distributed systems to choose from. Which vendor's offering is best for each plant? Here are the factors the engineer must understand and evaluate to make a proper selection.

Better use of refining energy
D. J. Ducote and R. Ragsdale, September 1981

If you are not trying to save energy, maybe you should be. Here are some ideas for energy savings in the hydrocarbon processing energy.

Stop emissions from liquid sulfur
J. A. Lagas, October 1982

Serious environmental and safety problems can arise in the handling of liquid sulfur. Fatal levels of hydrogen sulfide (H_2S) can accumulate in the vapor spaces above the sulfur—or even flammable levels. Here is the story and how to handle the problem.

Convert to microprocessor controls without shutting down
M. E. Leister and R. R. Sanders, April 1983

Here is how this refinery converted 12 units (3,000 loops) to microprocessor-based controls without a process shutdown.

Convert steam balances into dollar balances
W. V. L. Campagne, June 1983

Use this method to determine the real value of steam, condensate and brake horsepower.

What is cogeneration effectiveness?
M. P. Polsky and R. J. Hollmeier, July 1983

Several evaluation methods of cogeneration effectiveness are analyzed, and their strengths and weaknesses presented.

How to upgrade heavy feeds
B. Schuetze and H. Hofmann

Refiners have many options for converting heavy black oil to light white oil. Here is a review of the choices.

Integrate gas turbine cogeneration with fired heaters
G. Iaquaniello, S. Guerrini, P. Pietrogrande and H. Dreyer, August 1984

Heat and power cogeneration is a potentially rewarding technique for achieving energy savings when applied to process industry systems. This article presets an innovative solution which can improve the efficiency of large petrochemical plants and refineries.

Make phthalic anhydride with a low-air-ratio process
L. Verde and A. Nari, November 1984

A new catalyst permits cutting the air ratio in half and reduces investment in energy consumption. This article features a novel proprietary process to produce phthalic anhydride.

Basics of fire protection design
J. D. Soden, May 1985

Most hydrocarbon processing facilities have an inherent potential for fire from materials and from processes and reactions being conducted. Little can be done to reduce or eliminate this potential. Fire safety design, therefore, addresses reducing the probability of fire occurrence (preventive design) and minimizing the consequences should a fire occur (protective design).

Turbines lower NO$_x$ emissions
F. Giacobbe, Y. Lee, P. Pietrogrande and G. Iaquaniello, October 1985

Combining gas turbine and conventional heaters for power and process use reduces pollution while making electricity and saving money.

What went wrong? Case histories
T. A. Kletz, December 1985

Murphy's Law: "If anything can go wrong, it will." To prove the point, here are examples of HPI losses and what can be done to prevent them.

Selecting your next MMA process
R. V. Porcelli and B. Juran, March 1986

Technological changes and end-use developments will affect the next round of methyl methacrylate (MMA) plants.

Career success and your self-image
E. Raudsepp, March 1986

Here is a step-by-step walkthrough of what it takes to be successful in your career, and a profile of failure patterns that damage career progress.

Special Report: Gas Process Handbook
April 1986

This complete review of processes for operations includes natural gas, sulfur, hydrogen, flue gas and cleanup, liquids treating, gasification, shift and methanation, and C_3–C_5 conversion.

AI and MAP in the processing industries
L. A. Kane, June 1986

Here are the principles of artificial intelligence (AI) and manufacturing automation protocol, and examples of their use in the processing industries.

Redesign catalyst to save energy
J. A. Russell, S. E. Lyke, J. K. Young and J. J. Eberhart, July 1986

Theoretical limits show the energy savings found when a catalyst is designed for optimum operation of a catalytic cracking unit.

How refinery inventories threaten profitability
G. M. Intille, July 1986

Inventory control may be second only to fluctuating crude oil prices in its potent challenge to refinery managers.

Use performance indices for better control
V. A. Bhandari, R. Paradis and A. C. Saxena, September 1986

Would it not be easier to control fuel usage in your automobile if it had a gauge that showed miles/gallon or kilometers/liter? Here is how to use your distributed control system (DCS) to do the same thing for your processes.

Avoid self-priming centrifugal pump problems
G. G. Reeves, January 1987

Design and installation guidelines ensure that horizontal self-priming centrifugal pumps operate correctly.

How construction affects column control
P. Mizsey, H. Hajdú and P. Földes, February 1987

In the development of control strategies for distillation columns and absorbers, generally no attention is paid to the construction parameters and the type of built-in trays of the column. This article compares the responses of various trays to flow disturbances to show how column control is affected.

Europe's future gasoline options
May 1987

Legislative limits on engine emissions and fuel properties have severe consequences for Europe's cars and fuels. Estimates are given for refining options.

Include tech service engineers in turnaround inspections
J. E. Miller, May 1987

Startup problems can be reduced because of the unique perspective that process and technical service engineers have on equipment operation. Here is how to include them.

Advanced Process Control Handbook
March 1988

More than 100 strategies for advanced control of refining, gas processing, petrochemical and utility processes are presented. To make the handbook more complete, the best of previously published control strategies are included in abbreviated form without diagrams. New descriptions are presented with half-page diagrams so that more could be included.

Low-cost ammonia and CO$_2$ recovery
V. A. Shah and J. McFarland, March 1988

Using a low-energy CO_2 recovery process on the syngas intended for ammonia production results in an overall lower cost ammonia plant. Data are given to compare capital and operating costs.

Modern control tricks solve distillation problems
H. F. Bozenhardt, June 1988

Replacing old controls with a new DCS and implementing the advanced control algorithms described here provided a 2-mos payout on this azeotropic distillation column.

Ways to revamp urea units
F. Granelli, June 1988

Several factors should be examined when considering a revamp of a urea plant. Experience teaches which parts of the unit are likely to be involved.

Economics of new MTBE design
A. M. Al-Jarallah and A. K. K. Lee, July 1988

Methyl tertiary butyl ether (MTBE) is produced industrially by the catalytic reaction between methanol and isobutene. The catalyst that is widely used is an acidic ion exchange resin. This article explores design and economics when sulfuric acid is the catalyst.

Build an effective group for instrumentation systems
W. E. Fullen, August 1988

A skilled, experienced, efficient team is needed because of the advancement in recent years by microprocessing/electronics.

Magnetic bearings and dry seals improve compressor operation
J. Fort and J. Jehl, October 1988

An advanced oil-free compressor featuring active magnetic bearings and dry gas seals has been operating successfully for more than 7,500 hr. Here is a description of the project.

Better ethylene separate unit
V. Kaiser and M. Picciotti, November 1988

An ideal column concept guides improvements to ethylene plant gas separation. This results in better efficiency from limited investments.

Reduce olefin plant fouling
J. F. Martin, November 1988

Process-side fouling reduces the overall operating efficiency of an olefin plant. The fouling is commonly caused by the formation of organic polymers that can also contain small amounts of inorganic constituents. This article provides several case studies to show the results of effective remedies for fouling in various locations of the olefin plant.

Operational speed balancing: Should you be doing it?
L. Fisher, January 1989

Vibration is one of the primary enemies of rotating equipment and eliminating or lessening vibration can significantly improve operating efficiency and system longevity. Since a large portion of vibration problems in high-speed turbomachinery is due to an unbalanced motor, operational speed balancing of the rotor might achieve these objectives.

Refinery heat integration using pinch technology
K. L. Lee, M. Morabito and R. M. Wood, April 1989

Direct and indirect integration schemes for crude oil refining applications are compared using pinch technology procedures.

Data reconciliation: Getting better information
P. J. Lawrence, June 1989

Good data are essential to control and information systems. Here is how to use data reconciliation to improve instrumentation and corporate decision-making.

Bioremediation on the move
C. H. Vervalin, August 1989

The current frenzy in the HPI to meet groundwater protection needs is bringing with it some interesting developments in soil-contamination activity. For example, microbes with a taste for hydrocarbons can be grown to remove oily waste from dirt. These "bugs" promise to chew their way through some of the HPI's waste disposal problems. The future is not here yet, but it is coming.

Hydroprocess catalyst selection
C. T. Adams, A. A. Del Paggio, H. Schaper, W. H. J. Stork and W. K. Shifflett, September 1989

Flexibility in residuum hydroprocessing becomes a requirement as fuel oil demand weakens, crude slates tend to be heavier, and variability in crude oil cost and supply become the norm. One way of providing flexibility is to incorporate residuum hydrotreating ahead of a heavy-oil catalytic cracking unit that converts heavier components into lighter, more valuable products. Alternatively, significant conversion of the residuum to lighter products can be achieved by the operation of the residuum hydrotreater at a higher severity to facilitate hydrocracking reactions.

In both cases, the proper combination of catalysts for the desired feedstock selection and more of operation is critical for economic hydroprocessing operations. This article focuses on the design and selection of catalytic systems in the framework of a unified reactor modeling scheme for such residuum hydroprocessing applications.

Guidelines for rotating equipment
O. P. Goyal, October 1989

Engineers, designers and operators must know certain facts about rotating equipment process concepts, design aspects, operating needs and troubleshooting methods. Experience has shown that a list of selected guidelines makes their jobs more effective. In this article, guidelines are compiled for centrifugal pumps, centrifugal compressors, reciprocating compressors, electric motors and steam turbines.

HPI 1990 Outlook: A Special Report
December 1989

The HPI will spend $117.5 B in 1990, with $66 B earmarked for petrochemicals alone. Approximately $18 B will go into maintenance. Capital expenditures are forecast at $27.4 B, with around $13.7 B being spent on equipment and materials. A construction boom is helping to drive the "big bucks" outlay.

Simulator trains for new equipment use
H. Elston and D. Potter, December 1989

This "stepping stone" approach to training operators uses a process simulator as one of the steps. Trainees adapt quickly, willingly. **HP**

HP | Process Optimization

M. B. MATAR, A. AL-MANE and **A. Y. LAYRI,**
Kuwait National Petroleum Co., Ahmadi, Kuwait

MAA refinery's experience producing Europe's most-stringent diesel specification

The European climate has one of the harshest winter weather conditions—therefore, diesel products' cold flow properties [i.e., cloud point (CP) and cold filter plugging point (CFPP) parameters] are key to ensure diesel products' usability during these climate conditions. Kuwait National Petroleum Company's (KNPC's) Mina Al-Ahmadi (MAA) refinery has conducted studies and field trials to establish its capabilities to produce ultra-low sulfur diesel (ULSD) that adheres to a CFPP of –22°C and to achieve the ARAL (owned by bp, ARAL has the largest filling station network in Germany) test's requirements. Wax anti-settling flow improver (WAFI) additives were procured from different suppliers during two separate periods to carry out the studies while modifying the units' mode of operations. The MAA refinery's revamped gasoil desulfurization unit and new diesel hydrotreating (DHT) unit were utilized in the trials. The DHT unit was one of the processing units commissioned for KNPC's Clean Fuels Project (CFP), which was awarded *Hydrocarbon Processing's* Top Projects award in 2016.

This article provides a comprehensive analysis of cold flow properties of the ULSD product and the MAA refinery's experience in producing ULSD to adhere to the European Union's (EU's) most stringent diesel specification.

A guide for ULSD. ULSD was mandated by the U.S. Environmental Protection Agency (EPA) in 2006 by phasing in stringent regulations for diesel fuel with a sulfur content of 15 mg/kg parts per million (ppm).[1] In Europe, the European Parliament and the Council of the European Union mandated diesel fuel production with a maximum sulfur content of 10 mg/kg ppm. This mandate went into effect on January 1, 2009, with the aim of reducing emissions of conventional pollutants from the existing fleet of vehicles to improve air quality.[2]

Classification for Grade F diesel fuels for temperate climates and Class 0 diesel fuels for arctic zones in accordance with EN 590 standard specifications[3] are depicted in **TABLES 1** and **2,** respectively. Grade F diesel fuel is the most stringent limit for temperate climates, while Class 0 diesel fuel is the lowest limit for arctic climates.

Cold flow properties of diesel fuel are typically represented by CP and CFPP parameters. CP is the temperature at which wax precipitation occurs[4] and CFPP is like a low-temperature flow test (LTFT), which is used to estimate the filterability of diesel fuels in some automotive equipment at low temperatures with the following exceptions:

1. The fuel is cooled by immersion in a constant temperature bath, making the cooling rate nonlinear but comparatively much more rapid.
2. CFPP is the temperature of the sample when 20 ml of the fuel first fails to pass through a wire mesh in less than 60 sec.[4]

To improve cold flow properties in diesel fuel, a few techniques may be considered by refiners, such as reducing the distillation endpoint by considering the presence of n-paraffins in the heaviest fraction; reducing the initial point for better overlap with the kerosene cut; selecting more naphthenic and aromatic fractions than paraffinic fractions (mainly affected by crude oil origin); operating a dewaxing bed in the hydrotreating unit; and injecting additives in the form of middle-distillate flow improvers (MDFIs), along with waxy anti-settling additives (WASAs) or wax anti-settling flow improvers (WAFIs). The latter is a combination of MDFIs and WASAs, which are used to meet the cold flow property requirements and to ensure that diesel fuel passes the KPI 130 ARAL sediment test, as mentioned in Research Report 787 of the DGMK German Society for Sustainable Energy Carriers, Mobility and Carbon Cycles.

Background and challenges. Kuwait Petroleum Corporation (KPC), which is KNPC's parent company and marketing entity, wanted to market low-sulfur diesel fuels that adhere to the most stringent European specifications. In December

TABLE 1. Grade F diesel fuels (EN 590 standard) for temperate climates

Property	Lower limit	Upper limit
Cetane number	51	–
Cetane index	46	–
Density at 15°C, kg/m³	820	845
CFPP, °C	–	–20

TABLE 2. Class 0 diesel fuels (EN 590 standard) for arctic climates

Property	Lower limit	Upper limit
Cetane number	51	–
Cetane index	49	–
Density at 15°C, kg/m³	800	845
CFPP, °C	–	–20
CP, °C	–	–10

2017, a study was carried out to establish the company's capabilities for this goal. The scope of the study covered DHT units at both the MAA and Mina Abdullah (MAB) refineries.

The units can achieve the required CFPP limit with dewaxing and CFPP additives. However, the study did not elaborate on the specific requirements of feed and product needed for the additive to be effective. Furthermore, the study concluded that the additive's vendors will be the final entity in determining the quantity required to achieve the desired final specification. The study utilized kinetic programs to estimate the requirement for both DHT units at the MAA and MAB refineries, based on estimated unit design parameters.

The following crucial details were essential for chemical selection:

- Feed and product specific parameters and the distillation range required for the additives to be effective
- The feed blend and difficulty to meet the specific gravity limit in accordance with the EN590 standard
- The expected properties of the individual feed streams to the MAA refinery's DHT units
- Required additives
- Approval requirements for the additives
- Information about the type of additive (not limited to WASAs, MDFIs and WAFIs)
- A clear representation of economics (inclusive of the requirement details for kerosene to achieve final specifications).

Previously, KNPC had designed CFP units to meet a mild cold properties specification that was achievable, as tabulated in **TABLE 3.** The challenge was the ability to produce diesel with 10 ppm sulfur and adhering to a CFPP limit of −22°C. The study concluded that the MAA refinery has different options, including revamping the DHT unit, operating the dewaxing bed or testing a specialized chemical additive—or a combination of these options.

The CFP units have been designed for a 6-pt CP upgrade. To comply with the CFPP requirements as per EN590 Euro 5 diesel, a further 6-pt upgrade by means of cold flow improvers is required. The primary challenge is to investigate the consequences on the CFP units. The study provides insights on the capability of the CFP units' diesel product to either achieve a CFPP of −20°C (base case Euro 5 specification) or −22°C (stringent specification)

TABLE 3. KNPC DHT and gasoil desulfurization units (CFPP equals CP −2°C; an upgrade in CP means an upgrade in CFPP)

Unit	Δ CP, °C	CFPP, °C	Cold flow additives
DHT (MAA refinery)	6	-14	No
DHT (MAB refinery)	6	-14	No
New gasoil desulfurization unit (MAA refinery)	6	-14	No

TABLE 4. DHT and gasoil desulfurization units' feeds

Unit stream	Pour point, °C*	CP, °C	CFPP, °C
DCU diesel	2	4	2
ARD distillate 1	-14	-7	-8
ARD distillate 2	-12	-10	-12
CDU light diesel	-12	-6	-8
EOC light diesel	-51	-51	-44

TABLE 5. DHT and gasoil desulfurization feed properties

Properties	Coker diesel	Old ARD diesel	CFP ARD diesel	CDU light diesel	EOC light diesel
Specific gravity at 15°C (60°F)	0.882	0.863	0.8632	0.851	0.8607
Nitrogen, ppm	930	815	350	85	75
Sulfur, wt%	0.54	0.095	0.055	1.6	1.61
Monoaromatics, wt%	20	45	45	11.1	18.8
Diaromatics, wt%	15	9	9	5.7	6.1
Triaromatics, wt%	5	0	0	1.4	1
Total aromatics	40	54	54	18.2	25.9
Distillation	D86 lv%	D86 lv%	D86 lv%	D86 lv%	D86 lv%
Start, °C	263	189 (initial boiling point)	181 (initial boiling point)	186	172 (initial boiling point)
5°C	283	214	203	243	206
10°C	290	229	210	259	214
30°C	303	268	245	273	238
50°C	312	292	271	286	261
70°C	322	311	296	304	287
90°C	338	334	337	335	320
95°C	345	345	345	345	334
98°C	353	350 (end boiling point)	371 (end boiling point)	362	352 (end boiling point)

based on the original design feed or with a change in the catalyst bed operations. Also, the study evaluated the product properties for these cases to quantify any revamp scope. Furthermore, it also explored the use of additives [CFPP, lubricity, anti-static additive (ASA) and WASA], including the quantity required for the changed mode of operation. This also necessitated laboratory requirements for diesel specification based on new analytical methods.

All units are single-stage catalytic dewaxing DHT units. The hydrotreating process scheme is an integrated stripper concept with a vacuum dryer. To limit the diesel yield loss, the CFP units have been designed for a 6-pt CP upgrade.

The hydrotreater dewaxing (catalyst bed) scheme impacts product properties—some properties are intentionally changed, and others can be corrected due to the stripper and/or dryer design. Conversely, some properties are changed (improved or worsened) because of hydrotreating reactions, while some are feed-related properties that are determined by the inside cleanliness of the unit. However, most important are the properties that affect fluidity, like CP, which relates to catalyst bed operations and specification, including CFPP.

For most of the units, the feed is a mix of raw diesel and cracked and atmospheric residue desulfurization (ARD) units' distillate. **TABLE 4** summarizes the main parameters of the feed composition. The original blended design feed had a CP of –6°C. The product received a Δ improvement of 6°C for the winter cases. Without additives, the CFPP product in the winter case equaled –14°C. Therefore, the original CFPP specification of –20°C can only be met if CFPP additives are applied. The DHT and gasoil desulfurization feed properties are detailed in **TABLE 5**.

CFPP can be achieved by dewaxing bed operations and partly by CFPP additives. Furthermore, a lubricity additive, WASA and ASA must be added to achieve product specifications. The unit should be revamped to meet specifications, as the dewaxing capabilities are utilized to reach the CFPP specification for the base and the stringent specifications. However, the lubricity additive, WASA and ASA are still required to meet the specification.

To increase catalytic dewaxing capabilities, the weighted average bed temperature (WABT) in the dewaxing bed must

be increased compared to the original design. For a single-stage catalytic dewaxer, this means that the hydrogen desulfurization catalyst must be operated at higher WABTs, as well. There will be product giveaway with respect to sulfur. The product stripper overhead air cooler is too small in these cases. In addition, the reactor effluent trim cooler is too small, so the cold low-pressure separator offgas cooler in the hydrogen sulfide removal (HSR) unit, which is dedicated to the DHT unit offgas stream, was proposed to be replaced.

Due to the higher production of naphtha in these cases, the increase in vapor and liquid traffic in the product stripper might cause flooding. Currently, the product stripper is designed with conventional trays. The advice was to re-tray the stripper using proprietary trays. Some nozzles (naphtha streams) exceeded the maximum impulse momentum. A risk-based inspection was deemed an effective barrier to mitigate this. The gas load (impulse momentum) on the high-pressure absorber increased by approximately 22%. The high-pressure amine absorber is fitted with conventional trays.

It was advised to re-tray the column with high-capacity trays. The product stripper offgas is treated in the HSR unit. The low-pressure absorber for the HSR unit is likely to be replaced. Vacuum dryer packing should be increased without revamping the dryer. This will generate deteriorated slops quality. This is indicated by the fact that ASTM D86 T98 changes from 172°C to 226°C. The specific gravity changes slightly. The quantity will slightly increase (2.18 × the normal design rate), which will affect the crude distillation unit (CDU) if not designed for this function. Otherwise, the dryer slops can be safely routed to a slops tank, as the dryer slops have been stabilized. Vessels handling more naphtha will see lower holdup times as the capacity increases. The recycle gas compressor is a turbine-driven centrifugal compressor. As the megawatts (MW) increase by 22%, the compressor should be evaluated by the vendor if it cannot perform its duty.

Calculations show that increasing the dewaxing in the unit to meet the CFPP of –20°C or –22°C results in yield losses vs. the base case, as shown in **TABLE 6**.
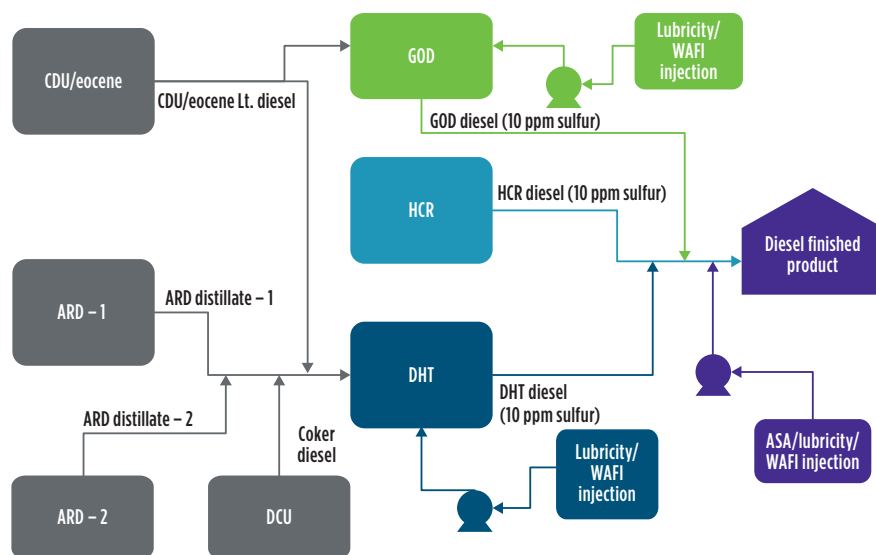

FIG. 1. Diesel configuration at the MAA refinery.

TABLE 6. DHT mode of operations

Property	Base Case	Winter	Stringent
Unit feed rate, bpd	45,000	45,000	45,000
CFPP, °C	–14	–20	–22
Naphtha, bpd	3,540	5,308	7,641
Diesel, bpd	42,488	40,445	37,966
Diesel yield, vol%	94.4	89.9	84.4

The main issue is diesel yield loss vs. the costs of CFPP additive injection. Increasing the dewaxing abilities of the catalyst to –20°C or –22°C results in substantial diesel yield loss, as diesel is converted to naphtha (slops) and offgas, as well as a reduced cycle length for the stringent CFPP –22°C case. For the dewaxing cases, a significant economic loss is incurred. Therefore, the costs for the revamp compound the financial losses; it is financially beneficial to achieve the required CFPP specification of –20°C or –22°C by using additives. The original design of the MAA units was promising, so a partial product upgrade by dewaxing and by CFPP additives was adopted.

A pilot plant was initiated with a licensor and a division of KNPC. However, due to the unavailability of a location and some other disputes, the Kuwait Institute of Scientific Research (KISR) was engaged to address some of the concerns. Unfortunately, due to confidentiality issues between KISR and the licensor, the pilot plant remained on hold and was sub-sequently canceled. After discussions with Kuwait Petroleum Corporation and obtaining required details/approvals for the additives considered, the MAA refinery decided to perform its own analysis and studies on producing winter-grade ULSD.

The process began by communicating with various vendors, performing initial unit trials, conducting analytical testing in both the vendors' and the MAA refinery's laboratory facilities to pinpoint the requirements based on reports from the vendors, procuring sample additives from selected vendors, and performing the field trial. The field trial is the final hurdle for the MAA refinery to confirm its capabilities to produce winter-grade ULSD in the actual plant environment.

Unit configuration. KNPC has two refineries—MAB and MAA—that can produce clean-burning fuels conforming to Euro 5 standards. It has a major share in boosting Kuwait's global position in the oil refining industry. In the MAA refinery, three processing units can produce ULSD: the revamped gasoil desulfurization unit, the CFP DHT unit and the hydrocracking (HCR) unit.

As per design, KNPC will produce Euro 5 diesels for the local market and export requirements from all units. The gasoil desulfurization unit will consume the diesel stream from the CDU and eocene (EOC) unit as its primary feed, while the feed streams going to the DHT unit are a combination of multiple diesel/distillate streams from the CDU, the EOC unit, the ARD unit, the delayed coker unit (DCU) and the fluidized catalytic cracking unit (FCCU). Therefore, feed blending is one of the critical considerations for DHT operation in the MAA refinery. Meanwhile, HCR consumed vacuum gasoil and produced 10 ppm sulfur diesel as one of its products. **FIG. 1** details the diesel configuration at the MAA refinery. No additive injection facilities are available at the HCR unit. This is compensated by higher injection at the gasoil desulfurization unit or offsite facilities (finished product site) in case of any off-specification situation. Simplified block flow diagrams of the MAA refinery's gasoil desulfurization and DHT plants are shown in **FIGS. 2** and **3,** respectively.

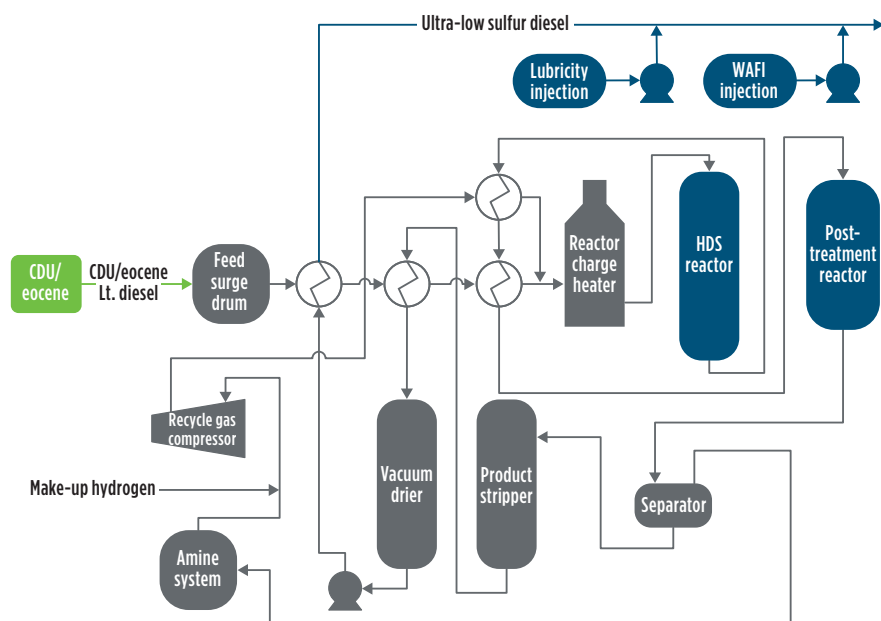**Lab-scale analysis.** Understanding diesel characteristics is essential in deter-

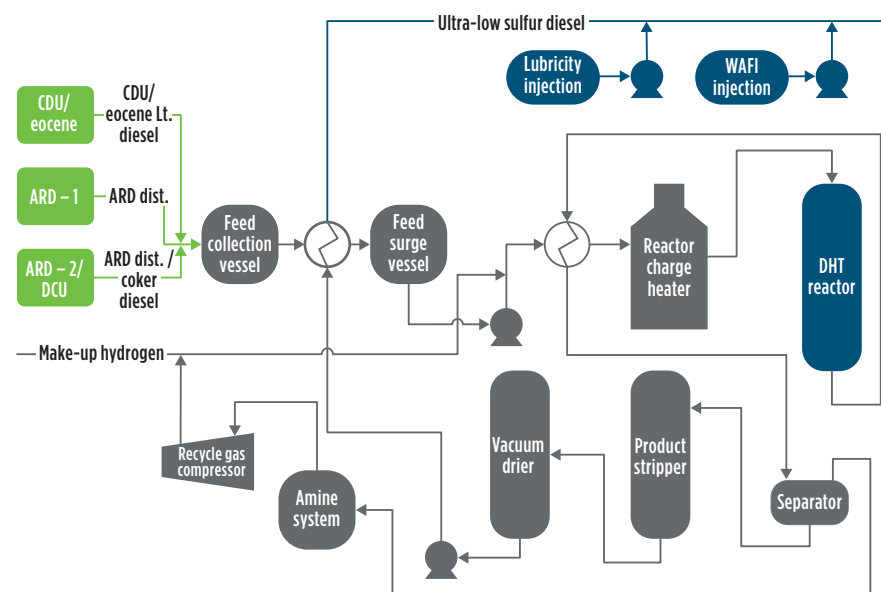**FIG. 2.** Simplified block flow diagram of the MAA refinery's gasoil desulfurization plant.

FIG. 3. Simplified block flow diagram of the MAA refinery's DHT plant.

mining suitable treatments for improving cold flow properties. Narrow boiling diesel is a fuel with a Δ (T90%–T20%) lower than 100. Such diesel is unresponsive to cold flow additives and requires high-performing WAFI solutions to meet both CFPP European winter-grade specifications and ARAL pass requirements. Ultra-narrow boiling diesel is a fuel with a Δ (T90%–T20%) lower than 80. This diesel is extremely unresponsive to cold flow additives and requires the latest top-tier additive technology to meet both CFPP European winter-grade specifications and ARAL pass requirements. In such cases, kerosene blending is a common option used by refiners.

Based on the results of the analytical testing conducted at the additive vendors' and MAA laboratories, the following characteristics are observed for both ULSD products from the gasoil desulfurization and DHT units. The results for the DHT sample are provided in the absence of dewaxing operations. The characteristics are divided into three main categories:

1. Cold flow properties—represented by CP and CFPP
2. Boiling distillation range—indicated by the actual distillation temperature at 90% recovery minus the actual distillation temperature at 20% recovery Δ (T90%–T20%)
3. Wax content.

FIG. 4 depicts the typical n-alkane distribution in diesel fuel. **Note:** The carbon numbers C23–C31 represent diesel fuel tail and normally characterize the wax content.

Cold flow properties. The gasoil desulfurization sample base characteristics do not meet the desired CP limit of –7°C; the CP for the product stream is –5°C. The DHT sample base characteristics meet the desired CP limit of –7°C. The dewaxing bed for the DHT unit is not activated for the sample collection.

Boiling distillation range Δ (T90%–T20%). In gasoil desulfurization, the diesel fuel has a narrow boiling distillation range of 90°C. In the DHT unit, the fuel has an ultra-narrow boiling distillation range of 75°C.

Wax content. In the gasoil desulfurization unit, the amount of wax at the CFPP target is in the average area, and the wax anti-settling should be achievable. In the DHT unit, the wax amount at the CFPP

target is remarkably high, and the wax anti-settling test is challenging to pass.

Two improvement techniques are considered for the cold flow properties during the laboratory analysis stage. These improvements are interrelated and consist of (1) adding kerosene, which is important to achieve a better additive treating rate, and (2) injecting additives by varying the dosage rate. The kerosene-blended sample provided a different treating rate than the original diesel fuel sample. Typical CFPP response curves are shown in **FIG. 5,** considering the CFPP target as per the CFP design and stringent targets.

Kerosene addition analysis. Adding kerosene will widen the distillation breadth between carbon number 8 (C8) and C13. This will slow the wax precipitation rate by reducing the steepness of the fuel tail (represented by C23–C31).

In the gasoil desulfurization unit, kerosene is blended to achieve a lower CP

by considering the minimum flash point constraint. Furthermore, the CFPP target is achieved at a lower treating rate.

In the DHT unit, kerosene blending widens the distillation breadth of the sample. The CP, which is already meeting the target, is lower than the CP limit, causing quality giveaway. In addition, the CFPP target of –22°C is achieved only with this sample.

Additive response curves. In the gasoil desulfurization unit, a CFPP of –22°C can be attained through additive injection. For the gasoil desulfurization sample diluted with kerosene, the CFPP target is achieved at a lower treating rate.

In the DHT unit, the CFPP target is not achievable for the DHT sample without kerosene dilution; however, this target can be achieved when using a sample with diluted kerosene.

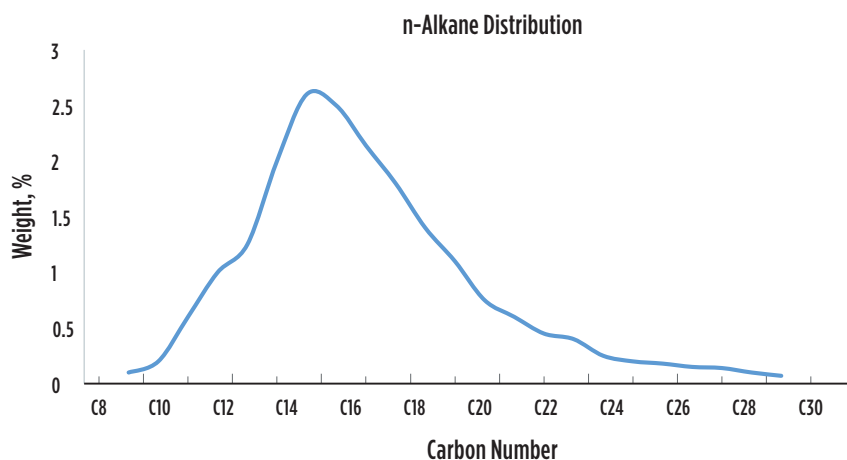**KNPC field test.** To diversify the target markets for the ULSD product, the MAA

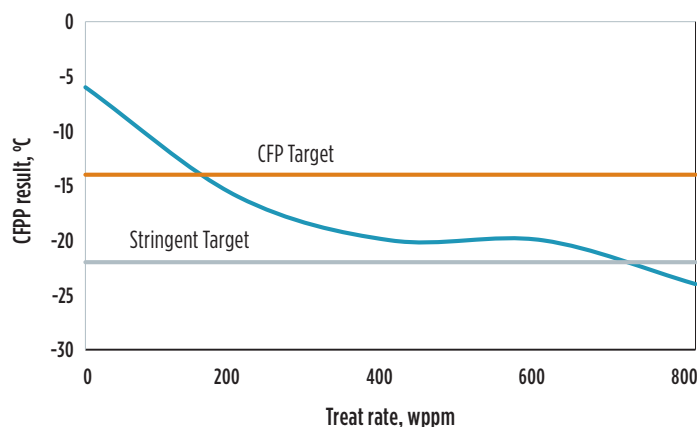**FIG. 4.** Distribution of n-alkane in diesel fuel.

FIG. 5. CFP response curves with additives treatment.

TABLE 7. Finished product results

Property	Additive A	Additive B
Cetane number	53.7	55.1
Cetane index	53.4	55
Density at 15°C, kg/m³	842	834
CFPP, °C	–29	–29
CP, °C	–15	–12

refinery evaluated WAFI additives from multiple suppliers to meet the target cold flow properties limit.

Preliminary studies conducted by two different suppliers concluded that ULSD produced from the MAA refinery's DHT unit has an ultra-narrow distillation range, which is less than 80°C. ASTM Test Method D86 determines the distillation temperature considered for the diesel fuel product. The target endpoint for the feed stream is between 350°C–355°C, with an initial point target of less than 197°C. Based on the narrow distillation range and wax content profiles, both suppliers offered a specific type of WAFI additive for a field trial (i.e., Additive A and Additive B). Upon completion of the lab-scale analysis and chemical procurement process, the WAFI field trial was scheduled to establish the MAA refinery's capabilities in actual refinery operation.

Preparation stage. A multidisciplinary team composed of operational planning (coordinator), process engineering, operations and the laboratory was formed to implement the field trial. The field trial was conducted in two phases with Additive A and with Additive B at different periods. The selection of finished tanks was significantly important to ensure that there was no interruption to the supply of committed diesel product for local and export customers.

In terms of diesel-producing units (i.e., gasoil desulfurization and DHT units) and the preparation of upstream units, the distillation initial point and endpoint for the feed streams were controlled to achieve a Δ (T90%–T20%) above 80°C. The operations and process engineering divisions monitored unit conditions closely prior to the target date of the field trial by adjusting the unit parameters, such as the column separation temperature and severity of the units. Subsequently, the dewaxing bed of the DHT unit was activated to achieve a preliminary CFPP of approximately –15°C to –17°C. These actions are to ensure a better additive response to the diesel product.

During the field trial. The additive was injected through the unit's injection facilities to achieve the desired CFPP temperature of less than –22°C. The injection dosage rate was closely monitored and controlled as per the recommended rate by each supplier. Samples were collected during every shift to test the key parameters and to ensure additive effectiveness and product qualities. Other important parameters that were monitored were the density at 15°C, which must be less than 845 kg/m³, as well as a CP of less than –7°C. Furthermore, other additives injected to meet lubricity and electrical conductivity parameters were controlled as per existing practice to meet the final specification. Once the tank filling was completed, the existing sampling and analysis procedure was undertaken against the winter-grade specification agreed upon with KPC. The final finished tank results for each field trial are shown in **TABLE 7.**

Various blends were used during both trials to ensure diversity in future conditions and to establish the additives response and behavior during these conditions. Blends consisted of gasoil desulfurization, and DHT and HCR products, while other blends considered only dewaxed DHT products and gasoil desulfurization and HCR products separately.

Post field trial. The challenges faced during the field trial were consolidated and then discussed by the team members. Some of the key challenges were resolved during the first phase of the field trial, such as injection pump failure and off-specification in one of the parameters during tank filling. Other challenges (e.g., a wild kerosene stream that was routed to slop, which was observed during the first phase, and which affected crude unit operations) were resolved prior to Phase 2 by routing the same to a kerosene desulfurizer unit. Furthermore, an economic assessment was carried out of the additional cost that was incurred during the field trial to evaluate the MAA refinery's competitiveness in selling winter-grade ULSD product.

Takeaways. To adhere to Europe's most stringent diesel specifications, KNPC performed two field trials with two different WAFI additives to achieve a CFPP limit of less than –22°C. This was accomplished by adjusting the upstream units' stream qualities to meet the required distillation range, the operation of the DHT unit's dewaxing bed and the controlled additives' dosing rate. Still, overall optimization is critical to ensure economic viability.

The CFPP limit can be achieved by controlling the feed stream's condition to achieve a Δ (T90%–T20%) of more than 80°C for better WAFI additive response toward the final diesel product. Further dosing rate controls of other additives are equally important to achieve the desired product specifications.

With this accomplishment, the MAA refinery is in the position to diversify its target market, strengthen KNPC's position in the export market and produce clean diesel products that conform to the latest European standards. HP

LITERATURE CITED

[1] U.S. EPA, "Final rule for control of air pollution from new motor vehicles: Heavy-duty engine and vehicle standards and highway diesel fuel sulfur control requirements," January 18, 2001, online: https://www.govinfo.gov/content/pkg/FR-2001-01-18/pdf/01-2.pdf

[2] EU, "Directive 2003/17/EC of the European Parliament and of the Council of 3 March 2003 amending Directive 98/70/EC relating to the quality of petrol and diesel fuels," March 2003, online: https://eur-lex.europa.eu/legal-content/EN/TXT/?qid=1435618704689&uri=CELEX:32003L0017

[3] European Committee for Standardization, "EN590: Automotive fuels and diesel requirements and test methods," October 2021.

[4] Rand, S. J. and A. W. Verstuyft, *Significance of Tests for Petroleum Products,* 9th Ed., ASTM International, West Conshohocken, Pennsylvania, January 2018.

MOHAMMAD B. MATAR is a chemical engineer and the Team Leader for Operational Planning at KNPC. He has experience in refinery operations, planning and process engineering.

ALI AL-MANE is a chemical engineer with more than 15 yr of experience. He works in operational planning and has played a significant part in the commissioning of the MAA CFP.

ABDUL AZIZ Y. LAYRI is the Operations Section Head for Hydrotreaters at KNPC's MAA refinery. He has more than 17 yr of experience in the refining industry and earned a BS degree in chemical engineering from the University of Dayton in Ohio.

HP | Process Optimization

B. BUECKER, ChemTreat, Lawrence, Kansas; and **J. POWALISZ,** Sentry Equipment Corp., Milwaukee, Wisconsin

HRSG water/steam sampling: Do it right or face potential consequences

Many large industrial facilities—including refineries, and chemical and petrochemical plants—are increasingly turning to co-generation for process steam and power production. Popular for many applications, including the power industry, are combined-cycle units with heat recovery steam generators (HRSGs). Many HRSGs operate at high temperatures and pressures, where the harsh conditions can transform seemingly minor chemistry upsets into major problems. Unit outages and employee safety are two primary concerns of poor water/steam chemistry. Online water/steam chemistry monitoring is critical not only for normal chemistry control, but also to detect upsets. However, if samples are not extracted and conditioned properly, the data may give false indications of actual conditions in the unit. This article examines three primary issues regarding HRSG water/ steam monitoring, including the:
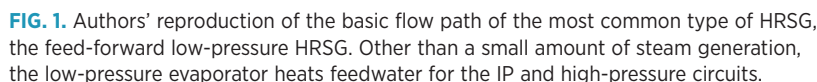
- Selection of critical measurements to maintain normal operating conditions, establish chemical feed control and detect chemistry upsets
- Importance of proper sample extraction and conditioning to ensure that online instrument data is accurate
- Benefits of iron monitoring, as these measurements provide direct data on the efficacy of steam-generator chemical treatment programs.

Regarding the last item, iron monitoring is particularly important for tracking flow-accelerated corrosion (FAC), which, over the last 30 yr, has caused several serious accidents—some with fatalities—at several conventional power plants. The tight radius elbows in HRSG low-pressure evaporators and economizers can be particularly susceptible to FAC.

Important monitoring parameters. The authors have seen many HRSG sampling system design specifications in which some important chemistry analyzers were omitted while others were overspecified. The following text offers a basic outline of the critical instrumentation for typical multi-pressure HRSGs, with the understanding that every project should be evaluated per the HRSG design and operating conditions. Much of this information is condensed and updated from literature.[1,2] In addition, references cited within this article offer expanded discussions on these topics.

Compared to coal-fired units, HRSGs have a radically different design. Most notably, the various waterwall tube and superheat/reheat panels (i.e., harps) are aligned in sections along the flue gas path. The water tubes in a coal unit basically form the walls (thus the name "waterwall") of a box that surrounds the combustion zone. This design is necessary to control the ash that forms during coal combustion. A positive aspect of the coal boiler configuration is that the tubes are reasonably accessible for repair in the event of a failure. The tight packing of tubes in an HRSG can make repairs very difficult, which further enhances the need for good corrosion control.

The most popular high-pressure HRSG design has three steam-generating networks (**FIG. 1**), where the low-

FIG. 1. Authors' reproduction of the basic flow path of the most common type of HRSG, the feed-forward low-pressure HRSG. Other than a small amount of steam generation, the low-pressure evaporator heats feedwater for the IP and high-pressure circuits.

pressure circuit essentially serves as a feedwater heater for the intermediate- and high-pressure circuits. Although

ments to monitor system performance, including pressure, temperature, flow and specific conductivity. The recommended

With a tight condenser, sodium levels in the condensate are normally very low (< 2 ppb) and, in many cases, are less than 1 ppb. An increase in sodium provides the earliest indication of a condenser tube leak.

> Many HRSGs operate at high temperatures and pressures, where the harsh conditions can transform seemingly minor chemistry upsets into major problems. Online water/steam chemistry monitoring is critical not only for normal chemistry control, but also to detect upsets.

once-through HRSG designs exist, most HRSGs are drum-type units. The common term for HRSG boilers is "evaporators," which will be used throughout the remainder of this article.

While coal ash issues are non-existent in HRSGs, some HRSG steam-generating tubes may have fins, which can collect particulates that impede heat transfer. While various methods have been developed (and continue to evolve) for external tube cleaning, the close packing of tubes can still make cleaning a complicated task.

The following sections outline recommended HRSG water/steam chemistry monitoring parameters, and why these choices are critical for reliable and safe operation.

HRSG water/steam chemistry monitoring recommendations. The sampling locations of primary importance throughout the steam-generating network are:
- Makeup treatment system
- Condensate pump discharge (CPD)
- Feedwater/economizer inlet
- Boiler water
- Saturated and main/reheat steam.

Makeup treatment system. No system is completely closed, and, even in the tightest steam generators, a small amount of process water/steam is lost via controlled blowdown or at leaking valves and other fittings. Losses must be made up with high-purity water. The most common makeup process is reverse osmosis (RO) followed by either mixed-bed ion exchange (MBIX) or electrodeionization (EDI) to polish the RO effluent. RO units are normally equipped with several instru-

instrumentation and normal limits of the ion exchange polisher effluent are:
- Specific conductivity: ≤ 0.1 µS/cm
- Silica: ≤ 10 parts per billion (ppb)
- Sodium: ≤ 2 ppb.

Continuous online measurement ensures consistent high-purity makeup water. An increase in any of the values indicates that either the MBIX resin has reached exhaustion or that a problem has occurred in the EDI unit; therefore, prompt corrective action is necessary.

CPD. In steam-generating power units, the primary spot for potential contaminant ingress is the condenser (if it is water-cooled), where a tube leak allows cooling water to infiltrate the high-purity condensate. Cooling water in-leakage will introduce a variety of impurities, including hardness ions, sodium, chloride, sulfate and silica, which, when subjected to the harsh environment in the steam generator, can cause serious corrosion or scaling problems. A condensate polisher can provide a buffer against contaminant ingress; however, polishers are often not installed on drum units, primarily to reduce project capital cost.

The following are recommended with online CPD analyses:
- Cation conductivity: ≤ 0.2 µS/cm
- Specific conductivity: Consistent with pH (as generated by ammonia or ammonia/amine feed)
- Sodium: ≤ 2 ppb
- Dissolved oxygen: ≤ 20 ppb
- pH: 9.6–10 (this is the pH range for the CPD/feedwater of the HRSG design in **FIG. 1;** the range may be lower for some other HRSG designs).

Sodium monitoring is very effective for detecting condenser tube leaks.

Cation conductivity is now often referred to as "conductivity after cation exchange (CACE)" to represent that the sample is routed through a cation exchange column to replace the cations (e.g., ammonium, sodium, calcium) with hydrogen ions. This creates a very diluted acid solution of primarily trace amounts of chloride and sulfate ions, whose conductivity is then measured. CACE eliminates the artificial influence of ammonia on conductivity and is more sensitive than specific conductivity. As with sodium, an increase in CACE indicates impurity in-leakage, although this measurement is influenced by carbon dioxide (CO_2) ingress (e.g., from increased air in-leakage at the condenser). Therefore, degasified CACE is becoming increasingly popular, which utilizes either a reboiler or nitrogen sparging compartment to remove CO_2. A low CACE value is a requirement for proper control of all-volatile oxidizing treatment [AVT(O)] chemistry, which is recommended for condensate/feedwater treatment to minimize FAC.[2,3] An issue that can influence CACE accuracy appears in units where a neutralizing amine is utilized as a supplement to, or in place of, ammonia. These compounds decompose to small-chain organics and CO_2 in high-temperature steam. The organic compounds are not removed in a degasifier, thus artificially increasing conductivity. CACE readings may become worthless in those cases.

Dissolved oxygen analyses are important for monitoring condenser air in-leakage. A sudden dissolved oxygen increase may indicate a mechanical failure at or near the condenser, which allows excess air to enter the system. However, with modern AVT(O) chemistry, some dissolved oxygen is required for the chemistry to be effective.[2,3]

Regarding specific conductivity and pH, ammonia (or sometimes an ammonia/amine blend) is the pH-conditioning agent for condensate/feedwater. However, the direct pH measurement of high-purity water can be tricky. Algorithms

have been developed to accurately calculate pH based on specific conductivity and CACE measurements. Specific conductivity in high-purity condensate is directly correlated to the ammonia concentration; therefore, specific conductivity measurements offer better control of ammonia feed than pH.

Total organic carbon (TOC) is a parameter that is not typically monitored continuously, but which can sometimes be of great importance. Organics can break down at high temperatures to form small-chain organic acids that can disrupt instrument readings such as CACE. TOC is often performed on a periodic grab sample basis, but, at co-generation facilities where organic compounds may infiltrate condensate return, online TOC can be quite valuable.

Note: At co-generation facilities where condensate from steam heating processes is returned to the boilers, the potential exists for impurity ingress from many other locations. This added complexity may require additional or supplemental analyses to those described in this article. Extra condensate treatment methods may also be required to minimize corrosion and deposition in steam generators. Additionally, any number of waste heat boilers may exist at large industrial plants. These may require additional sampling parameters to those outlined in this article.[4,5]

Low-pressure economizer inlet/ boiler feed pump discharge. Unlike conventional fossil units, feedwater heaters (apart from economizers) are not common in HRSGs. Accordingly, recommended feedwater sample points and normal limits are like CPD. These include the following:

- CACE: ≤ 0.2 µS/cm
- Specific conductivity: Consistent with pH
- Sodium: ≤ 2 ppb
- Dissolved oxygen (range): 5 ppb–10 ppb
- pH: 9.6–10.0 (this is the pH range for the HRSG design shown in **FIG. 1;** the range may be different for other HRSG designs)
- Iron: ≤ 2 ppb.

The 5 ppb–10 ppb dissolved oxygen range is in line with the AVT(O) guidelines recommended for nearly all HRSGs—unless, for some reason, the feedwater system contains copper alloy materials. With proper chemistry control to minimize corrosion, the iron limit should be readily achievable. Higher values suggest FAC in the system.

Evaporator water. Evaporator water sampling is critical for two primary reasons. First, poor chemistry control and/ or poor monitoring can allow unacceptable carryover of impurities to the steam. Secondly, and as is the same in conventional units, the highest heat fluxes occur within the evaporator circuits, and particularly in the HP evaporator of HRSGs. Therefore, the effects of impurity ingress or poor chemistry are magnified by the high temperatures and pressures in these circuits.

The recommended boiler water analyses include the following criteria:

- pH (< 8, immediate boiler shutdown)
- CACE
- Specific conductivity
- Chloride
- Silica
- Phosphate (for those units on phosphate treatment)
- Iron: < 5 ppb.

There are no direct limits for most parameters. Limits or recommended ranges are variable, based on boiler pressure and treatment chemistry. Detailed guidelines are available directly from the International Association for the Properties of Water and Steam (IAPWS).[6,7] A key aspect of these guidelines is to maintain sufficient alkalinity to prevent corrosion by chloride and sulfate. Also, evaporator readings in conjunction with steam analyses are important for monitoring impurity carryover to steam.

Regarding the limit for iron, the low-pressure drum in an HRSG can suffer from a phenomenon known as two-phase FAC. In this mechanism, much of the ammonia injected for feedwater pH control flashes off with steam, leaving a mixture of water droplets and steam at a lower pH, which can induce FAC of the drum internals.

For decades, tri-sodium phosphate has been a core boiler water treatment chemical in many drum units. However, control of phosphate concentrations is challenging due to the compound's reverse solubility above approximately 250°F (**FIG. 2**).

The reverse solubility (hideout) of tri-sodium phosphate above approximately 250°F can cause significant difficulties for plant chemists or operators, especially where units regularly cycle up and down in load. The guidelines outlined in literature[4] offer a valuable tool for phosphate chemistry control.

Some plant personnel, especially at conventional units, have switched to caustic (sodium hydroxide) boiler water treatment to eliminate phosphate hideout. Great care is required with these programs to prevent caustic gouging of waterwall tubes. The control of such issues for balancing chemistry may be beyond the experience of HRSG operators.

Steam. Steam purity measurements are very important, particularly if the steam drives a turbine. Contaminant deposition on turbine blades can lead to corrosion and possibly to blade failures, which can cause a potentially catastrophic situation with the turbine spinning at several thousand revolutions per minute. Core monitoring parameters include the following:

- CACE: ≤ 0.2 µS/cm
- Sodium: ≤ 2 ppb
- Silica: ≤ 10 ppb.

Sodium provides a direct indication of salt or sodium hydroxide carryover to steam. Salts—particularly chloride salts—will settle in the last stages of the low-pressure turbine, where they can cause pitting and subsequent stress corrosion cracking (SCC) and corrosion fatigue of turbine blades and rotors. Sodium hydroxide carryover is a very serious issue, as caustic can quickly induce SCC in turbine components.

CACE provides an indirect measurement of chloride and sulfate carryover, and the ≤ 0.2 µS/cm normal limit has been a long-time guideline for turbine manufacturers. However, data indicates
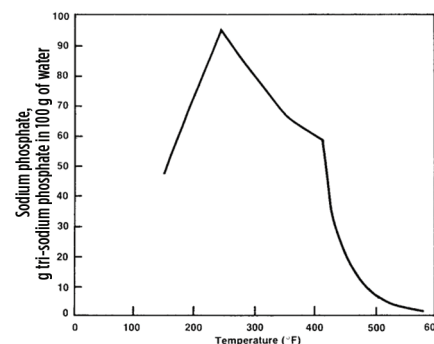

FIG. 2. The solubility of tri-sodium phosphate vs. temperature.

that chloride and sulfate may be well above 2 ppb at the recommended CACE limit. A relatively new instrument offered by an instrumentation provider[a] allows analyses of these two impurities down to a 0.1-ppb level.[8] The instrument separates ions via the process of capillary electrophoresis. The ions are then measured by a conductivity analyzer.

It has long been known that silica in steam will precipitate on turbine blades. While the compound is not corrosive, it can influence turbine aerodynamics and reduce efficiency. Therefore, 10 ppb is the recommended limit.

Sampling with saturated, main and reheat steam is normally recommended for power boilers. Main and reheat steam are the most important, as they provide data on impurities directly entering the turbine. Besides drum carryover, impurities can come from contaminated attemperation water. Such contamination should also be detected by feedwater instruments. Conducting saturated steam sodium measurements on a periodic basis is typically recommended to evaluate mechanical carryover from steam drums. Failed or damaged steam separators in evaporator drums are common causes of

mechanical carryover. Rapid load swings can also induce carryover.

The criticality of proper sampling and conditioning. The quality of data from the sample analysis system is dependent on the integrity of the samples provided to the sensors and analyzers. It is imperative to consider all aspects of the sample path from point of extraction, sample transport, sample conditioning, and analyzer care and maintenance.

The objectives of any good sampling system are to provide a statistically significant sample to the measurement tool that is representative of the process. In the case of high-pressure, high-temperature steam and water sampling, this includes controlling the temperature, pressure and velocity of the sample from the point of extraction to the sensor.

Sample extraction. Liquid samples can be effectively extracted from a process line via a side of a pipe entry. Three o'clock or nine o'clock positions are best. The sample tap should never be placed at the bottom of the pipe.

For years, isokinetic nozzles were recommended for all steam samples (FIG. 3), as these nozzles are designed to

extract steam at the same velocity as the flow in the pipe to ensure representative samples. In recent years, however, some experts have questioned the need for isokinetic sampling on superheated steam lines, while recognizing that it is needed for saturated steam.

Another design detail that is important for high-temperature and/or high-pressure sample lines is a double isolation/root valve (FIG. 4). The double valves provide added protection for isolating a live sample. Some guidelines also call for the primary steam sample cooler to be placed remotely at the sample tap to convert the steam to condensate for its journey to the sample panel. However, these remote coolers are often difficult to access and to maintain with high ambient air temperatures. In most applications, superheated steam is brought to the sample panel as a vapor and is then condensed.

Sample transport. Depending on velocity, flowing samples, and especially liquids, can deposit or pick up solids. This effect is minimized when the linear velocity is 6 ft/sec. Additionally, high velocities could induce some erosion of the tube walls—although this would probably be minor, given that the recommended material is usually either 304 or 316 stainless steel.

For a standard 0.25-in. outside-diameter tube with a wall thickness of 0.049 in., a 6-ft/sec linear flowrate equates to 1,200 cc/min. More often selected is 0.375-in. outside-diameter tubing, where a 6-ft/sec linear flowrate corresponds to 3,300 cc/min, which can be much greater than the common requirement of 1,800 cc/min–2,200 cc/min. As a compromise, a linear flowrate range of 3 ft/sec to 6 ft/sec is standard, as this still ensures accurate analyses.
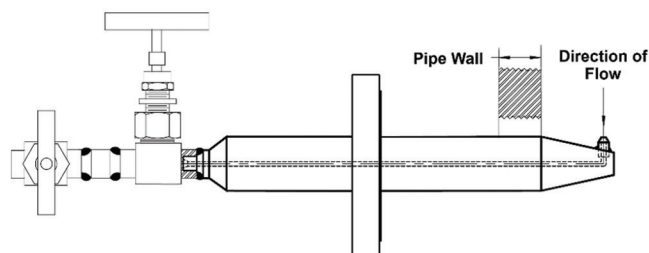

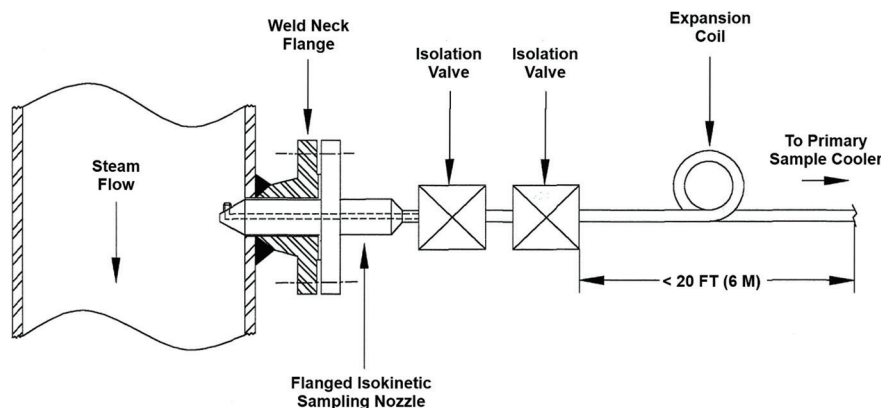**FIG. 3.** Diagram of an isokinetic steam sampling nozzle. Illustration courtesy of Jonas Inc.

FIG. 4. Diagram of a steam sample tap with a double isolation valve. Illustration courtesy of Jonas Inc.
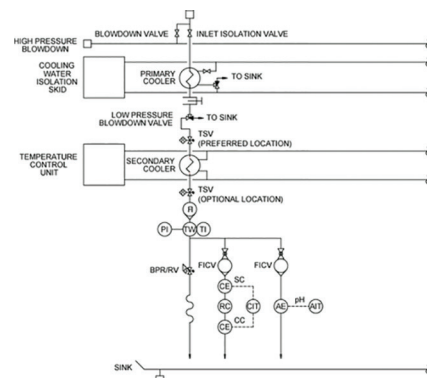

FIG. 5. Sample conditioning diagram.

Fittings and tubing bends should be kept to a minimum to limit pressure drop. Also, whenever possible, long sample runs should be avoided.

Sample panel conditioning details. **FIG. 5** outlines the common control devices and equipment for samples when they reach the sample panel. This diagram is for a sample with pH, specific conductivity and CACE online instruments. Virtually all the coolers, valves and other equipment shown in **FIG. 5** are recommended in various guidelines, including those of the Electric Power Research Institute (EPRI), ASTM International (formerly known as the American Society for Testing and Materials), and others.

Inlet isolation valves. An inlet isolation valve for each sample line should be used. Cases may arise where the entire sample panel must be isolated; however, much more frequent is the need to isolate a single line for equipment repairs and/or maintenance while the other lines remain in service. Isolation valves should not be used for throttling or pressure reduction and should remain either fully open or fully closed.

High-temperature blowdown valves. High-temperature blowdown valves should be periodically opened for a short duration to flush sample lines. Longer flushes are often necessary during startup after an outage. The valves discharge to piping that has been specially designed to handle high temperatures.

Primary cooling systems. A primary cooler is standard for lowering sample temperatures from process conditions to less than 122°F (50°C), with a common guideline of 100°F (38°C).

Filters. Once standard on many sample panels were sample filters, either mesh pads or magnetic filters, to protect downstream equipment. However, filters can affect the integrity of samples, particularly for iron monitoring, and the co-author's company does not officially recommend their use.

Pressure reduction. For sample pressures over 500 psig, a variable rod-in tube-pressure-reducing device is recommended. Below this pressure, traditional pressure control valves are sufficient. Panel design should include calculations for sample transport reduction induced by these valves.

Thermal protection. An automatic thermal shutoff valve on all high-temperature samples is recommended to protect operators and instruments in the event of the loss of cooling water to the primary sample coolers.

Secondary cooling systems. A standard feature of sampling systems is a secondary cooling circuit to moderate sample temperatures to 77°F (25°C), +/- 2°F. Most chemistry guidelines are based on this temperature. Many modern instruments have automatic temperature compensation, but variations in the chemical matrix and excessive temperatures can generate erroneous results. Secondary cooling systems provide uniformity across all samples, as variations in temperature from primary sample coolers are common. While some primary cooling systems may push the limit of primary cooler capacity, these secondary systems enable correction for these cases.

Total flow indication. A total flow rotameter is standard. It offers a straightforward method to observe if the sample flowrate is correct, or if it is too low or too high. Individual instruments also have rotameters to ensure that each sample is receiving the correct flow.

Grab sample pressure regulation. A typical feature of the sample panel is a grab sampling line for each sample. These ports enable operators and chemists to spot check conditions throughout the steam-generating network. Without a pressure-regulating valve (PRV), the low resistance through this line would short-circuit flow to the instruments. Grab sample PRVs can be adjusted in conjunction with the primary pressure-reducing valves to ensure that a consistent flow is provided to the analyzers throughout a range of conditions.

Iron monitoring. Iron monitoring continues to emerge as a primary tool for evaluating the efficacy of any HRSG corrosion control chemistry program. It is also a key tool to monitor for FAC. The industry has seen a continuous improvement in monitoring techniques, with four primary methods available:

- Continuous particulate monitoring
- Corrosion product sampling
- Grab sample analysis, using digestion to reach low detection limits
- Online nephelometric detection.

Note: Usually more than 90% of iron corrosion products in a steam generator exist as iron oxide particulates. Too often, plant personnel test for only dissolved iron. Serious corrosion may be underway, but when only testing for dissolved iron is used, this corrosion can go undetected by plant personnel.

Particulate monitoring. In the high-purity water of high-pressure steam generators, most particulates will be iron oxide corrosion products. Accordingly,

FIG. 6. A corrosion product sampler.

FIG. 7. Suspended particles of magnetite (black) and hematite (red) in water. Photo courtesy of Hach.

online particulate monitoring offers real-time measurements of these particulates, which, when converted to iron concentrations via grab sample tests, can provide suspended iron data. However, the lower size limit for detection is approximately 2 microns; therefore, very fine corrosion products may go unobserved.

Corrosion product samplers. A corrosion product sampler (CPS) has both a particulate filter and an ion exchange column or ionic filter papers to collect suspended and dissolved metal corrosion products (**FIG. 6**). Usually, samples are collected over a period of 1 wk–2 wk, and then the filter and ion exchange resin are analyzed for total iron and copper, if necessary. The product sampler has a
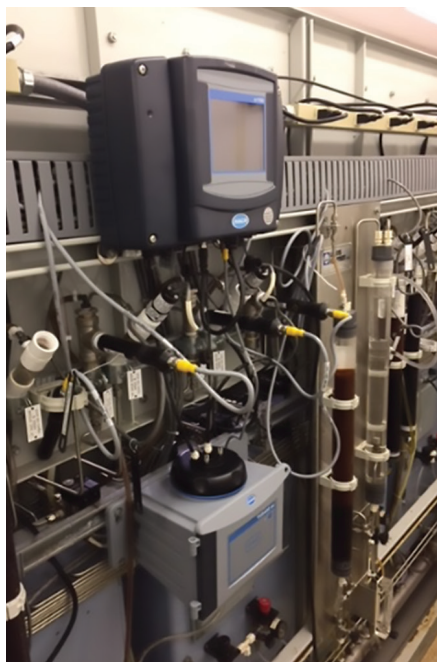

FIG. 8. An installed laser nephelometer. Photo courtesy of Hach.

flow totalizer, so that the average concentration of the products can be calculated.

A disadvantage of using a CPS is that it cannot track transients, and may miss a condition that has caused a significant problem.

Grab sample iron analyses. Straightforward colorimetric methods have long been available to monitor dissolved iron concentrations. However, most steam-generator carbon-steel corrosion products exist as iron oxide particulates. Modern chemistry is available to dissolve either magnetite or hematite particles to make total iron measurements (**FIG. 7**).[9]

A methodology developed by a water analysis solutions company[b] allows complete dissolution of particulate magnetite and hematite in a 135°C (275°F), 30-min closed vessel digestion using 240 µl of combination reagent and 12 ml of sample. The digestion is carried out in a 20-ml glass vial heated in an aluminum block. After the sample has cooled, the absorbance can be determined with a spectrophotometer and a 1-in. cell. Using this procedure, the calibrated range is 1 µg/l (ppb) to 100 µg/l (ppb), with a method detection limit of 0.3 µg/l.

Online nephelometric iron analyses. Straightforward colorimetric total-iron laboratory analyses combined with a sensitive laser nephelometric analyzer (**FIG. 8**) can provide cost-effective, quantitative, real-time corrosion monitoring. When the laser beam passes through high-purity water samples, any particulates scatter the light. The nephelometer captures the light deflected at a 90° angle to the laser beam.

When properly calibrated, the readings from a nephelometer can be correlated to total iron concentration values. Each spe-

cies produces a different nephelometric response. Black magnetite absorbs more and reflects less light than red hematite. Dissolved iron does not produce any nephelometric response (**FIG. 9**).

Variables (such as species, color and particle size) associated with iron corrosion products make it impossible to create a universal nephelometric calibration for the quantification of corrosion products. A calibration that is appropriate for a particular location with corrosion characteristics will be inaccurate for a different location with different corrosion characteristics. Therefore, quantification of total iron via nephelometry must be accomplished through site-specific calibration.

Takeaway. As much of the world transitions away from coal-fired units to renewables and other low-carbon technologies, combined-cycle power generation has evolved into a bridge technology. HRSGs are an important part of combined-cycle plants, where diligent monitoring and control of water/steam chemistry are essential for reliable operation. **HP**

LITERATURE CITED
[1] Buecker, B., "Monitoring of water and steam chemistry for steam generators," *Chemical Engineering,* September 2019.
[2] Buecker, B., S. Shulder and A. Sieben, "Fossil Power Plant Cycle Chemistry," 39th Annual Electric Utility Chemistry Workshop, June 4–6, 2019, Champaign, Illinois.
[3] EPRI, *Guidelines for Control of Flow Accelerated Corrosion in Fossil and Combined Cycle Plants,* The Electric Power Research Institute, Palo Alto, California, 2017.
[4] Buecker, B. and K. Kraetsch, "Advanced methods for controlling boiler tube corrosion and fouling—Part 1," *Hydrocarbon Processing,* October 2021.
[5] Buecker, B. and K. Kraetsch, "Advanced methods for controlling boiler tube corrosion and fouling—Part 2," *Hydrocarbon Processing,* November 2021.
[6] International Association for the Properties of Water and Steam, "Technical Guidance Document—2015 Revision: Instrumentation for monitoring and control of cycle chemistry for the steam-water circuits of fossil-fired and combined cycle power plants," 2015.
[7] International Association for the Properties of Water and Steam, "Technical Guidance Document—2015 Revision: Phosphate and NaOH treatments for the steam-water circuits of drum boilers of fossil and combined cycle/HRSG power plants," 2015.
[8] Buecker, B., "An advancement in steam turbine chemistry monitoring," *Power Engineering,* March 2018.
[9] Buecker, B., K. Kuruc and L. Johnson, "The integral benefits of iron monitoring for steam generation chemistry control," *Power Engineering,* January 2019.
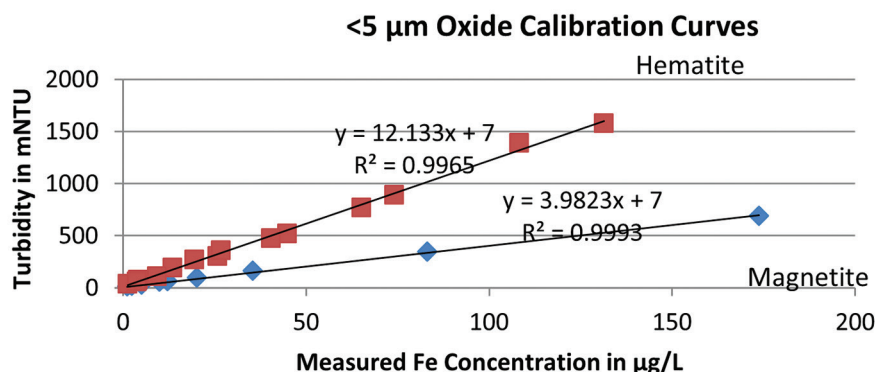
FIG. 9. An example of hematite and magnetite calibration curves. Illustration courtesy of Hach.

Caustic tower design guidelines and recommendations

A caustic tower is a critical piece of equipment in an ethylene plant that supplies feed to the downstream section after removing impurities. It mainly absorbs contaminants such as carbon dioxide (CO_2), hydrogen sulfide (H_2S) and acid gases that are harmful to the downstream process. If left untreated, CO_2 can freeze at lower (negative) temperatures and H_2S can deactivate the activity of catalyst for the acetylene reactor and hydrogenation reactor, which in turn leads to off-spec product. Additionally, any upset in the caustic tower may lead to reduced throughput and can force a complete plant shutdown, which directly affects a company's gross refinery margin.

FIG. 1 depicts a plant's caustic system where cracked gas is compressed with the help of a compressor and treated in the caustic tower to eliminate contaminants. The compressor may have 2–5 stages based on the pressure requirements along with a provision for the caustic tower between the stages.

A caustic tower is a combination of packing and trays that splits into different stages, such as weak, medium and strong caustic sections, based on concentration.

Cracked gas from a compressor's first-stage discharge enters the tower bottom section and comes in contact with weak caustic. In the weak caustic section, most acid gases are absorbed (compared to the remaining stages) and the remaining unabsorbed acid gases are later routed to the medium and strong caustic sections. A wash (water) section facility is also provided to wash over the entrained caustic from the cracked gas. All sections are provided with individual pumps for circulation of the caustic solution, shown in **FIG. 2.**

This article addresses major concerns associated with caustic towers during normal operation and startup, as well as troubleshooting and resolving these issues.

Small errors can quickly turn into larger issues if not corrected. These errors can be eliminated during design or resolved later to avoid abnormal condi-
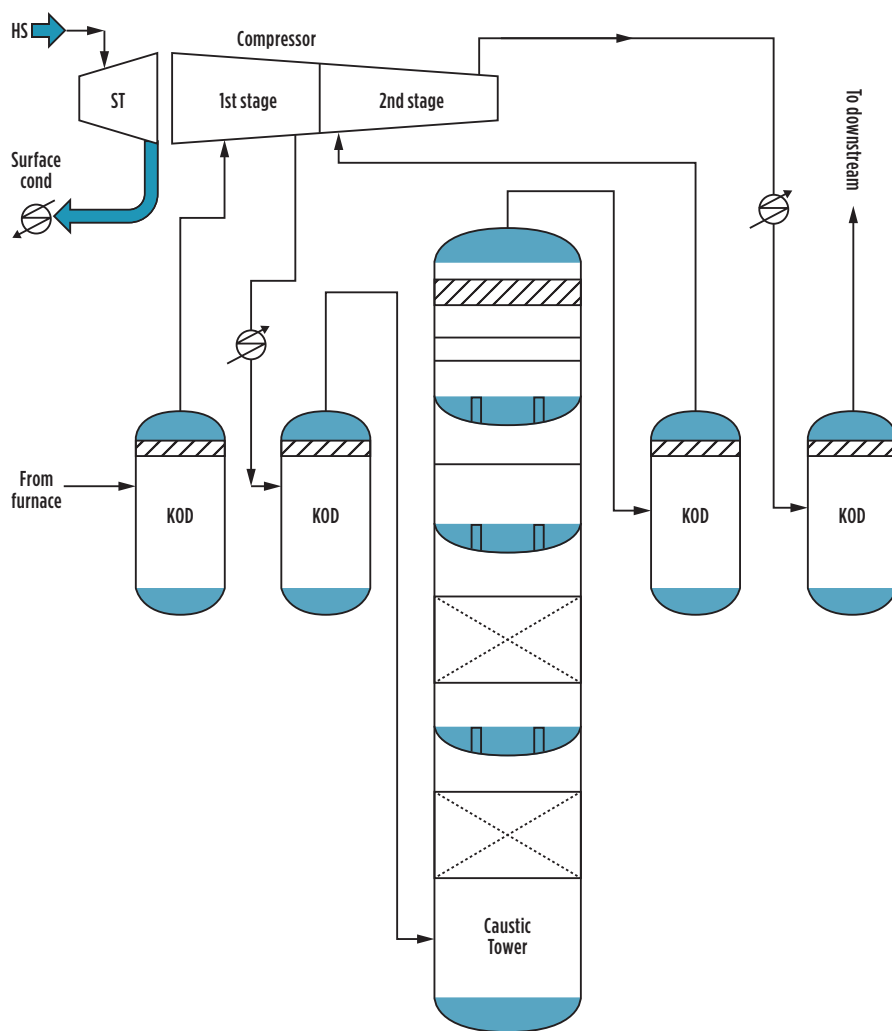

FIG. 1. Overview of a cracked gas compressor and caustic tower system with two stages and four knock-out drums. The flow direction of hydrocarbon is from the furnace to the compressor and the compressor to downstream through the caustic tower.
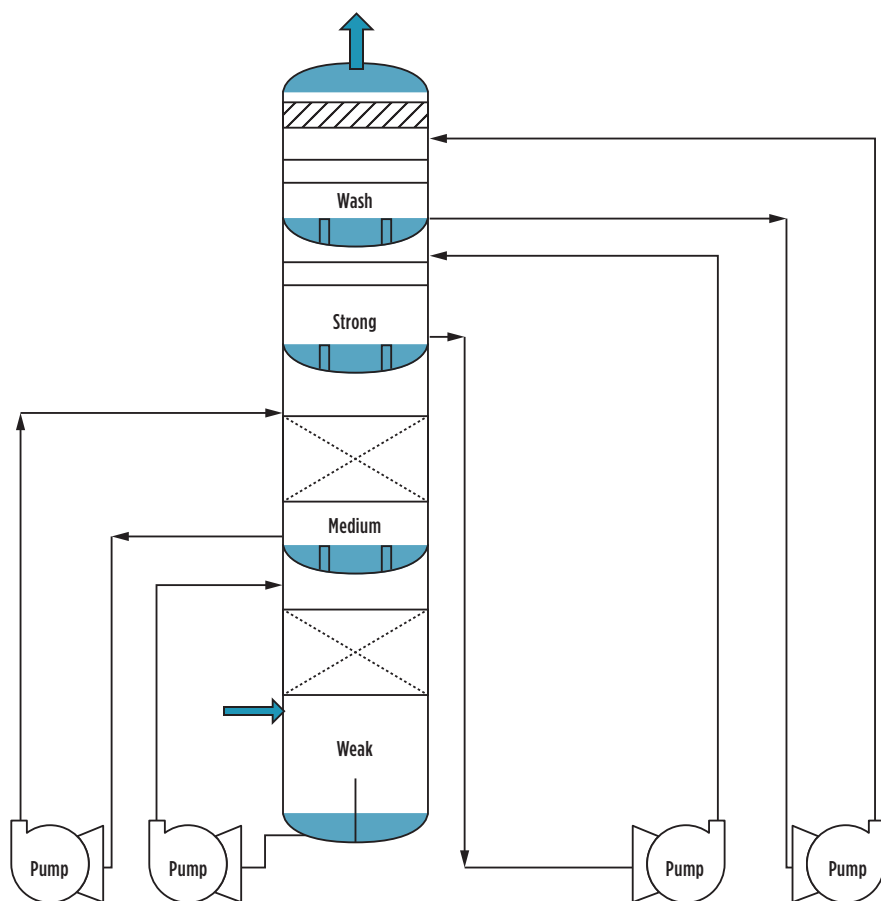
FIG. 2. Overview of a caustic tower with a circulating pump system. The column is classified into four sections: strong, medium and weak sections with caustic of 10%, 5% and 2% concentrations, respectively, along with a wash water section.

FIG. 3. Liquid dumping from packing to the riser and overflow pipe.

tions or upsets. Guidelines and a qualitative or heuristic approach are discussed for better understanding—learning from experience is good, but learning from the mistakes of others is wise and helps avoid any perilous event before it happens.

PROBLEMS ASSOCATED WITH CAUSTIC TOWERS

Liquid (an aqueous solution of caustic) dumping during startup and normal operation. Possible causes include:

- An aqueous solution of caustic (NaOH) dump from the upper section of the strong caustic (10%) to the medium caustic (5%) and weak caustic (2%) sections, leading to a reduction in levels of the strong caustic and medium caustic sections. As a result, a cavitation in the circulating pump is possible, or it may cause a trip if the makeup

of caustic is not compensating the quantity, leading to dumping. This is similar to throwing away valuable and unused things into a dustbin, which is costly and creates environmental pollution.
- Strong caustic dump through the riser pipes during startup (**FIG. 3**).
- Liquid dripping through an overflow pipe from the upper section to the lower (**FIG. 4**).
- Leakage through bolts of the bottom sump and tray support ring (TSR), as shown in **FIG. 5**.
- The use of a nonstandard gasket can lead to high corrosion and leakage.
- Liquid is distributed over the packing, and some part of that liquid is dumping through an overflow pipe (**FIG. 3**). If the overflow pipe arrangement is just below the seal pan of the tray due to a manufacturing defect, then a large
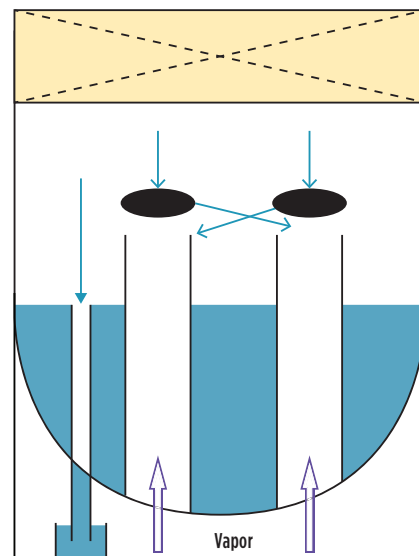
quantity of caustic solution will dump via the overflow pipe (**FIG. 4**). Solutions and recommendations include:
- The riser cap diameter should be at least 15% larger than the riser pipe diameter to avoid liquid ingress to the lower section. Additionally, it can be sloped (**FIG. 6**).[1]
- It is advisable that the overflow pipe and bottom sump should be seal welded (rather than bolted) to the shell of the column to reduce leakages (**FIG. 5**). If this is not the case, then a standard gasket made of polytetrafluoroethylene (PTFE) should be used to withstand the caustic environment. A sump can be welded with the shell rather than bolted since there is negligible thermal expansion due to high temperature (2°C–5°C temperature rise only).
- It is recommended to place the overflow pipe away from the seal pan or between the vapor riser, as shown in **FIG. 7**. If this is infeasible, then a cap (hat) arrangement should be provided on the overflow pipe to completely close it, and a V-notch on the side of overflow pipe should be provided to prevent caustic ingress (**FIG. 8**).
- An overflow pipe (downpipe) should be extended in the bottom; it should also be liquid sealed with a seal pan to avoid vapor blow (**FIG. 8**).
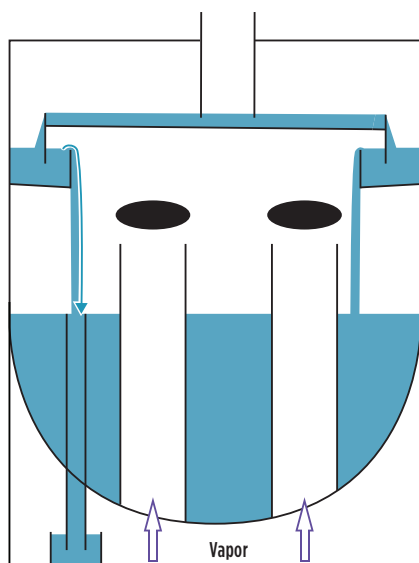
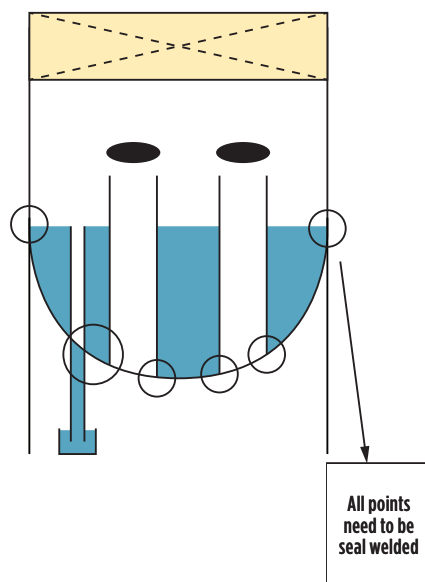**FIG. 4.** Liquid dumping from the seal pan to the overflow pipe.

All points need to be seal welded

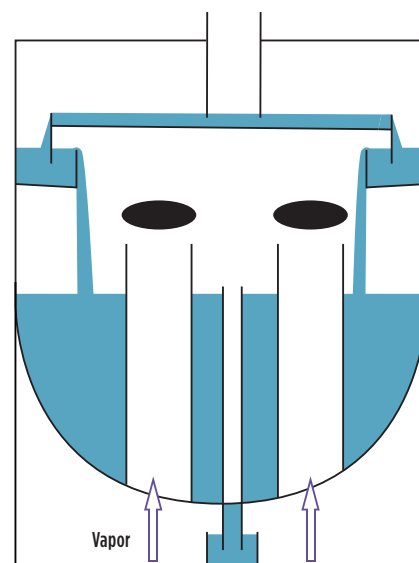**FIG. 5.** Leakage if not seal welded.

Vapor

FIG. 7. The downpipe is in the correct location and sealed.

Choking of demister pad and overloading with regard to liquid.
Possible causes include:
- The formation of yellow oil or red oil (an oligomer of hydrocarbons that is formed by an aldol condensation reaction) due to side reactions that can be entrained to the top demister by high velocity of gas during any upsets, such as surging and trip/startup of a compressor (**FIG. 9**).
- Carryover of fouling material and caustic salts can choke and plug the demister pad, potentially reducing the flow area and resisting the flow of gas to the compressor.
- Caustic/salts precipitation and entrainment during high velocities.
- Liquid can lead to carryover of caustic to downstream due to overloading of the demister pad.

Solutions and recommendations include:
- Individual pressure differential transmitters (PDTs) can be placed in demisters rather than a common PDT in addition to trays.
- A water wash facility can be provided across the demister pad whenever an increase in ΔP exists across the demister.
- A vane type demister that can withstand high liquid capacities can be used instead of a typical mesh type.
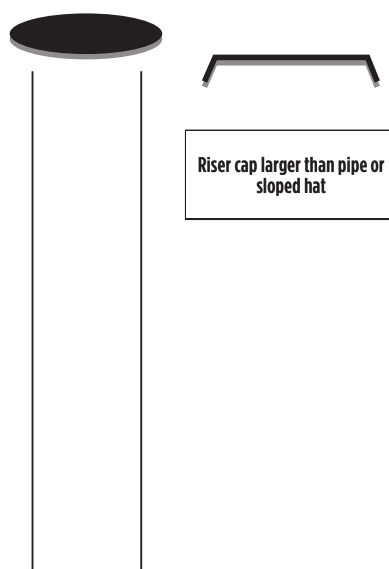

Riser cap larger than pipe or sloped hat

FIG. 6. The riser cap diameter should be greater and sloped.

- A demister pad should be made of stainless steel and have a higher efficiency (> 99%).

Instrument glitches.
Possible causes include:
- The formation of yellow/red oil due to side reactions and polymerization due to contaminants (e.g., vinyl acetate, hydroxide) from downstream units (HDPE/polypropylene). These polymers and gums can plug

Overflow pipe top closed and v notch
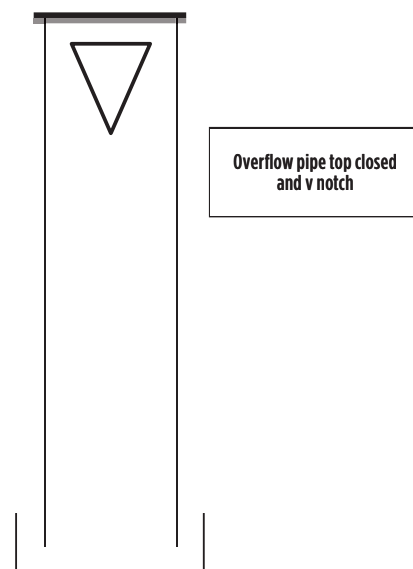
FIG. 8. The top of the overflow pipe is plate welded and V-notched.

the level transmitter tapping and show inaccurate level indication.
- At the bottom of the tower, two phases of spent caustic and hydrocarbon liquid (gasoline, yellow oil and red oil) exist simultaneously. Most of the level transmitters (LTs) calibrate with regard to water density only rather than both water and HC densities, which can lead to incorrect readings at the tower bottom due to density
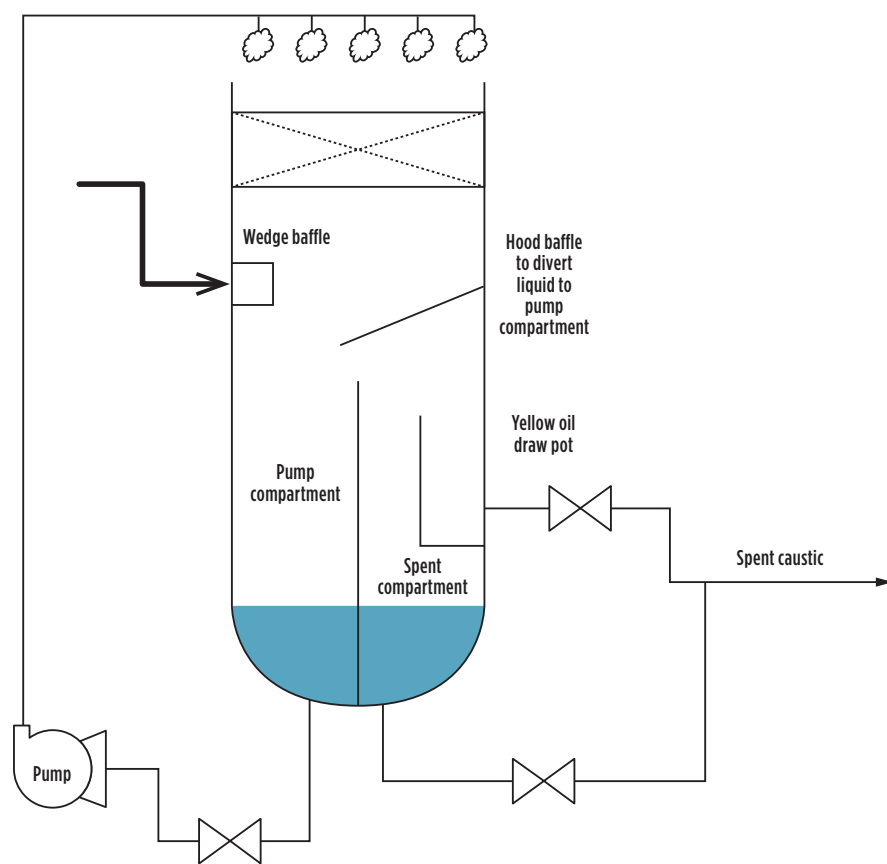
FIG. 9. Caustic tower bottom portion for phase separation, showing the pump circulation compartment (left) and the spent caustic compartment (right).

TABLE 1. Typical density values	
Strong caustic (10%)	Density: 1,112 kg/m³
Medium caustic (5%)	Density: 1,058 kg/m³
Weak caustic (2%)	Density: 1,014 kg/m³
Water	Density: 1,000 kg/m³

differences. These types of level transmitters (differential pressure) cannot detect the exact level of liquid because hydrocarbon density is 30% lower than the caustic solution.

- The mixture of aqueous caustic and hydrocarbon has a greater tendency to form an emulsion/foam (fouling is the root cause of the foaming) that can lead to inaccurate level detection.
- All LTs calibrated with the same density across the tower in most of the plants.

Solutions and recommendations include:

- Provision of an LG in the pump circulation compartment to continuously check the level (**FIG. 10**).
- Instead of a typical DP type, one interface-level transmitter can be considered in the spent caustic compartment (**FIG. 10**).
- Skimming facility to remove yellow oil (**FIG. 10**).

- Accurate densities should be considered for calibration across the tower for LTs. Typical values are mentioned in **TABLE 1.**
- A permanent water wash facility can be considered for all level transmitters and pressure transmitters.
- All pressure transmitter tapping should be in the vapor phase (along with an inclined slope toward the column) to prevent liquid accumulation. A pressure indicator should be above the tapping altitude.
- Two-level gauges can be installed at different elevations[2] to detect foaming.
- Level transmitter tapping should be in the spent caustic compartment rather than the pump circulation compartment.
- Hydrocarbon density should be used for the draw-off pot of yellow oil skimming level transmitter calibration

instead of caustic (**FIG. 10**).

- All temperature sensors should be long enough to accurately read the liquid temperature.
- Antifoaming and emulsion breaker facilities, if required.

Flow fluctuation in compressor. Possible causes include:

- Dislodging of trays and packing due to abnormal compressor condition, such as surge/choke during startup/trips.
- Entrainment of caustic to the downstream line to the knock-out drum of the compressor.
- Sticking of tray valves can prematurely flood the tower.

Solutions and recommendations include:

- All caustic tower trays and packing should be mechanically designed and support should be strengthened to withstand abnormal compressor conditions.
- The caustic tower should have provision for a wedge baffle or impingement plate in front of the feed nozzle to counter gas momentum. This also avoids flow hitting the level transmitter and hood baffle.
- The overhead line and successive knock-out drum should be designed for caustic.
- Tower metallurgy should be stress released to reduce corrosion. Any welding work after manufacturing should be avoided.[3]

General problems. Possible causes include:

- Salt out (precipitation of salts on tray) of caustic
- Liquid holdup or flooding due to blockage of packing with support
- Foaming and emulsion at the bottom section
- Corrosion
- Pyrophoric FeS formation ($H_2S + Fe = FeS + H_2$)
- Fouling (aldol condensation)[4]

- Pump hydraulics, such as net positive suction head (NPSH)
- Valve erosion problems and valve packing issues
- Fouling and deposition of polymers.

Solutions and recommendations include:

- The provision of a permanent steam facility for steam out and washing in each section
- Packing open area should not be blocked by the TSR and support beam by more than 10%[5]
- An antifouling/antifoaming agent should be used
- Temperature must be maintained within 5°C above dewpoint to avoid condensation of hydrocarbon; higher temperature can lead to caustic precipitation/salt formation
- The hood plate must be seal welded rather than bolted to inhibit leakage
- Venting provision should be provided for the hood plate, otherwise the level filled beyond the hood baffle elevation could break down the hood plate
- Overfilling the caustic tower with caustic or water can fill the cracked gas inlet line up to the compressor casing, so the inlet line must be elevated more than 4 m–5 m to avoid filling of inlet line
- The tower bottom sump's partition baffle should be without holes to avoid mixing the liquids of both compartments
- The yellow oil draw pot should have no drain hole
- All valves related to column isolation or working in alkaline service should be sleeved/coated with PTFE or any other equivalent
- A valve stem should be installed at vertical or at a 45° angle to vertical to avoid any contact of caustic, and the deposition of caustic in the gland packing of valves should be PTFE or equivalent
- Wash oil provision should be provided for washing of fouling or polymers during shutdown and normal operation.[6]

Takeaway. Applying these recommendations supports the smooth startup and operation of the caustic tower. These
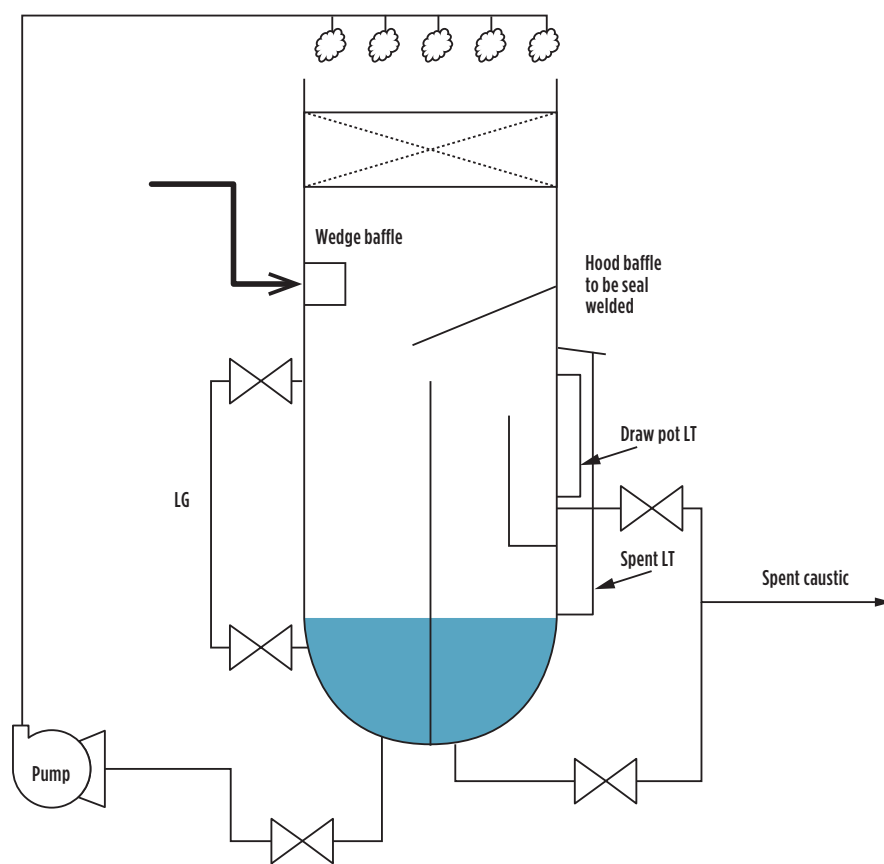

FIG. 10. Level transmitter and hood cover plate of the bottom section of the caustic tower. The hood plate diverts the total liquid into the pump circulation compartment and the caustic overflow to spent caustic. Both compartments are separated by a partition baffle.

guidelines can be checked either at the time of design review of a tower drawing or later—this article can be used as a checklist for a drawing review; however, once the tower is operational, it becomes difficult and expensive to shut down the plant and modify it. Numerous published case studies detail the reasons for various caustic tower flaws and provide recommendations and solutions. As stated here, it is better to learn from other's experiences.

The fundamental guidelines of the article are: to avoid direct contact with caustic, all level and flow transmitters should be capillary type with a water washing facility; gas impingement on the tower's shell must be avoided; the open area of packing should be checked by the process engineer; all gaskets should be PTFE or equivalent; and caustic spills must be avoided for the safety of people, processes, plants and the environment. **HP**

NOTES
These general guidelines are based on the author's experiences and are not affiliated with any company.

LITERATURE CITED
[1] Kister, H. Z., *Distillation operation,* McGraw-Hill Education, New York, 1990.
[2] Lieberman, N. P. and E. T. Lieberman, *A working guide to process equipment,* McGraw-Hill Education, 4th Ed., 2014.
[3] Kister, H. Z., *Distillation troubleshooting,* John Wiley & Sons Inc., 2006.
[4] Wikipedia, "Aldol condensation and formation of polymer."
[5] Lieberman, N. P., *Process design for reliable operation,* Gulf Publishing Company (1998).
[6] Sharma, A., "Preferential baffle reboiler—Part 1," *Hydrocarbon Processing,* April 2022.

ABHISHEK SHARMA is a process engineer at an ethylene plant, and has more than 4 yr of experience in the steam cracker unit. He completed his B.Tech degree in chemical engineering from the National Institute of Technology Raipur, India with honors and completed a process equipment design course from IIT Roorkee. He is an active professional member of the American Institute of Chemical Engineers and an associate member of IChemE. He has published five articles and participates in the smooth operation and troubleshooting of the plant.

HP | Catalysts

S. DYKE, PetroQuantum, Northland, New Zealand; and **N. PONGBOOT,** Global R&D, Samut Prakan, Thailand

Hydroprocessing catalyst reload and restart best practices—Part 1

Hydroprocessing (hydrotreating and hydrocracking) units are high-pressure, high-temperature units that have multiple reactors, multiple beds per reactor and specialized metallurgy. Catalysts in these units are replaced on a 2 yr–5 yr cycle, depending on feed quality, unit design, catalyst selection, operational constraints and performance.

One of the key drivers for a catalyst change-out turnaround on these high-margin units is minimizing the time that the unit is offline—the cost of downtime is high, particularly when a turnaround is extended.

Managing a catalyst change-out turnaround is vastly different than normal refinery maintenance activities: the complexity is higher, the risks and consequences of unplanned events are much greater, and the required resources are significant but limited (**FIG. 1**). The experience of the key personnel involved is a significant factor during this activity; however, decades of experience are disappearing from refineries due to economic pressures and the age profile of operations/engineering/maintenance personnel.

The responsibilities of refinery process engineers change every 2 yr, so building and promoting experience and expertise in-house for hydroprocessing catalyst reloads is difficult. In the past, the catalyst vendor often provided much of the necessary technical expertise, specifically for the catalyst loading and unit restart activities. However, the impact of the COVID-19 pandemic and ongoing restrictions means that catalyst vendors are generally unable to provide this level of onsite support.

This situation leads to the question of how to best manage the complexities and risks associated with a catalyst change-out and restart for refinery hydroprocessing units, as well as hydroprocessing units for renewable fuels (e.g., vegetable oils and fatty acids).

This article (Part 1 of 2) will discuss the activities associated with turnaround planning and shutdown, catalyst unloading and reactor inspection. Part 2, which will appear in the August issue, will discuss the activities associated with catalyst loading and the restart. The two articles cover the entire process across the full catalyst cycle, as well as many of the best practices that are used to manage and mitigate the underlying risks for these units.

Turnaround planning for catalyst change-out. The best performers understand the risks associated with catalyst turnarounds and turnaround work, in general, compared to maintenance and inspection work during normal operation. For example, decommissioning and commissioning of a unit are the periods of maximum risk of unexpected events. Each time equipment is accessed or "opened up," new risks are introduced. Safety incidents and labor disruptions have a greater impact during a turnaround than during normal operation. On startup, operators must have a high level of confidence that the unit will run the full cycle, without interruption.

For numerous reasons, the priorities for a turnaround should be safety, quality, time and cost—in that order. Too often, decisions are made in the planning and execution phases of a turnaround with an obsessive focus on minimizing costs. In many cases, this singular focus has resulted in massive losses because the unit had to be shut down again to rectify a problem resulting from these cost-minimizing decisions, or the performance of the unit was affected because shortcuts were taken during the catalyst reload, or the quality of the reload was compromised to save time or reduce cost. Two examples that illustrate this point are given here:

- Avoid compromising on the quality of the ceramic catalyst support material (normally ceramic balls). In some instances, trying to save $10,000–$20,000 on the cost of ceramic balls has cost millions of dollars because the cheap ceramic materials have broken or failed at the bottom of a large catalyst bed.

FIG. 1. Multi-reactor, multi-bed hydrocracker catalyst change-out.

- Ensure a catalyst handling contractor has the experience, expertise, equipment and resources to complete the catalyst unload and reload. Saving $100,000–$200,000 on the cost of the catalyst handling contractor can easily result in a multi-day delay in completion of the turnaround, particularly during the unloading of the catalyst.

During a catalyst change-out turnaround, surprises and issues—impossible to predict—will arise that must be resolved. Managing the surprises is a critical success factor and begins with the planning phase.

Planning for a catalyst reload turnaround should begin soon after the completion of the last catalyst reload. The first item to address is the catalyst evaluation and selection for the next catalyst cycle, once data is available on how the current cycle is tracking against the predicted performance.

Ideally, the catalyst selection process should begin at least 18 mos–24 mos before the next catalyst change-out to provide sufficient time for all requisite tasks. Typically, catalyst lead time is 6 mos–12 mos, leaving the remaining time for planning, evaluation and internal processing. To put it simply: the earlier, the better.

Best practices. As a general practice, it is best to apply a multi-discipline approach to set the key catalyst requirement or strategy [e.g., longer run length or more difficult (cheaper) feedstocks]. Refinery management and the economics and scheduling departments will have input into the future catalyst strategies. Additionally, the refinery's focal point (usually a unit process engineer) should also incorporate current operating issues (e.g., high reactor pressure drop, feed contamination levels) into the invitation to bid (ITB) so the catalyst supplier can properly address these problems in the next cycle.

While some refiners still rely on vendor estimations/predictions, pilot plant testing has become more popular as a tool to unveil or expose actual catalyst performance. This evaluation approach is particularly vital to a critical unit like a hydrocracker, where a slight difference in product yield can result in multi-million dollars of profit/loss per year over the whole cycle.

Comparing paper estimates/predictions from different catalyst vendors is not an apples-to-apples comparison, but this approach is nonetheless prevalent among refiners due to its simplicity. Catalyst vendors employ different design assumptions, feed characterization techniques, kinetic models and product property estimators (e.g., basic to non-basic nitrogen ratio, aromatics distribution). Consequently, it is fundamentally inaccurate to compare estimates/predictions between catalyst vendors at face value; unfortunately, many refiners are unaware of the errors inherent in this simplistic approach.

It is, however, acceptable to use a paper-based evaluation for less critical applications (e.g., for a naphtha or kerosene hydrotreater), although the best practice is still to have the catalysts tested before evaluating the options.

For refiners without an in-house pilot plant testing facility, several companies can provide an independent pilot plant testing service. Two primary methods are available: full pilot-scale and high throughput bench-scale approaches. Each method has its own advantages/disadvantages, and refiners must select the best independent pilot plant testing laboratory to suit their requirements and constraints. Based on experience, both approaches provide adequate essential information for hydrocrack-

ing catalyst evaluation and selection. It must be noted that some laboratories are more preferred by refiners than others. At least one independent laboratory requires 24 mos pre-booking before the actual test date. As such, a refiner should proactively contact these independent laboratories as soon as the new cycle starts.

The testing fee for each catalyst loading scheme can range between $45,000 and $95,000. So, who pays for the pilot plant testing? The refiner may have to pay the total cost, or the catalyst suppliers may agree to share this cost. In general, the willingness of the catalyst supplier to share the testing cost increases with the value of the catalyst package.

Accurately interpreting the results of the pilot plant testing is complex and requires experience and expertise.

A catalyst change-out turnaround is a large, complex logistical undertaking and a structured and disciplined approach to planning—along with attention to detail—is the foundation upon which good catalyst turnaround execution is based. A small, empowered, multi-discipline pre-shutdown team should be given the responsibility to conduct all planning and preparation activities and then provide the continuity throughout the turnaround execution phase. Established project management practices should be used in the planning phase and an integrated operations and maintenance schedule should form the basis of the turnaround plan.

Critical path activities should be subject to careful risk assessment and challenged and optimized aggressively throughout the planning and execution phases. Contingency plans should be prepared for the most likely and high-consequence events that may impact the turnaround (e.g., weather-sensitive work like catalyst loading, uncertain or risky activities, and critical materials or spares that may be required). Confirm the quantities of fresh catalyst onsite prior to the turnaround and ensure the catalyst is stored in a safe, dry, cool warehouse. Do not add additional maintenance or engineering work that could be conducted during normal operations just because the unit is down.

A detailed plan is required for the catalyst handling work, covering the spent catalyst unloading and fresh catalyst loading, along with a dedicated health, safety and environment (HSE) plan. Detailed procurement and logistics plans should involve the catalyst vendor and the catalyst handling contractor as early as possible.

The area around the reactor(s) must be a controlled space with only authorized entry due to the elevated level of activity involving people, cranes, vehicles, equipment and, consequently, the high risk attached to these activities happening in a small area. Clear planning and communication of how the space is to be used and controlled (crane locations, truck and forklift access ways, etc.) are required.

Utility requirements and availability, particularly air and nitrogen (N_2), must be understood and provided with a high degree of certainty. The N_2 requirement during catalyst unloading is often underestimated, especially when unloading from more than one reactor at a time, when N_2 usage is high elsewhere for purging vessels and columns of hydrocarbons and hydrogen (H_2). Ample N_2 supply and distribution capacity will reduce delays caused by high oxygen levels in the reactor(s) resulting from insufficient N_2 supply capacity. A dedicated air supply to the catalyst dense-loading machine is preferred to avoid fluctuating supply pressure caused by offtake of other users.

Do not assume the catalyst loading diagrams provided by the catalyst vendor are free of errors. Challenge any details that do not appear to be correct, based on your understanding. For example, if the vendor proposes to use 6-mm ceramic balls to directly support 1.7-mm extrudate hydrotreating catalyst it should be challenged, especially if the hydrotreating catalyst is to be sock loaded. In this case, 3-mm support material should be used under 1.7-mm extrudate catalysts (a maximum size factor of 3:1 is normally applied) to avoid catalyst migration.

A minimum 150-mm layer of large-diameter ceramic balls should be used above the outlet collector, and minimum 75-mm layers of finer ceramic balls are deemed appropriate to support the catalyst. Layers of less than 75 mm have an increased chance of allowing migration due to variations in the layer depth due to poor loading practices. Ceramic hold-down material is not used above 3-mm extrudate catalyst beds (i.e., more catalyst can be loaded). For smaller catalyst, the hold-down material is still used to guard against the potential for reverse flow.

Shutdown and startup procedures should be reviewed in detail prior to the turnaround to build in changes in catalyst conditioning requirements, lessons learned from the last shutdown and startup, newly acquired best practices from other locations, and to consider specific requirements or opportunities for the coming turnaround.

The turnaround planning and execution phases should be a cooperative effort between engineering/maintenance and operations, with an integrated plan and schedule (starting with feed out) all the way to product rundown on grade to storage. This integrated plan should define when each piece of equipment will be handed over from operations to engineering/maintenance in a gas-free condition and when it is expected back for startup preparations.

Prior to the turnaround, a detailed discussion with the catalyst vendor and the catalyst handling contractor should finalize the detailed plans and contingencies for catalyst unloading and loading activities.

Throughout the catalyst change-out turnaround, the highest probability of delays and errors occur during handovers and transitions, such as the handover of equipment from operations to engineering/maintenance after shutting down the unit and gas-freeing individual systems and equipment, the handover between engineering/maintenance to the catalyst contractor, and when inspectors are requested to perform equipment inspection.

Safe work permit renewals for confined space entry, for example, occur at the start of every shift (2–3 times per day), so any delays in this process can add a considerable amount of time to the entire turnaround. All delays on each interface can add hours and sometimes days to the turnaround—by managing these interfaces and handovers efficiently, considerable time can be potentially saved during the turnaround.

Shutdown, catalyst unloading and reactor inspection. As discussed here, the process of shutting the unit down is one of the highest risk periods for hydroprocessing units. During this non-steady-state operation, conditions (temperature, pressure, composition, etc.) are fluctuating significantly and, in some steps, very close to engineering limits. An incident on shutdown can impact the scope of the turnaround (e.g., a heat exchanger leak or a heater tube failure).

In the case of a hydrocracker unit, the whole complex is likely to be shutting down at the same time, including the vacuum distillation unit, hydrogen plant and sour gas treating units. Particularly for a hydrocracker unit, ensure that the gasoil flush and hot hydrogen strip are performed thoroughly to remove as much heavy hydrocarbon from the catalyst as possible. If these steps are cut short, the probability of a delayed entry into the reactor will be higher due to lingering hydrocarbon on the catalyst [high hydrocarbon vapor (LEL) in the reactor]. Do not exceed maximum cooling rates of 28°C/hr for heavy wall equipment, especially the reactors, as it can lead to hydrogen stress cracking and overlay disbonding.

Cooling of the reactor and catalyst system at lower temperatures is the rate-controlling step that determines when the reactor can be opened. Ambient temperature is a key factor and some locations have experience with accelerated cooling using liquid nitrogen injection (as shown in **FIG. 2**); however, the metallurgy, piping design and equipment at and downstream of the injection point must be rated for the lower temperature operation. The composition of the recycle gas changes significantly during the accelerated cooling operation (nitrogen injection), and the impact on the recycle gas compressor must be evaluated prior to implementing this practice.

For most units, maintaining full hydrogen pressure for as long as possible down to the minimum pressurization pressure (MPT), as well as other cooling strategies, will allow for an acceptable cooling rate. Most refiners use the nominal MPT (to

FIG. 2. Accelerated cooling using liquid nitrogen injection.

Quench Zone 1
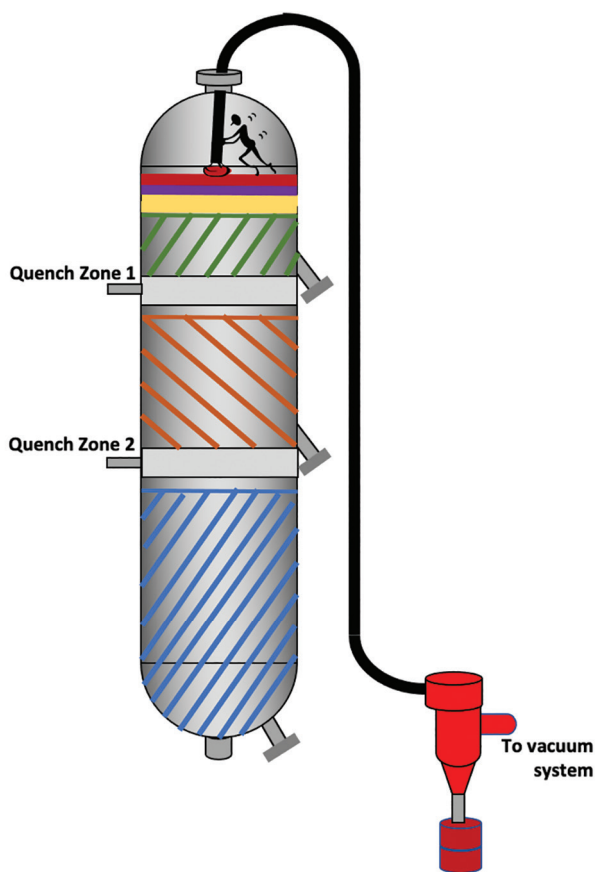
Quench Zone 2

To vacuum
system

FIG. 3. Vacuum unloading.

prevent the risk of brittle fracture or temper embrittlement) for their reactor system, which is determined by the bulk metal composition of the reactor base metal. It is worthwhile to request a specific MPT to be calculated by the reactor fabricator (J-factor calculation) for the reactor(s), based on impact testing (Charpy-V impact testing) of the base metal test blocks and welded coupons from the actual retained material used in the reactor fabrication. Most reactors have an actual MPT well below the nominal MPT of 66°C for post-1990 metallurgy (2¼ Cr – 1 Mo–0.25 V and 3 Cr – 1 Mo–0.25 V) (i.e., closer to ambient temperatures). Note: Naphtha hydrotreating (NHT) and kerosene hydrotreating (KHT) reactors (1¼ Cr – ½ Mo) do not have an MPT constraint above ambient temperatures.

Once the reactor(s) are cooled and blinded from the rest of the high-pressure circuit, the inlet elbow is removed and nitrogen purge connections are made to the reactor(s), the catalyst handling contractor can begin catalyst unloading. Strict control of reactor isolation (blinds), nitrogen connections and the inert/air atmosphere inside the reactor(s) must be maintained throughout the full process of unloading spent catalyst and reloading fresh catalyst. Fatalities have occurred during catalyst unloading, mostly due to nitrogen asphyxiation or to accidents in the inert atmosphere of the reactor. A detailed safety and rescue plan should be produced and agreed upon before work commences.

The environment inside the reactor is non-life supporting (almost 100% nitrogen) and risks associated with the potential presence of hydrocarbons and pyrophoric metal sulfides must be managed, as well. If oxygen ingress cannot be controlled, the carbon on the catalyst will oxidize to form carbon monoxide CO, carbon dioxide (CO_2) and potentially nickel carbonyl (an extremely poisonous gas), along with generating excess heat. These risks must be actively mitigated, including continuous monitoring of the reactor(s) for temperature, oxygen and other contaminants mentioned above.

Once the top distribution tray is opened and any physical filter material is removed by the inert entry team, the graded bed material and any demetalization catalyst layers are normally removed by vacuum (**FIG. 3**). Sampling of the spent catalyst in these top layers, including the first hydrotreating bed, is important to confirm the level of feed contaminants (V, Ni, As, Si, Na, etc.) during the previous cycle. The top hydrotreating catalyst bed in a hydrocracker unit is often very hard and difficult to remove; this is caused by a very hard crust or agglomerated catalyst. It is common for this bed to require the use of jack hammers to break it up before the catalyst can be removed.

The other beds in the reactor system are normally gravity-dumped from dump nozzles at the base of each catalyst bed (**FIG. 4**). Only 65%–75% of the catalyst will flow from the bed under gravity. The inert entry team then enters the reactor and "chases" the remaining catalyst and ceramic balls from the bed manually, although robots are being developed for some of this work. The manway sections are then removed from the catalyst support grid and the quench zone trays to access the next catalyst bed, where the process is repeated until the reactor is empty.

During catalyst removal in the bottom of the reactor, it is possible that catalyst and small-diameter ceramic balls fall

through the outlet collector and into the reactor outlet elbow. This debris must be removed prior to catalyst loading or it will be pushed through to a downstream reactor or feed/effluent heat exchanger on startup.

The inert entry crew should take extreme care of multi-point thermocouple arrays in the top and bottom of the catalyst beds during unloading of the spent catalyst, as these instruments are easily damaged.

After removing all catalyst and support material from the reactor(s), the internal, austenitic stainless-steel surfaces must be neutralized with an aqueous soda ash solution to protect against polythionic acid stress corrosion cracking (PASCC).[1,2] This failure mechanism is caused by polythionic acids that are formed by the reaction of sulfide corrosion products [sulfur, hydrogen sulfide (H_2S), metal sulfides] with oxygen and water. Normally, TP-347 and TP-321 stainless steel grades are used for the weld overlay and internals of hydroprocessing reactors. Austenitic stainless steels are sensitized for PASCC by welding and/or high temperatures (370°C–815°C). Newer, chemically stabilized grades of stainless steels resist sensitization for some time and therefore are less susceptible to PASCC (e.g., TP-347AP). Soda ash neutralization applies to all sensitized austenitic stainless-steel surfaces, not just reactor internals, that are exposed to the mix of sulfur, air and moisture (e.g., heater tubes and some feed/effluent heat exchangers).

When the soda ash wash is complete, the reactor can be turned over to an air atmosphere. All nitrogen connections to the reactor(s) must be positively isolated (blinded or physically disconnected).

Prior to loading, the reactor must be cleaned of all loose scale, debris and other deposits fouling the internals. Of particular importance are the outlet collector, distribution trays, other quench zone trays and the catalyst support grids (profile wire or mesh screens), which must be 90%–95% clear to ensure good distribution in the bottom of the catalyst beds.

The inspection requirements of the reactor and its internals should be detailed in the inspection plan and will include:

- General cleanliness and condition of the reactor, nozzles and internals
- Reactor internal overlay cracking: spot dye penetrant testing is utilized to detect cracking in the weld overlay, especially in areas adjacent to nozzles and at load-bearing, high-stress areas
- All reactor seams and support skirt-to-shell seams should be inspected on a set frequency.

The authors emphasize that the shutdown of the unit and the catalyst unloading are the phases of greatest uncertainty and hold the highest risk of unplanned events. Therefore, the completeness of the planning, attention to detail and the presence of refinery and contract people with experience and expertise to deal with these potentially schedule-destroying events cannot be overemphasized.

Part 2 of this article (August 2022) will address the activities associated with catalyst loading and the restart of the unit. **HP**
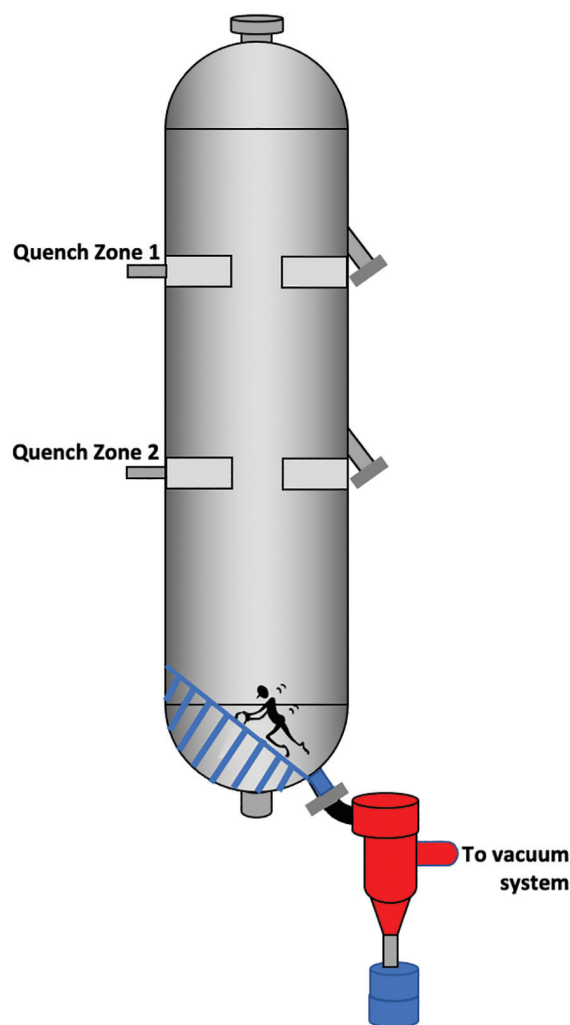
FIG. 4. Gravity dumping.

LITERATURE CITED

[1] The National Association of Corrosion Engineers (NACE) NACE Standard RP0170-2004, "Protection of austenitic stainless steels and other austenitic alloys from polythionic acid stress corrosion cracking during shutdown of refinery equipment," 2004.
[2] American Petroleum Institute (API) Standard 571, "Corrosion and materials: (Section 5.1.2.1) Polythionic acid stress corrosion cracking (PASCC)," September 2010.

SHAUN DYKE is an experienced chemical engineer who has worked in the refining and petrochemical industries for more than 40 yr in numerous technical, managerial, governance and consulting roles around the world. He lives in and works from New Zealand and writes in his spare time. Mr. Dyke earned a BSc degree (First Class Honors) in chemistry from Massey University, New Zealand.

NATTAPONG PONGBOOT is an experienced chemical engineer with extensive experience in refining and petrochemical technologies, specializing in hydroprocessing technology. Before partnering with Global R&D, he held various technical roles with Honeywell UOP, PTT Global Chemical and SCG Chemicals, with broad exposure to process and equipment design, refinery operation, plant troubleshooting and process optimization. Additionally, he is also a technical instructor for www.chemengedu.com. Mr. Pongboot obtained B.Eng. and M.Eng. degrees in chemical engineering from Kasetsart University. The author can be reached at nat.pongboot@gmail.com or nattapong.globalrd@gmail.com.

HP | Maintenance and Reliability

M. ALSAIARI and **F. ALGHAMDI**,
Saudi Aramco, Kingdom of Saudi Arabia

Storage tank settlement and soil-side corrosion assessment with optimized repair strategy

Aboveground storage tanks are used in several industries with different fluid services. These industrial tanks are normally huge structures built at a bigger scale to store the selected valuable fluids. However, the structures of these tanks are often thin and are subject to failure under any unexpected ground deformation.[1]

Most aboveground storage tanks are supported on soil, concrete slabs, gravel compaction, ring walls and pile cap foundations.[2] Aboveground storage tanks are classified into two main categories, based on their operating pressure range: atmospheric and low pressure (not exceeding 15 psig), according to API-650/620 standards.[3,4] Tanks usually are constructed with either metallic or non-metallic materials. However, these tanks are designed and manufactured with a flat bottom and a cylindrical vessel shape.[5,6]

Tanks typically have different types of roofs,[5] but some are operated without roofs and others have either fixed or floating roofs.[5,7] Aboveground storage tanks have two main concerns that impact their reliability: corrosion and bottom-supporting configuration. Throughout the oil and gas industry, tank bottom plate corrosion is a typical issue that causes high maintenance cost and equipment outage.[8,9] Conversely, storage tank-supporting configuration failure may lead to catastrophic damages that affect the environment and human life, since they contain large volumes of hazardous products.[2]

Several studies were conducted to analyze and evaluate storage tank settlements and bottom plate support configuration.[10,11] Tank settlement classifications, per API-653, are uniform settlement, planar tilt, non-planar settlement, shell settlement, edge settlement, bottom settlement near the shell, and localized bottom settlement remote from the shell.[12] API-653 does not consider the foundation stiffness influence, plate-shell section stiffness and plate thickness, which give approximately 20% allowable edge displacement of the maximum amplitude.[13]

Overview and assessment of a tank failure. An aboveground storage tank used to store distilled water in a processing facility—constructed in 1940s—suffered soil-side corrosion in several locations in the bottom plate critical zone (within 3 in. away from the shell). Edge settlement was also observed, as shown in **FIG. 1.** Based on these findings, a risk assessment and technical evaluation based on inspection findings were deemed urgent before returning the tank to service.

Magnetic flux leakage (MFL) floor scanning was conducted on the tank bottom plates. Additionally, ultrasonic thickness testing was carried out within 18 in. from the weld of the bottom to the shell joint where MFL is inaccessible. The tank bottom plates were observed with corrosion from both sides. Additionally, localized pitting corrosion was noticed close to the shell-to-bottom weld joint. However, the most severe metal losses were caused by underside (soil side) corrosion located at the critical zone.

The bottom plate's original thickness was 6 mm, while detected thickness readings ranged from 1.6 mm–2.7 mm. These values are very low (i.e., below the minimum required thickness) and it was determined that repair was required. The root causes of this corrosion formation are attributed to an ineffective cathodic protection system and lack of drip ring. The tank was constructed with a ring wall foundation type, but that was 70 yr ago when there were no standards that mandated drip ring installation to prevent water ingress between the bottom plates and the foundation.

The settlement was evaluated structurally, particularly on the deflected bottom plate at the tank perimeter. Additionally, an integrity inspection of the bottom-to-shell weld joints was completed and found satisfactory. The tank settlement was classified as edge settlement, according to API-653.[12] The tank settlement appearance was uniform, and this type of settlement does not cause any serious stresses in the tank structure.[14] Moreover, most standards do not express concern about the uniform tank settlement structurally, except for the associated piping system.[1] In this case example, the existing piping system had sufficient piping flexibly with no risk that might require enforcement.

Repair methodology. A specialized engineering team evaluated the tank

FIG. 1. Tank edge settlement layout.

settlement structurally, considering all involved parameters (tank service age, type of service, settlement severity, etc.). It was recommended to continue operating this tank with close monitoring (i.e., measuring the settlement during every operation outage window). Due to the corrosion severity in the tank bottom critical zone, bottom plate replacement was crucial for long-term safe operation. A specific repair procedure was created to replace all corroded bottom plates that were below the minimum required thickness. Replacing the tank bottom plate is very demanding and requires installing an additional supporting system to prevent shell deformation after its cutting. Because of this, external supports were welded to the tank shell to stiffen the tank shell, as shown in **FIG. 2.**

The tank bottom plate replacement sequence was implemented with a skip-on-plate replacement technique by replacing one plate and keeping the other. To prevent water ingress underneath the bottom plate, especially at the critical zone, a drip ring around the tank was installed, as seen in **FIG. 3.**

Storage tank and asset integrity management systems. The use of asset integrity management systems is widespread in the oil and gas industry to integrate and enhance asset performance according to its desired design functionality. An asset integrity management system is defined as a system or sets of systems that protect life, environment and property by constructing a well-maintained management environment that governs the asset's main critical elements.[15] The main asset's critical elements comprise process, personnel, practices and methodologies that ensure asset integrity performance to prevent accident. Successful implementation of an asset integrity management system will ensure the safe and reliable operation of processing hazards fluids. One of the main effective integrity management models used in the oil and gas industry (among others) is called the Swiss Cheese Model. This model is divided into barriers with classification categories: prevention, protection and escalation control. These barriers act as a first defense to prevent failures. Storage tanks fall under pressure vessels below the process containment barrier, as shown in **FIG. 4.**

Storage tank integrity is monitored

with integrity performance standards (IPSs), where sets of assurance requirements are assigned to ensure the integrity of the pressure envelope. However, the IPS will be ineffective unless well-designed assurance requirements and verification tasks are adequately allocated. In this storage tank case study, the drip ring installation was not included in the minimum assurance integrity requirements. This allowed the water to accumulate below the tank bottom plates—this failure was not anticipated due to an outdated IPS.

Takeaway. This article describes a systemic assessment and repair methodol-

FIG. 2. An example of a support welded to the tank shell.

ogy for an aboveground liquid storage tank. This tank was in service for approximately 70 yr in well-maintained condition. Recently, the tank experienced combined damages mechanisms: settlement and soil side-plate corrosion. The tank has a uniform edge settlement that poses no risk to the connected piping system due to its sufficient flexibility. On the other side, the tank suffered from severe soil side-plate corrosion that mandated plate replacement to operate the tank safely.

These damages necessitated a well-structured assessment and repair strategy to identify the most affordable repair methodology, considering the tank ser-

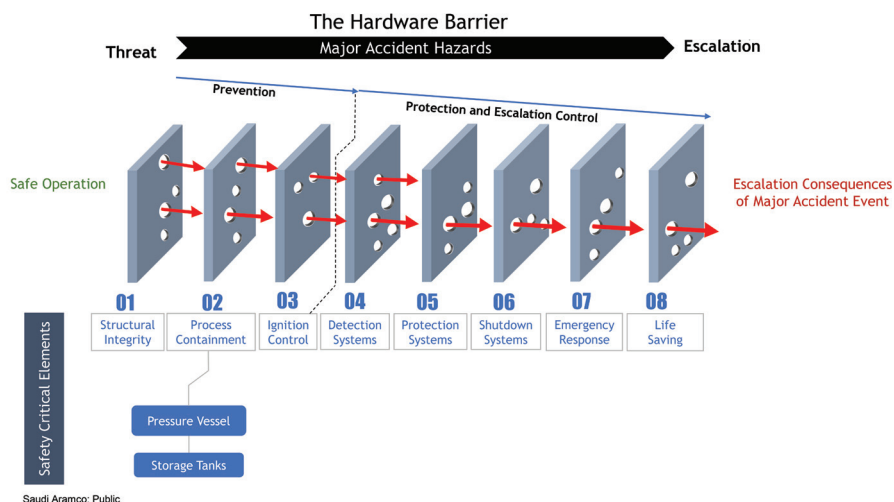**FIG. 3.** A typical example of an installed drip ring around a tank.

FIG. 4. The Swiss Cheese Model Risk Escalation.

vice age. The tank was evaluated visually along with MFL and ultrasonic examinations. The ultrasonic testing report demonstrated a metal loss of 50%–75% from the original thickness due to inadequate cathodic protection and lack of drip ring where water ingress underneath the tank plate occurred.

Adhering to API STD 653 requirements, a specific repair approach was proposed to rehabilitate this corrosion while maintaining the existing tank condition. The repair procedure focused on the tank bottom critical zone due to its impact on the tank shell stability. As a result of this assessment, a new drip ring and cathodic protection system were installed and tested to verify their effectiveness. A major finding of this study was the benefit of enhancing the asset integrity management system program by updating the integrity performance standards through revamping the minimum assurance requirements and verification tasks that are reviewed quarterly by the process owner and field inspection team to prevent future such failures. **HP**

LITERATURE CITED

[1] Hamidi, B. and S. Varaksin, "Ground improvement of tank foundations in the Middle East," Soil Testing, *Soil Stability and Ground Improvement,* 1st GeoMEast International Congress and Exhibition Egypt, Egypt 2017 on Sustainable Civil Infrasturctures.

[2] Wisnugroho, J. and S. Guntoro, "Numerical study of oil storage tanks during planar settlement," *Applied Mechanics and Materials,* February 2018.

[3] American Petroleum Institute (API) Standard 650, "Welded tanks for oil storage," 13th Ed., 2020.

[4] American Petroleum Institute (API) Standard 620, "Design and construction of large, welded, low-pressure storage tanks," 10th Ed., 2004.

[5] M. Gulin, M., I. Uzelac, J. Dolejš and I. Boko, "Design of liquid-storage tank: Results of software modeling vs calculations according to eurocode," *Elektronički časopis građevinskog fakulteta Osijek,* December 2017.

[6] Jerath, S. and M. Lee, "Stability analysis of cylindrical tanks under static and earthquake loading," *Journal of Civil Engineering and Architecture,* January 2015.

[7] Zhao, Y., Q. S. Cao and X. Y. Xie, "Floating-roof steel tanks under harmonic settlement: FE parametric study and design criterion," *Journal of Zhejiang University-SCIENCE A,* Vol. 7, 2006.

[8] Martinez, S., "Estimating internal corrosion rate and internal inspection interval of aboveground hydrocarbon storage tanks," *Goriva i Maz : časopis za tribologiju, tehniku podmazivanja i primjenu tekućih i plinovitih goriva i inžinjerstvo izgaranja,* Vol. 52, No. 2, 2013.

[9] Feng, Y., Y. Yang and B. Huang, "Corrosion analysis and remaining useful life prediction for storage tank bottom," *International Journal of Advanced Robotic Systems,* September 2019.

[10] Dimov, L. A., I. L. Dimov and E. M. Bogushevskaya, "Large oil tank settlement and tilt during hydraulic testing," *Soil Mechanics and Foundation Engineering,* 2017.

Complete literature cited available online at www.HydrocarbonProcessing.com.

MESHAL ALSAIARI works with Saudi Aramco as a piping and structural engineer. He earned a BS degree in mechanical engineering from Prince Mohammed University and has more than 10 yr of experience working extensively in the inspection and engineering fields with static equipment and piping components. He is an Incorporated Engineer from the UK Engineering Council and a Certified Corrosion Technologist from the National Association of Corrosion Engineers (NACE). Mr. Alsaiari has published several technical papers in the field of piping and static equipment engineering.

FAYEZ ALGHAMDI works with the Saudi Aramco Consulting Services Department (CSD) as a pressure vessels and tanks consultant with extensive experience in the design and repair of pressure vessels and storage tanks. He earned an MS degree in mechanical engineering from King Fahad University of Petroleum and Minerals (KFUPM) in Dhahran, Saudi Arabia in 2003. He previously worked as Vessels Standards Chairman from 2015–2019.

I. WADE, Belzona Polymetrics Ltd., Harrogate, UK

Developing and utilizing a novel, toughened epoxy adhesive

When identifying solutions that can offer assurance and longevity, the maintenance and reliability of asset repairs can be challenging. This article will examine the use of structural adhesives as the first-choice solution.

Since structural adhesives provide high modulus and high strength, they can be used for affixing metal substrates or components. Even though adhesives are used in a wide range of industries (including aerospace, rail and construction), they are not presently recognized internationally like traditional methods.

Traditional practices—such as welding, riveting, nuts and bolts, and mechanical fixing—are perceived as the go-to methods. However, they all have their inherent inadequacies. Welding, for instance, can be hazardous to health. Riveting, nuts, bolts and fasteners can concentrate stress.

This article introduces a novel, two-component, solvent-free toughened epoxy adhesive material that provides high adhesion to metallic substrates, while also being able to withstand high movement or cyclic fatigue vs. general epoxy materials.

In addition to potential application areas, this article also discusses several benefits of this adhesive material, including its ease of use, and its load bearing and impact-resistance properties.

Maintenance and repair procedures. Most industrial maintenance or repair procedures can involve either welding or the use of mechanical fasteners, as these methods can be perceived as easy and quick fixes; however, while these procedures might initially seem to correct the issue, they may cause more harm than good. Depending on the repair situation, welding or drilling to connect mechanical fasteners on a storage tank containing flammable liquid is not recommended for obvious reasons. This is where a structural adhesive can offer a solution for that type of maintenance repair.

There are many structural fixings used across a range of industries that may be part of any maintenance or repair, including support brackets (e.g., cable trays, antennas, heating coils, filter pans) or any other internal fixtures in vessels that suffer from corrosion, impacts or vibration damage.

Process equipment or piping can suffer from steel thinning or even from wall defects, which will require either monitoring or repairing depending on the severity of the integrity lost. Structural fittings are generally used for fixing static members, but they may be subjected to forces unbeknown at the time of installation, including thermal cycling of the joints, cyclic loading or vibration due to the fatigue of a component. If repairs are needed, the contractor may be in a situation where a choice of solutions can be made. If so, before a decision is made on a course of action, the strengths and weaknesses of the possible solutions should be identified.

Welding is regularly used for repairs since it is widely available. Although welding is well regulated and results in a high-strength repair, it does come with inherent risks (including heat stress and other types of harm to the user), as welding can cause both acute and chronic health risks.[1] The application of welding repairs onto piping sections, storage tanks, or process systems and equipment should not be undertaken due to the high temperatures involved and the combustible nature of the process fluids or gases running through these systems or being stored in these components.

Bolted joints are a simple and low-cost repair because of their ease of disassembly/reassembly. However, bolted joints often use dissimilar metals, which contributes to galvanic corrosion, adds weight to the joint, and requires routine inspection and tensioning. Also, drilled holes in the support material create uneven stress distributions.

Structural adhesives have a high bond strength and are lightweight. In addition, adhesives that are applied to cover the entire joint result in a uniform stress distribution, reducing metal distortion under strain.

The importance of a strong bond. Adhesive bonding is the joining of similar or dissimilar members together, while creating permanent high-strength bonds that can transfer structural stress without loss of structural integrity.

Regardless of the joint type used, it is important to understand the different stresses that are imparted onto a bonded assembly. Adhesives perform the best when the stress is two-dimensional to the adhesive, allowing the force to be applied over the entire bond area.

Joints that are well designed for adhesives place most of the stress into compression or shear modes. Adhesives perform the worst when stress is one-dimensional to the adhesive, concentrating the load onto the leading edge of the bond line. Joints that are placing stress on peel or cleavage adhesion concentrate this stress onto the leading edge, which may lead to premature bond failures, especially if subjected to vibration, impact or fatigue.

High-strength bonds are obtained after cleaning the substrate by removing all contaminants, followed by roughing the substrate—usually in the form of grit blasting—according to internationally recognized standards.[2] This is why surface preparation is critical to success, regardless of what type of adhesive is used.

There are three types of bonding that are important to ensure good adhesion: adhesive, chemical and mechanical. Adhesive bonding relies on surface energy to generate adhesion to the substrate, while chemical bonding relies on a chemical bond formation and on electronic bonding to produce adhesion. Mechanical adhesion is due to the creation of an irregular profile that allows a deeper profile to be produced. The types of structural adhesives available are summarized in **TABLE 1.**

The following are two types of failure mechanisms associated with structural adhesives:

1. Cohesive failure occurs in the bulk layer of the adhesive material. This failure mode is limited by the strength of the adhesive material and can be caused by insufficient curing of the adhesive and/or by applications at a greater thickness than what is recommended.
2. Adhesive failure occurs when the mechanical adhesion between the adhesive and the parts being joined is overcome by the loading. This failure mode is associated with inadequate surface preparation, the presence of contaminants, or insufficient curing of the adhesive, among other factors.

The creation of a novel adhesive. Design considerations for a proprietary fatigue-resistant adhesive[a] were based on both technical target requirements and a practicality approach. Technical design considerations included the following:

- **Excellent adhesion to metallic substrates:** The adhesive was optimized for metal-to-metal adhesion.

- **Suitable service temperatures:** The adhesive had to withstand service temperatures between –30°C and 60°C.
- **High resistance to peel/cleavage forces:** Most standard epoxies do not perform well when subjected to peel or cleavage forces; therefore, an epoxy that could withstand both forces would be advantageous.
- **Superior resistance to cyclic fatigue:** The new adhesive should show no signs of deterioration or cracking when subjected to cyclic loading.
- **Data package for engineering design:** Performance data collection was required for the adhesive to be modelled through finite element analysis (FEA).
- **Solvent-free formulation:** Solvent-free epoxy systems show greater mechanical properties vs. formulations with solvents. Experiments have shown that solvents remaining within the epoxy can hinder the cross-linking process, resulting in lower exotherm, and affecting the initial curing rate reaction order and glass transition temperatures.

The practical design considerations included the following:

- **High build paste structure:** The adhesive should be able to hold its own structure and not slump in vertical applications.
- **Ease of application:** The system should be able to be conveniently applied by brush, applicator or cartridge injection.
- **Fast return to service:** The structural adhesive should have shorter curing times to provide appeal for asset owners.

The proprietary adhesive[a] was subjected to the following tests and evaluation protocols to ensure that it met the design criteria previously discussed. Where possible, internationally recognized standards were used. These tests/evaluations included:

1. Cleavage adhesion—ASTM D1062-08 (2015): Standard Test Method for Cleavage Strength of Metal-to-Metal Adhesive Bonds
2. Tensile shear adhesion—ASTM D1002 (2019): Standard Test Method for Apparent Shear Strength of Single-Lap-Joint Adhesively Bonded Metal Specimens by Tension Loading (Metal-to-Metal)
3. Tensile fatigue resistance—ISO 9664:1993: Adhesives—Test Methods for Fatigue Properties of Structural Adhesives in Tensile Shear
4. Impact resistance—ASTM D256-10 (2018): Standard Test Methods for Determining the Izod Pendulum Impact Resistance of Plastics.

Cleavage adhesion: ASTM D1062-08 (2015). Cleavage adhesion is used to assess the strength of an adhesive bond between two substrates when exposed to cleavage stress. The proprietary adhesive[a] was applied between two identical grit-blasted metallic cleavage test pieces to create a fixed bond area of 125 mm² of minimal bond-line thickness (**FIG. 1**).

The specimen was allowed to cure, and then it was attached to a 25-kilonewton (kN) tensometer, using suitable grips. The tensometer then applied a load at a fixed rate of 1.3 mm/min, exerting a cleavage force on the specimen until bond failure. This test was repeated five times to calculate an average force.

Tensile shear adhesion: ASTM D1002 (2019). Tensile shear adhesion (or lap-shear adhesion) is used to determine the

TABLE 1. Types of structural adhesives

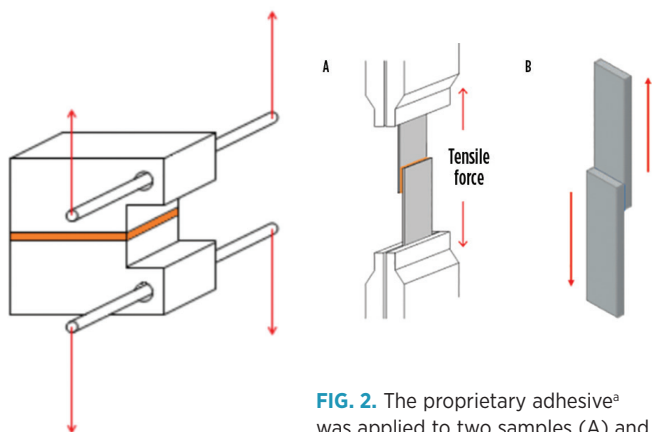| Type	Strengths	Weaknesses
Standard epoxies	Lap-shear adhesion, temperature resistance	Peel and cleavage forces
Toughen epoxies	Highest bond strength (metal-to-metal)	Temperature resistance

FIG. 1. Cleavage adhesion test.

FIG. 2. The proprietary adhesive[a] was applied to two samples (A) and then tested (B) using the tensile adhesion test.

adhesive strength of a material when bonded between two ridged metallic substrates. Two samples with dimensions of 100 mm × 25.4 mm × 2 mm were overlapped lengthwise by approximately 12.7 mm and bonded to a minimal bond-line thickness with the proprietary adhesive[a] (**FIG. 2**). The specimen was allowed to cure before being attached to a 25-kN tensometer using suitable grips. The tensometer then applied a load at a fixed rate of 1.3 mm/min, exerting a cleavage force on the specimen until bond failure.

Fatigue resistance: ISO 9664:1993. Fatigue resistance is the highest stress that a material can withstand for a given number of cycles without breaking. A standard static tensile shear adhesion test was conducted to determine the mean breaking stress—24.17 MPa was used as the mean stress in fatigue testing. The mean breaking stress value was 35%; therefore, the 35% mean shear stress was 24.17 MPa × 35% = 8.461 MPa. At four different alternating stresses, fatigue testing was conducted at 30 Hz until failure. Results were as follows:

1. 80% = 6.8 MPa (8.461 MPa × 80%) stress amplitude cycles between
2. 60% = 5.1 MPa (8.461 MPa × 60%) stress amplitude cycles between
3. 57.5% = 4.9 MPa (8.461 MPa × 57.5%) stress amplitude cycles between
4. 55% = 4.7 MPa (8.461 MPa × 55%) stress amplitude cycles between.

The ISO 9664:1993 fatigue stress cycle is shown in **FIG. 3.**

Impact resistance: ASTM D256-10 (2018). Impact tests can be used to assess the toughness of a material. A material's toughness is a factor of its ability to absorb energy during plas-

tic deformation. Brittle adhesives have low toughness due to the small amount of plastic deformation that they can endure. Conversely, tougher materials can absorb greater energy during fracture; therefore, they have improved impact resistance.

The Izod impact test enables samples to be tested in two forms: notched or unnotched. In this case, the testing was notched, with a V-shaped notch of approximately 2.5 mm in depth, and a total defect angle of 45° in the center of the specimen sample, with dimensions of 12.7 mm × 12.7 mm × 65 mm. The notch concentrates stress and enables a crack propagation measurement.

Three-point load test. This non-standard test was used to assess the relative flexibility of adhesives when applied to a metallic substrate. In this test, mild steel panels of dissimilar dimensions (Panel 1's thickness was 550 mm × 50 mm × 10 mm, and Panel 2's thickness was 225 mm × 50 mm × 10 mm) were stressed to the point that the adhesive failed. The panel was held in position at two points—one at either end of the sample—and was gradually stressed at a single point in the center of the specimen via a hydraulic press (**FIG. 4**). The greater the displacement (i.e., the further the press travels until failure), the more flexible the adhesive. The thickness of the adhesive will influence the degree of flexibility, so the analysis should be duplicatable for repeatability purposes.

In the case of this testing (the manufacturing stage), the specimens were compressed by hand pressure only to replicate in-field applications of achieving below the maximum bond-line thickness of 2 mm.
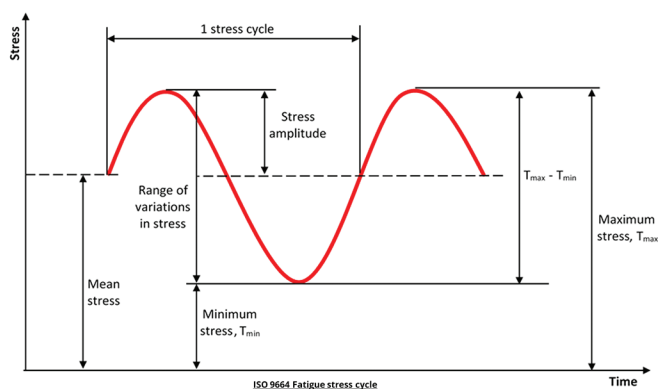

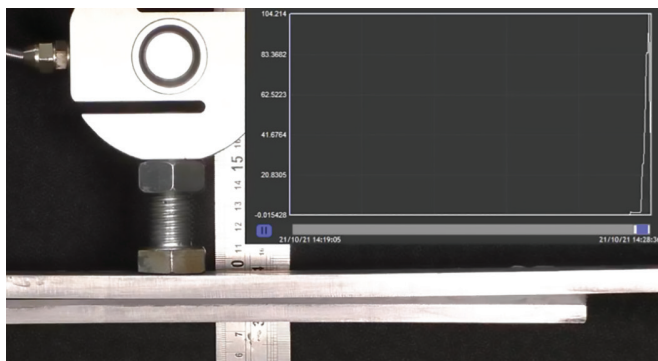
FIG. 3. ISO 9664:1993 fatigue stress cycle.

FIG. 4. Three-point load testing.

TABLE 2. Cleavage adhesion test results

Grit blasted (ISO 8501-1 Sa 2.5)	Cleavage adhesion
20°C (68°F) applied, cured and tested	360 N/mm (2,050 pli)
20°C (68°F) applied, 60°C (140°F) cured and tested	300 N/mm (1,710 pli)
60°C (140°F) applied, cured and tested	330 N/mm (1,880 pli)

TABLE 3. Tensile shear adhesion test results

Grit blasted (ISO 8501-1 Sa 2.5)	Tensile shear adhesion
20°C (68°F) applied, cured and tested	33.4 MPa (4,840 psi)
20°C (68°F) applied, 60°C (140°F) cured and tested	20.9 MPa (3,030 psi)
60°C (140°F) applied, cured and tested	24.8 MPa (3,600 psi)

TABLE 4. Cyclic fatigue test results

Stress amplitude cycles	Results, MPa
80% = 6.8 MPa (8.461 MPa x 80%)	15.23–1.69
60% = 5.1 MPa (8.461 MPa x 60%)	13.54–3.38
57.5% = 4.9 MPa (8.461 MPa x 57.5%)	13.33–3.6
55% = 4.7 MPa (8.461 MPa x 55%)	13.11–3.81

TABLE 5. Impact-resistance test results

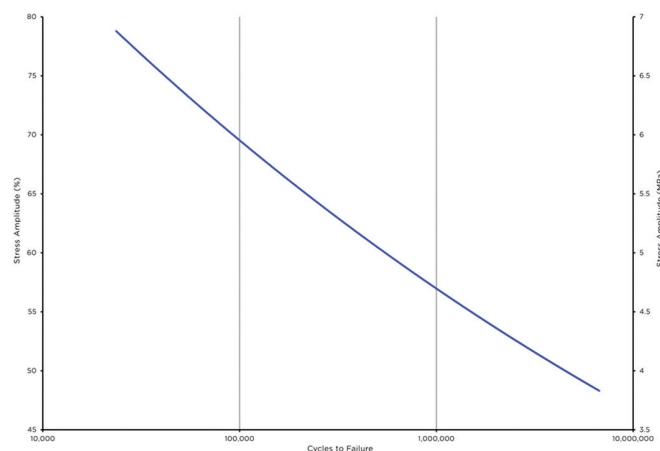| Specimen	Reversed-notched Izod impact strength
20°C (68°F) applied, cured and tested	15.9 KJ/m^2 (165.2 J/m)
20°C (68°F) applied, 60°C (140°F) cured and tested	16.2 KJ/m^2 (171.4 J/m)
60°C (140°F) applied, cured and tested	9.7 KJ/m^2 (100.5 J/m)

TABLE 6. Three-point load test results

Specimen	Deflection
20°C (68°F) applied, cured and tested	11 mm
20°C (68°F) applied, cured and tested	13 mm
20°C (68°F) applied, cured and tested	13 mm

FIG. 5. The S-N curve of the proprietary adhesive[a]

Testing results and discussion. Results of the cleavage adhesion test are shown in **TABLE 2.** Tensile shear adhesion test results are detailed in **TABLE 3.** Tensile fatigue resistance test results are shown in **TABLE 4.** From a mean breaking stress of 35% (8.461 MPa), the proprietary adhesive[a] will survive 10^6 cycles at 56.6%, with an alternating stress amplitude of ± 4.791 MPa = 13 MPa–3.67 MPa. The S-N curve of the proprietary adhesive[a] is shown in **FIG. 5.** Results of the impact-resistance tests and the three-point load tests are detailed in **TABLES 5** and **6,** respectively.

Takeaways. The following takeaways can be drawn from the use of the proprietary adhesive[a] as a solution for the repair and/or maintenance of assets:

1. The proprietary adhesive[a] offers high resistance to structures that are subjected to forces such as peel, cleavage, vibration or cyclic loading. These include, but are not limited to, support brackets for fire deluge systems, internal and external fixtures on process equipment, wear pads, and wind girders on storage tanks.
2. As the proprietary adhesive[a] offers an array of additional practical features (i.e., ease of application, the ability to hold its own structure when placed in vertical applications and superior adhesion to metallic substrates), the toughened epoxy can be used on structural support reinforcements, load transfer supports, and metallic staircases and ladders.
3. Plate bonding to repair thinning walls or wall defects on areas such as pipe/piping, process equipment, storage tank floating roofs and platform decks can utilize the proprietary adhesive, as it offers high impact resistance and flexural properties.
4. The fatigue-resistant adhesive has been optimized for metal-to-metal adhesion, and it exhibits an extensive data list with more than 20 tests solely based on adhesion. This performance data can be used for FEA or other simulations to aid in bond designing and/or qualification of the adhesive in areas (such as handrails and walkways) that would normally be seen as high risk for standard epoxies. **HP**

NOTE

[a] Belzona 7311 fatigue-resistant adhesive

LITERATURE CITED

[1] Health and Safety Executive, "Health risks from welding," UK Government, online: https://www.hse.gov.uk/welding/health-risks-welding.htm
[2] International Organization for Standardization, "ISO 17212:2012: Structural adhesives—Guidelines for the surface preparation of metals and plastics prior to adhesive bonding," February 2012.
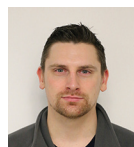
IAN WADE is a Technical Services Supervisor for Belzona Polymerics Ltd. in Harrogate, UK. He is AMPP CIP L2 qualified, and has been with the company since 2010. Mr. Wade is also a participating member of the British Standards Institute (BSI). He is studying toward a Bch degree in engineering from The Open University.